
A GPU-Accelerated Moving-Horizon Algorithm for Training Deep Classification Trees on Large Datasets

Jiayang Ren[†], Valentín Osuna-Enciso[‡], Morimasa Okamoto[†], Qiangqiang Mao[†],
Chaojie Ji[†], Liang Cao[†], Kaixun Hua[†], Yankai Cao^{†*}

[†]University of British Columbia

[‡]Universidad de Guadalajara

Abstract

Decision trees are essential yet NP-complete to train, prompting the widespread use of heuristic methods such as CART, which suffers from sub-optimal performance due to its greedy nature. Recently, breakthroughs in finding optimal decision trees have emerged; however, these methods still face significant computational costs and struggle with continuous features in large-scale datasets and deep trees. To address these limitations, we introduce a moving-horizon differential evolution algorithm for classification trees with continuous features (MH-DEOCT). Our approach consists of a discrete tree decoding method that eliminates duplicated searches between adjacent samples, a GPU-accelerated implementation that significantly reduces running time, and a moving-horizon strategy that iteratively trains shallow subtrees at each node to balance the vision and optimizer capability. Comprehensive studies on 68 UCI datasets demonstrate that our approach outperforms the heuristic method CART on training and testing accuracy by an average of 3.44% and 1.71%, respectively. Moreover, these numerical studies empirically demonstrate that MH-DEOCT achieves near-optimal performance (only 0.38% and 0.06% worse than the global optimal method on training and testing, respectively), while it offers remarkable scalability for deep trees (e.g., depth=8) and large-scale datasets (e.g., ten million samples).

1 Introduction

Decision trees, as a supervised learning technique, offer exceptional interpretability, making them suitable for many domains requiring clear decision-making (Morgan and Sonquist, 1963). Their tree-like structure systematically partitions the feature space to address classification or regression problems. However, building an optimal decision tree is an NP-complete problem (Laurent and Rivest, 1976), leading to heuristic strategies like ID3 (Quinlan, 1986), C4.5 (Quinlan, 1993), and CART (Breiman et al., 1984). These methods utilize a top-down, greedy approach to construct trees. Despite their widespread use, heuristic techniques are limited by their focus on individual tree splits, neglecting potential impacts of future splits (Bertsimas and Dunn, 2017). Consequently, these algorithms risk arriving at sub-optimal solutions, potentially compromising the decision tree’s predictive capabilities.

Addressing greedy problems, optimal classification trees (OCT) that induce the entire tree at once have gained significant attention in recent years. Two primary approaches to solving OCT are mixed integer programming (MIP) (Bertsimas and Dunn, 2017; Verwer and Zhang, 2017, 2019; Günlük et al., 2021; Aghaei et al., 2022; Hua et al., 2022; Mazumder et al., 2022) and dynamic programming (DP) (Hu et al., 2019; Aglin et al., 2020; Lin et al., 2020; Demirović et al., 2022; McTavish et al., 2022). MIP methods learn optimal trees with a fixed depth as a MIP model and employ general

*corresponding author: yankai.cao@ubc.ca.

or specific-purpose MIP solvers to attain global optimum. State-of-the-art methods RS-OCT (Hua et al., 2022) and Quant-BnB (Mazumder et al., 2022) expanded solvable regions to datasets with one million samples through well-designed lower and upper bounds and sophisticated branch-and-bound frameworks. However, these methods still face substantial computational costs, as they can only handle shallow decision trees with two or three layers. RS-OCT offers theoretical convergence to the global optimal solution but relies heavily on the parallelization of large computing clusters (e.g., 1000 cores). Quant-BnB exhibits minimal computing time for two-layer trees but is limited to shallow trees up to three layers, due to the exponential increase in both tree nodes and computing time with each increment in tree depth. As for DP, studies conducted have demonstrated promising results in solving OCT problems. Nonetheless, the majority of these DP approaches can only deal with shallow trees and primarily focus on binary features (Demirović et al., 2022). Converting continuous features into binary features can lead to a significantly expanded feature space, potentially disrupting the relationship between values of numerical features (Mazumder et al., 2022). In conclusion, existing OCT methods face difficulties when computing optimal decision trees with continuous features, particularly for large-scale datasets and deep trees.

In addition to OCT that aim to achieve the optimal solution, there are alternative approaches focused on enhancing greedy algorithms by introducing stochastic elements into the process. One noteworthy method in this category is the local search method proposed by (Bertsimas and Dunn, 2017). Similar to the conventional approach of CART, the local search method traverses a single current node to generate an initial solution. However, it diverges in its strategy for refinement—improving the initial tree through node swapping and continuous evaluation of the objective function until further enhancement is unattainable. Empirical studies conducted on extensive datasets demonstrate that local search consistently outperforms CART. Nevertheless, the computational overhead introduced by node swapping renders local search less efficient, especially when dealing with large datasets and deep trees. Additionally, the implementation’s reliance on a caching technique complicates parallelization on modern computers. A more detailed overview of related works can be found in Appendix A.

In this paper, we introduce a gpu-accelerated moving-horizon differential evolution algorithm for optimal univariate binary trees on classification tasks with continuous features (MH-DEOCT). Differential evolution (DE) is a metaheuristic method that can search extensive spaces of candidate solutions for a black box optimization problem. There are several metaheuristic-based methods proposed for inducing decision trees (Kuo et al., 2007; Cho et al., 2011; Dolotov and Zolotykh, 2020; Ersoy et al., 2020; Rivera-Lopez et al., 2022). However, these methodologies require searching the entire tree simultaneously, while the tree nodes increases exponentially with tree depth. Given that black-box optimization methods are typically designed to handle a limited number of variables, these methodologies tend to underperform when applied to deep trees. In our experiments, the plain DE algorithm, without the moving-horizon strategy and warm-starts, could not even outperform CART when the depth was 8. To address this issue, we propose utilizing a moving-horizon strategy that optimizes shallow subtrees at a time to balance the vision of trees and the ability of optimizers.

Our contributions: First, we devise a discrete tree decoding method from DE individuals that eliminates duplicated searches between adjacent samples, thereby enhancing the efficiency in handling continuous features. Second, we implement a population-based, GPU-accelerated fitness evaluation algorithm for OCT along with the corresponding population-based DE algorithm. This powerful combination drastically reduces the running time. Finally, we propose a moving-horizon strategy that optimizes shallow subtrees at each node incrementally to strike a balance between the vision and the optimizer capability.

Performance: Our comprehensive studies on 68 UCI datasets demonstrate that the proposed MH-DEOCT outperforms heuristic methods like CART, enhancing training and testing accuracy by an average of 3.44% and 1.71%, respectively. Moreover, these numerical studies empirically demonstrate that MH-DEOCT achieves near-optimal performance with significantly reduced running time, trailing the global method Quant-BnB by an average of 0.38% and 0.06% on training and testing, respectively. Furthermore, our approach extends its performance to deeper trees (e.g., depth=8) and large-scale datasets (e.g., ten million samples), making it a promising solution for a broad range of applications.

2 Preliminaries and Notations

Differential Evolution is a population-based meta-heuristics optimization algorithm consisting of four operators, including initialization, mutation, crossover, and selection (Storn and Price, 1997). For an optimization problem with a m -dimensional solution, DE starts by randomly initializing a population consisting of N vectors with m dimension corresponding to the solution. Each vector in this population is called an individual. We denote the population at the g th generation as $\mathcal{S}^g = \{\mathbf{s}_1^g, \mathbf{s}_2^g, \dots, \mathbf{s}_N^g\}$ and the r th individual at the g th generation as $\mathbf{s}_r^g = [s_{r,1}^g, s_{r,2}^g, \dots, s_{r,m}^g] \in \mathbb{R}^m$. After population initialization, the mutation operator generates mutant vectors $\mathbf{v}_r^g = [v_{r,1}^g, v_{r,2}^g, \dots, v_{r,m}^g] \in \mathbb{R}^m$ from the parent population \mathcal{S}^g :

$$\mathbf{v}_r^g = \mathbf{s}_{best}^g + M \cdot (\mathbf{s}_{r_1}^g - \mathbf{s}_{r_2}^g) \quad (1)$$

where \mathbf{s}_{best}^g is the individual with the best fitness in the current generation, $r_1, r_2 \in \{1, \dots, N\}$ are two randomly selected indices and M is the mutation factor. Subsequently, an offspring individual $\mathbf{u}_r^g = [u_{r,1}^g, u_{r,2}^g, \dots, u_{r,m}^g] \in \mathbb{R}^m$ is generated by the crossover operation:

$$u_{r,q}^g = \begin{cases} v_{r,q}^g & , \text{ if } rand(0, 1) \leq CR_r \text{ or } q = q_{rand} \\ s_{r,q}^g & , \text{ otherwise} \end{cases} \quad (2)$$

where $rand(0, 1)$ is a uniform random number within a range of $[0, 1]$ for each individual $r \in \{1, \dots, N\}$ and each dimension $q \in \{1, \dots, m\}$, CR_r is a pre-specified cross probability, q_{rand} is a random index chosen from $\{1, \dots, m\}$. Then, a fitness value $f(\mathbf{s}_r^g)$ is used to perform the selection:

$$\mathbf{s}_r^{g+1} = \begin{cases} \mathbf{u}_r^g & , \text{ if } f(\mathbf{u}_r^g) \leq f(\mathbf{s}_r^g) \\ \mathbf{s}_r^g & , \text{ otherwise} \end{cases} \quad (3)$$

The above procedure iterates until the maximum generation number G arrives. A detailed description of the classic DE procedure can be found in Appendix B, Algorithm 3.

Optimal Classification Tree (OCT): We consider univariate binary trees with continuous features and depth D for classification. "Binary" implies each node has at most two child nodes. "Continuous" differs from "categorical" features in the dataset, while the later one can be incorporated using encoding methods like one-hot encoding. "Univariate" denotes that only one feature can be selected for splitting at each node.

To facilitate ease of reading, we primarily adopt the notation system used in Bertsimas and Dunn (2017). Denote the training dataset as (\mathbf{X}, \mathbf{Y}) and the samples in the dataset as (\mathbf{x}_i, y_i) , where $i = 1, \dots, n$ and n is the number of samples. Each sample consists of a pair of P features $\mathbf{x}_i \in \mathbb{R}^P$ and a class indicator $y_i \in \mathcal{K} = \{1, \dots, K\}$, with K representing the total number of classes. Notably, we scale \mathbf{x}_i with the min-max value of each feature, resulting in a range of $[0, 1]$.

Figure 1 illustrates a typical example of a binary tree with depth $D = 3$. The tree comprises branch nodes that apply a split and leaf nodes that assign a class. The total number of nodes in a complete tree with depth D is $T = 2^{(D+1)} - 1$. Each node in the binary tree is assigned an index $t \in \mathcal{T} = \{1, \dots, T\}$, counted from top to bottom and left to right, as shown in Figure 1. We further denote the index set of branch nodes as $\mathcal{T}_B = \{1, \dots, \lfloor T/2 \rfloor\}$ and leaf nodes as $\mathcal{T}_L = \{\lfloor T/2 \rfloor + 1, \dots, T\}$.

The univariate binary tree is described using a vector tuple (\mathbf{a}, \mathbf{b}) , where $\mathbf{a} = [a_1, \dots, a_{\lfloor T/2 \rfloor}]$ and $\mathbf{b} = [b_1, \dots, b_{\lfloor T/2 \rfloor}]$. Specifically, $a_t \in \{0, 1, \dots, P\}$, $t \in \mathcal{T}_B$, represents the selected feature to split at branch node t . If $a_t = 0$, it means there is no split at this node. $b_t \in [0, 1]$, $t \in \mathcal{T}_B$ represents the threshold to split at branch node t . For a branch node t and a sample \mathbf{x}_i , if the a_t th feature $x_{i,a_t} < b_t$, the sample is assigned to the left child node; otherwise, it is assigned to the right child node. To maintain the complete structure of a decision tree with depth D , we assign all samples at branch node t to the right child node if no feature is selected by forcing $b_t = 0$ when $a_t = 0$.

We utilize $z_{i,t} = 1$ to indicate that a sample \mathbf{x}_i is assigned to a leaf node $t \in \mathcal{T}_L$ following the assignment procedure described above; otherwise, $z_{i,t} = 0$. Besides, $z_{i,t}^k$ is denoted as the class flag representing if sample \mathbf{x}_i of class k is assigned to the leaf node t , with $z_{i,t}^k = 1$ if $z_{i,t} = 1$ and $y_i = k$, otherwise, 0. In this manner, the assigned class of each leaf node $c_t \in \{1, \dots, K\}$, $t \in \mathcal{T}_L$ can be calculated using:

$$c_t = \arg \max_k \{z_t^k\}, \hat{z}_t^k = \sum_{i=1}^n z_{i,t}^k, k \in \mathcal{K}, t \in \mathcal{T}_L, \quad (4)$$

where \hat{z}_t^k is the number of assigned samples that belong to class k on the leaf node t . The optimal classification tree aims to find the optimal solution to the following problem:

$$\min_{\mathbf{a}, \mathbf{b}} \sum_{i=1}^n \ell_{0-1}(\hat{y}_i, y_i) + \alpha \sum_{t \in \mathcal{T}_B} \mathbf{1}_{\mathbb{N}}(a_t), \quad (5a)$$

$$\text{s.t. } \hat{y}_i = f_{tree}(\mathbf{a}, \mathbf{b}, \mathbf{x}_i) \quad (5b)$$

$$n_t \geq n_{min} \times \mathbf{1}_{\mathbb{N}}(n_t), t \in \mathcal{T}_L \quad (5c)$$

where $\hat{y}_i = f_{tree}(\mathbf{a}, \mathbf{b}, \mathbf{x}_i)$ is the predicted class of sample \mathbf{x}_i through the univariate binary tree (\mathbf{a}, \mathbf{b}) ; $f_{tree}(\mathbf{a}, \mathbf{b}, \mathbf{x}_i) = c_t$ for t with $z_{i,t} = 1$; ℓ_{0-1} is a 0-1 misclassification loss, where $\ell_{0-1}(\hat{y}_i, y_i) = 1$ if $\hat{y}_i \neq y_i$, and 0 otherwise; $\mathbf{1}_{\mathbb{N}}(\cdot)$ is the indicator function on the set of natural numbers; $\sum_{t \in \mathcal{T}_B} \mathbf{1}_{\mathbb{N}}(a_t)$ is the complexity of the tree representing the number of splits included in the tree; α is the complexity penalty parameter; $n_t = \sum_{i=1}^n z_{i,t}$ is the number of samples assigned to leaf node t , and constraint 5c ensures n_t is larger than the minimum sample size n_{min} when $n_t \neq 0$. From the perspective of leaf nodes, the misclassification loss in the cost 5a can also be represented as: $\sum_{i=1}^n \ell_{0-1}(\hat{y}_i, y_i) = n - \sum_{t \in \mathcal{T}_L} \max_{k \in \mathcal{K}} \hat{z}_t^k$.

3 Differential Evolution for Optimal Classification Tree (DEOCT)

3.1 Decoding Tree Candidates from Individuals Discretely

In differential evolution, the individual \mathbf{s}_r is a real-valued vector. However, the univariate binary tree consists of a set of nodes with an integer scalar a_t , a real-valued scalar b_t . Therefore, we need to decode the univariate binary trees from DE individuals. Here, the individual of a univariate binary tree with the depth of D is consist of $\mathbf{s}_r = [\hat{a}_1, \dots, \hat{a}_t, \dots, \hat{a}_{\lfloor T/2 \rfloor}, \hat{b}_1, \dots, \hat{b}_t, \dots, \hat{b}_{\lfloor T/2 \rfloor}]$, where $\hat{a}_t \in [0, P + 1)$, $\hat{b}_t \in [0, 1)$, $t \in \mathcal{T}_B$.

Sequentially, we can decode the selected feature a_t in a tree from \hat{a}_t in a DE individual:

$$a_t = \lfloor \hat{a}_t \rfloor, \quad \hat{a}_t \in [0, P + 1), \quad t \in \mathcal{T}_B \quad (6)$$

As for the split threshold b_t , it is obviously that we can directly utilize $b_t = \hat{b}_t$ to decode. However, this direct method will introduce duplicated splits between two adjacent samples, which won't influence the training loss. Hence, instead of directly decoding the values of b_t , we propose a discrete decoding approach that utilize \hat{b}_t to represent the index of b_t in a sorted threshold set.

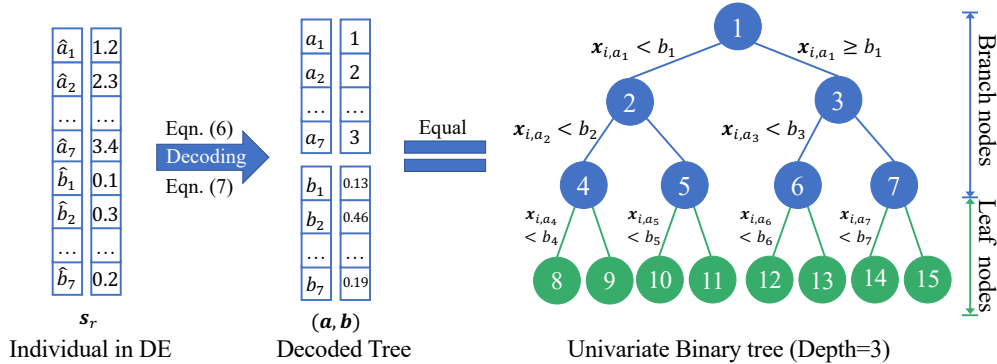


Figure 1: Example of a binary tree with depth=3 and the decoding procedure from a DE individual

Specifically, we denote $\hat{x}_{i,p}$ as the unique elements in the p th feature of the original dataset, subject to the constraints $\hat{x}_{i,p} < \hat{x}_{i+1,p}, i = 1, \dots, n_p$. Here, n_p is the number of unique elements in the p th feature. Then, the threshold set for p th feature is generated by splitting at the mean values of adjacent $\hat{x}_{i,p}$, which is $\mathcal{B}_p := (\beta_{p,i})_{i=1}^{n_p+1} = (0, \frac{\hat{x}_{1,p} + \hat{x}_{2,p}}{2}, \dots, \frac{\hat{x}_{n_{p-1},p} + \hat{x}_{n_p,p}}{2}, 1)$. Finally, the split threshold b_t for node t with the split feature a_t is decoded from \hat{b}_t utilizing the following equation:

$$b_t = \beta_{a_t, i}, i = \lfloor \hat{b}_t \times (n_p + 1) \rfloor + 1, t \in \mathcal{T}_B, \quad (7)$$

where a_t is the selected feature to split, i is the index of split threshold b_t in the threshold set \mathcal{B}_p . Note that these threshold sets only need to generate once at the beginning of the algorithm, ensuring minimal additional costs. Figure 1 shows an example of a univariate binary tree (a, b) with depth $D = 3$ decoded from an individual \mathbf{s}_r .

3.2 Parallel Fitness Evaluation of Tree Candidates Using GPU

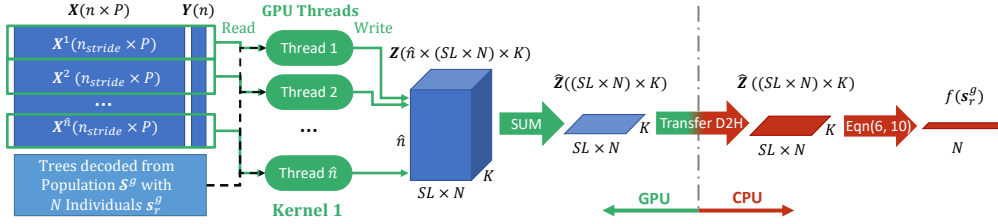


Figure 2: SIMD parallelization model for OCT fitness evaluation in GPU (Line 6-20 in Algorithm 1)

Differential Evolution relies on individual fitness values $f(\mathbf{s}_r)$ to select the best candidate over generations. A key challenge in applying DE to the OCT problem is designing a suitable fitness function. Since DE does not support constraints other than range constraints, we transform constraints (5c) in the OCT problem (5) into soft constraints within the objective function as $f(\mathbf{s}_r^g) = n - \sum_{t \in \mathcal{T}_L} \max_{k \in \mathcal{K}} \hat{c}_t^k + \alpha \sum_{t \in \mathcal{T}_B} \mathbf{1}(a_t) + \sum_{t \in \mathcal{T}_L} V_t$, where $V_t = 1$ if $n_t < n_{min} \times \mathbf{1}_{\mathbb{N}}(n_t)$, otherwise, 0.

The OCT fitness function’s computational cost significantly impacts the overall training time, as DE requires fitness evaluation for each individual. Most heuristic methods like CART employ a sorted and cached approach to reduce costs. However, DE relies on random individual movements and cannot utilize this method for OCT fitness calculation. Fortunately, examining the fitness function $f(\mathbf{s}_r^g)$, we notice that operations for each sample \mathbf{x}_i are identical, enabling GPU parallelization using SIMD (single instruction, multiple data). Algorithm 1 and Figure 2 detail the procedure for computing fitness values for a population \mathcal{S}^g . The algorithm starts by decoding trees from individuals, transferring necessary data to GPU’s global memory, and processing the dataset in parallel. Then, the class count matrix \hat{Z} , representing the number of assigned samples that belong to each class on the leaf nodes, is aggregated and transferred back to the host. Finally, the fitness values for individuals are calculated in CPU.

The algorithm’s efficiency comes from leveraging the parallel architecture of GPUs. Notably, we process n_{stride} adjacent samples in one thread, and store the class flags’ sum value in Z . Here, Z is the matrix of the class flag $z_{i,t}^k$ representing if sample i of class k is assigned to the leaf node t . This operation reduces expensive random access for adjacent samples. The dimension of Z is also reduced for faster sum operations in Line 17. Furthermore, by calculating fitness for the entire population at once, we only need to read the adjacent samples once for all the individuals.

3.3 Optimal Classification Tree Induction via Differential Evolution

As mentioned in Section 3.2, we need to modify the classic differential evolution algorithm to treat the entire population as the fundamental unit for fitness evaluation in GPU. To achieve this, we first generate a new generation population by performing mutation and crossover operations based on the best individual from the previous generation, rather than the current best one as illustrated in Equation 1. We then employ the GPU-parallelized OCT fitness evaluation (Algorithm 1) to assess the fitness of the new individuals and select the better individual accordingly. This approach generates a non-descending sequence of fitness values, ultimately leading to a near-optimal solution. Furthermore, to expedite the initialization process, we offer warm-start options such as CART solutions in our algorithm. Besides, we set the mutation factor $M = rand(0, 1)$ to enlarge the exploration range. Comprehensive DEOCT is detailed in Appendix B, Algorithm 4.

Algorithm 1 GPU-parallelized OCT Fitness

- 1: **Input:** Training dataset (\mathbf{X}, \mathbf{Y}) with n samples and K classes, DE population \mathcal{S}^g with N individuals, number of branch nodes SB , number of leaf nodes SL , and minimum sample size n_{min} .
- 2: **Output:** Fitness value set $\{f(s_r) \mid s_r^g \in \mathcal{S}^g\}$.
- 3: **CPU:** Decode trees $(\mathbf{a}, \mathbf{b})_r^g$ from $s_r^g \in \mathcal{S}^g$ by Equation (6) and (7).
- 4: **H2D:** Transfer (\mathbf{X}, \mathbf{Y}) (if not exist on the device) and all the decoded trees to GPU global memory.
- 5: **GPU:** Initialize the number of samples per thread as n_{stride} ; number of required threads as $\hat{n} \leftarrow \lceil n/n_{stride} \rceil$; class flag matrix $\mathbf{Z} \leftarrow \mathbf{0}^{\hat{n} \times (SL \times N) \times K}$.
- 6: **begin GPU (Kernel 1)** on GPU threads executed parallelly and asynchronously):
- 7: Read dataset $(\mathbf{X}^j, \mathbf{Y}^j)$ of thread j with n_{stride} adjacent samples from GPU global memory.
- 8: **for** r th tree $(\mathbf{a}, \mathbf{b})_r^g$ **in** all the decoded trees **do**
- 9: **for** $(x_i^j, y_i^j) \in (\mathbf{X}^j, \mathbf{Y}^j)$ **do**
- 10: $t \leftarrow 1$.
- 11: **while** $t \leq SB$ **do**
- 12: $t = x_{i,a_t}^j < b_t ? t \times 2 : t \times 2 + 1$.
- 13: **end while**
- 14: $\mathbf{Z}[j, (r-1) \times SL + (t-SB), y_i^j] += 1$.
- 15: **end for**
- 16: **end for**
- 17: $\hat{\mathbf{Z}} = \text{sum}(\mathbf{Z}, \text{dims}=1)$.
- 18: **end GPU.**
- 19: **D2H:** Transfer the class count matrix $\hat{\mathbf{Z}}$ to host
- 20: **CPU:** Calculate the OCT cost of each individual $f(s_r)$.

Algorithm 2 Moving-Horizon DEOCT

- 1: **Input:** Training set (\mathbf{X}, \mathbf{Y}) , tree depth D , minimum leaf sample number n_{min} , complexity parameter α , moving-horizon depth D_{MH} . DE: warm-start trees $\{(\mathbf{a}, \mathbf{b})\}^0$, other parameters in DEOCT.
- 2: **Output:** The best tree $(\mathbf{a}, \mathbf{b})_{best}$.
- 3: **for** $t \in \mathcal{T}_B$ **do**
- 4: Induce the subset of training set for t th node $(\mathbf{X}_t, \mathbf{Y}_t)$ according to the path to node t .
- 5: **if** $|\mathbf{X}_t| > n_{min}$ and $\text{unique}(\mathbf{Y}_t) > 1$ **then**
- 6: Determine the effective moving-horizon depth for t node, $D_{t,MH} = \min\{D_{MH}, D - D_t\}$.
- 7: **if** $D_{t,MH} \neq 1$ **then**
- 8: Retrieve the warm-start subtrees $\{(\mathbf{a}, \mathbf{b})\}_t^0$ from the warm-start trees $\{(\mathbf{a}, \mathbf{b})\}^0$ with the same shape and location as the corresponding moving-horizon subtree.
- 9: Calculate the CART solution for the MH subtree and add to the warm-start subtrees.
- 10: Optimize MH subtree with depth $D_{t,MH}$ using DEOCT Alg.4 and warm-start subtrees.
- 11: **else**
- 12: Optimize the MH subtree with depth 1 using CART with the misclassification loss.
- 13: **end if**
- 14: Save the first node of the optimized MH subtree in the t th node of $(\mathbf{a}, \mathbf{b})_{best}$.
- 15: **else**
- 16: Save an artificial node with $\{a_t = 0, b_t = 0\}$ in the t th node of $(\mathbf{a}, \mathbf{b})_{best}$.
- 17: **end if**
- 18: **end for**

4 Moving-Horizon DEOCT

In a binary tree, the quantity of branch nodes grows exponentially with the tree depth D . DEOCT, which optimizes the entire tree simultaneously, leads to individual sizes that also expand exponentially at a rate of $O(2^{D+1} - 2)$. This causes substantial computational costs for deep trees (e.g., depth=8), leading to suboptimal performance. Our tests indicate that DEOCT, if warm-started with CART, slightly outperforms standalone CART at a tree depth of 8. However, without a CART warm-start, DEOCT underperforms compared to CART at the same depth.

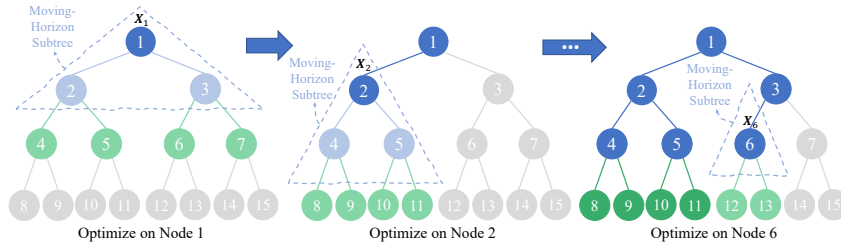


Figure 3: Training procedure of Moving-Horizon DEOCT (Depth=3, Moving-Horizon Depth=2)

To tackle the challenge of rapidly growing node numbers and individual sizes with increasing tree depth, we propose a Moving-Horizon (MH) strategy. Similar to greedy approaches, MH optimizes node by node, but it optimizes a multi-layer subtree rooted at each node (called moving-horizon subtree) and adopts its first node in the final tree. While several moving-horizon algorithms for decision trees have been suggested in previous literature (Murthy and Salzberg, 1995; Dong and Kothari, 2001; Esmeir and Markovitch, 2004; Roizman and Last, 2006; Last and Roizman, 2013), they typically optimize the moving-horizon subtrees by employing greedy methods, such as CART,

supplemented with additional post-processing. However, they generally achieve only marginal performance improvements over purely greedy methods. In contrast, our method, referred to as Moving-Horizon DEOCT (MH-DEOCT) in Algorithm 2, employs DEOCT to optimize the entire moving-horizon subtrees simultaneously. This approach provides a more comprehensive global view within a moving-horizon subtree, resulting in improved performance compared to both the purely greedy methods and the DEOCT methods.

Figure 3 illustrates the training procedure for a tree with depth=3 and moving-horizon depth=2. The effective moving-horizon depth of the t th node ($D_{t,MH}$) is dynamically determined based on node depth D_t , tree depth D , and moving-horizon depth D_{MH} using $D_{t,MH} = \min\{D_{MH}, D - D_t\}$. For example, when optimizing node 6 in Figure 3, the effective moving-horizon depth is 1, as the child nodes’ absolute depth in the subtree reaches the original tree’s maximum depth.

5 Numerical Results

In this section, we evaluate the proposed algorithms, DEOCT and MH-DEOCT, alongside the classical heuristic method, CART (Breiman et al., 1984) and the state-of-the-art heuristic method, local search OCT (LS-OCT) (Bertsimas and Dunn, 2017), as well as state-of-the-art global optimal methods, namely RS-OCT (Hua et al., 2022) and Quant-BnB (Mazumder et al., 2022) on continuous datasets and GOSDT-Guess (McTavish et al., 2022) on binary datasets. Our analysis addresses the following questions: **Q1.**How do our algorithms compare to heuristic and global optimal methods in terms of training accuracy? **Q2.**Can conclusions drawn from training accuracy be extended to testing accuracy? **Q3.**How does the training time of our algorithms compare to other methods with respect to dataset size and tree depth? **Q4.**What is the impact of moving-horizon depth on performance? **Q5.**How does the warm-start influence performance, and can our methods outperform heuristic methods without any warm-starts? **Q6.**How do our algorithms behave on binary datasets comparing to global methods designed for binary datasets?

Experiments We utilize 68 UCI classification datasets (Dua and Graff, 2017) with continuous and categorical variables for binary and multi-class tasks, and a sample size range of 47 to 11,000,000. Datasets are split into 75% training and 25% testing sets, repeated 10 times with varied random seeds. All the following results are compiled from these repetitions. The computations are performed on a server with a 24-core AMD 2.65GHz CPU, 498 GB RAM, and an NVIDIA A100 (40 GB) GPU. For tree hyperparameters, Quant-BnB disregards minimum sample size (n_{min}) and complexity parameters (α). To make the comparison fair, unless stated otherwise, we set n_{min} to 1 and α to 0 for all algorithms. Additionally, we also provides the results of α tuning with validation sets in Table 1 and Appendix C.

The proposed DEOCT and MH-DEOCT are implemented in Julia and run in parallel on a GPU using CUDA.jl (Besard et al., 2018; Cook, 2012). The implementations will be open-sourced after acceptance. Notably, DEOCT utilize CART solutions as warm-starts; MH-DEOCT utilize CART and DEOCT solutions as warm-starts in solving the MH subtrees as described in Algorithm 2. The recorded training time of our algorithms include the calculation time to obtain the warm-starts. As for the parameter for DE, we follow the general guidelines in Ahmad et al. (2022): crossover probability (CR) is set to 0.1, maximum generations (G) to 600, and population size (N) to 100 in Normal mode (G increased to 4,000 and N to 200 in Long mode; unless otherwise stated, all DE-related experiments run in Normal mode). We highlight that this parameter setting is used for all datasets. Comparison methods include CART using DecisionTree.jl (Sadeghi et al., 2022) running in the serial mode; LS-OCT, self-implemented in Julia in serial mode as no open-source code is provided; Quant-BnB from the official repository, executed in Julia in serial with a four-hour limit; and RS-OCT from the official repository in Julia with CPLEX, running on 40 CPU threads in parallel with a four-hour limit.

5.1 Comparison with heuristic and global optimal methods

Table 1 compares accuracy and training times for 65 datasets with up to 1 million samples. In terms of training accuracy (**Q1**), MH-DEOCT outperforms heuristic methods CART and LS-OCT by average relative differences of 2.99% and 1.05% across all tree depths and datasets, respectively, and this performance gap extends to 3.44% and 1.48% in Long mode. The global method Quant-BnB reaches global optima on 65 and 55 datasets at depths 2 and 3, respectively, while MH-DEOCT trails by 0.27%

Table 1: Comparison with heuristic and global methods on 65 datasets within 1 million samples

Performance	Depth	Heuristic Method		Global Method		Our Method				
		CART ⁴	LS-OCT ⁴	Quant-BnB ⁴	RS-OCT ⁴	DEOCT ⁴	MH-DEOCT ⁴	DEOCT ⁴ (Long)	MH-DEOCT ⁴ (Long)	MH-DEOCT ⁴ (α tuned)
Train (%)	2	79.41	81.47	81.86 ¹	81.42 ³	81.56	81.64	81.66	81.75	81.25
	3	84.30	86.04	87.37 ²	-	86.43	86.82	87.03	87.23	86.26
	4	(84.05)	(85.78)	(87.43)	-	(86.19)	(86.54)	(86.75)	(86.93)	(85.92)
	8	87.62	88.87	-	-	89.33	90.24	90.26	90.80	89.19
Test (%)	2	76.91	78.19	78.20	78.23	78.20	78.21	78.15	78.27	78.85
	3	80.45	81.57	81.90	-	81.48	81.78	81.64	81.74	82.71
	4	(80.02)	(81.10)	(81.72)	-	(81.09)	(81.31)	(81.25)	(81.32)	(82.26)
	8	82.42	83.32	-	-	83.45	83.60	83.63	83.74	84.81
Time (s)	2	0.03	140.34	2.96	7,701.63	0.72	1.51	8.54	17.17	29.46
	3	0.05	231.98	2204.39	-	1.15	3.58	14.46	43.14	69.56
	4	0.06	366.77	(1059.91)	-	1.81	6.96	22.99	84.32	127.38
	8	0.12	869.29	-	-	14.71	68.77	178.33	731.07	973.11

¹ All datasets achieve global optimality at Depth 2 in Quant-BnB. ² 55/65 datasets reach global optimality at Depth 3 in Quant-BnB. (·) is the average accuracy or time of these 55 datasets. Besides, Quant-BnB failed to give a solution for 5/65 datasets. ³ 35/65 datasets attain global optimality at Depth 2 in RS-OCT. ⁴ α is set to 0 without α tuning.

and 1.09%. Remarkably, given more time, MH-DEOCT (Long) achieves closer accuracy to Quant-BnB with only 0.14% and 0.63% differences, respectively. Besides, Quant-BnB failed to give a solution for 5 out of 65 datasets. For trees deeper than 3, MH-DEOCT continues to outperform heuristic methods in a reasonable time, while Quant-BnB cannot solve these deeper trees. Meanwhile, RS-OCT reaches global optima on 35 datasets at depth 2. It lags behind MH-DEOCT in terms of average accuracy on all datasets and fails to perform at depths larger than 2.

Regarding testing accuracy (Q2), MH-DEOCT exceeds CART and LS-OCT by average relative difference of 1.65% and 0.35% across all depths (1.71% and 0.40% in Long mode), respectively. MH-DEOCT marginally outperforms Quant-BnB at depth 2 and slightly underperforms at depth 3. Figure 4 displays the number of datasets with relative differences between MH-DEOCT and CART. As depicted, MH-DEOCT outshines CART on most datasets for all depths. Detailed results on all datasets for Table 1 are provided in Appendix E.

Moreover, we present outcomes of hyperparameter α tuning using validation sets in Table 1 and Appendix C. The parameter α plays a crucial role in balancing the tree node number (complexity) and the training accuracy. After tuning, MH-DEOCT improves its testing accuracy by an average of 1.37% relatively, despite a 1.29% drop in training accuracy. Tuned MH-DEOCT also outperforms tuned CART and IAI-OCT by 1.92% and 0.80%, respectively. Here, IAI-OCT is a commercial OCT method with hyperparameter α tuning (Bertsimas and Dunn, 2017; Interpretable AI, 2023).

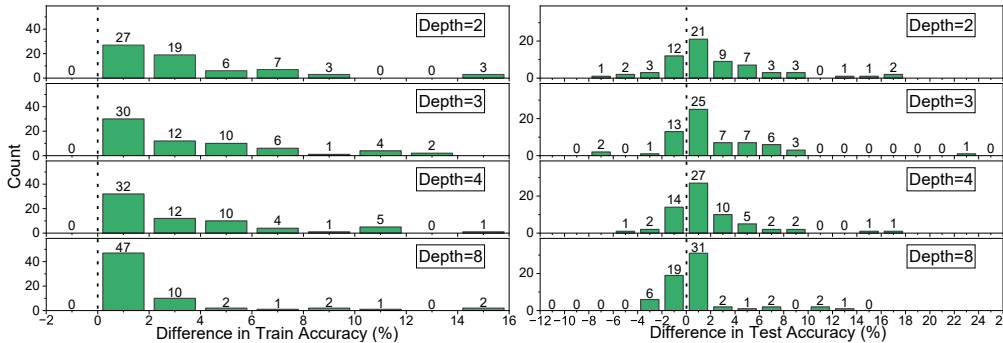


Figure 4: Comparison of MH-DEOCT with CART in relative difference ($\frac{\text{Acc}_{\text{MH-DEOCT}} - \text{Acc}_{\text{CART}}}{\text{Acc}_{\text{CART}}} \times 100\%$) on 65 datasets within 1 million samples

Concerning training time (Q3), CART performs the fastest, albeit at the expense of performance quality, while MH-DEOCT provides a balance between time efficiency and performance. Figure 5 illustrates the training time in relation to dataset sizes. Generally, CART and MH-DEOCT exhibit linear

growth as sample numbers increase. LS-OCT shows an accelerated growth pattern. Quant-BnB, on the other hand, demonstrates a seemingly linear trend at depth 2, but becomes less stable at depth 3.

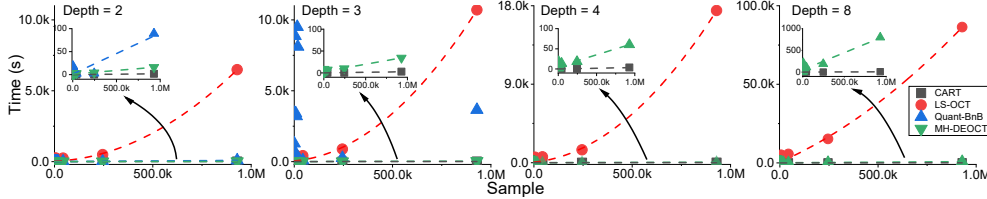


Figure 5: Comparison of the training times regarding to the dataset sizes

We also present comparisons with a global method requiring binary datasets, GOSDT-Guess (McTavish et al., 2022) (Q6). As outlined in Appendix D. Our algorithm, MH-DEOCT, performs commendably, with only a marginal decrease of 0.10% and 0.12% in average train and test accuracy when compared to the global methods on binarized datasets. Additionally, we observe that the global methods encounter challenges in obtaining optimal solutions within a reasonable time for large datasets and deeper trees. In contrast, our algorithm adeptly manages these complexities, efficiently solving problems involving larger datasets (up to 11,000,000 samples) and deeper trees, marking a groundbreaking achievement in the field. Comparing the outcomes of continuous and binarized datasets, our results highlight the superiority of continuous datasets in terms of average train and test accuracy when contrasted with their binarized counterparts. This disparity suggests a potential information loss during the binarization process, aligning with prior observations in (Mazumder et al., 2022). Consequently, MH-DEOCT consistently attains higher average accuracy on continuous datasets in comparison to the global methods applied to their corresponding binarized equivalents.

5.2 Ablation experiments

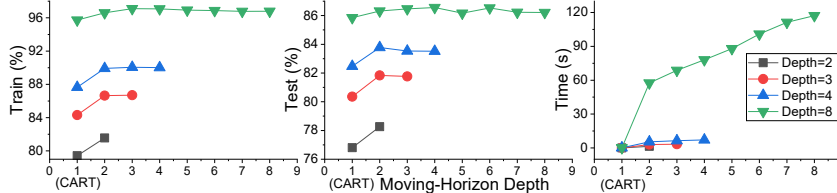


Figure 6: Influence of Moving-Horizon Depth on accuracy and training times

Figure 6 illustrates the effect of moving-horizon (MH) depth on accuracy and training times in the normal mode (Q4). Training accuracy generally improves for MH depths up to 3 and stabilizes or slightly decreases beyond. Training time increases with MH depth, thus we choose MH depth 2 for tree depth 2 and MH depth 3 for deeper trees as the optimal MH depth. This observation may be due to the fact that, under the normal mode, DEOCT can only yield reasonable solutions for depths ≤ 3 . Larger generation and population sizes could yield a larger optimal MH depth. Moreover, by comparing the training and testing accuracy plots, we observe that testing accuracy increases proportionally to training accuracy at depths 2, 3, and 4, and to a lesser extent at depth 8. This result suggests that our algorithms do not suffer extensively from overfitting in deeper trees.

Table 2 displays the impact of warm-starts (WS) on accuracy (Q5). Several key observations can be drawn: first, from rows 1, 3, and 7, with CART warm-starts, both DEOCT and MH-DEOCT exhibit improved training accuracy compared to CART. Second, from rows 1, 2, and 6, even without any warm-start, MH-DEOCT consistently outperforms CART across all depths, while DEOCT falls behind at depth 8. Third, we extend the iterations of DEOCT to 1800 to match the training time of MH-DEOCT without DEOCT warm-starts. Rows 4, 5, 6, and 7 demonstrates that MH-DEOCT without DEOCT warm-starts surpasses DEOCT while maintaining similar running times. Finally, from rows 8, 9, 10, and 11, MH-DEOCT with DEOCT warm-starts can achieves substantially better training accuracy compared to DEOCT, with the significance increasing as tree depth grows.

Table 2: Ablation study on DEOCT and MH-DEOCT with/without warm-starts (WS)

No.	Methods & Factors	D=2			D=4			D=8				
		Train (%)	Test (%)	Time (s)	Train (%)	Test (%)	Time (s)	Train (%)	Test (%)	Time (s)		
1	CART	79.41	76.91	0.03	87.62	82.42	0.06	95.67	85.78	0.12		
	DEOCT											
	CART WS in DE		D=2		D=4		D=8					
2	-	81.50	78.31	0.70	88.45	83.27	1.63	91.22	84.51	14.91		
3	✓	81.56	78.20	0.72	89.33	83.45	1.81	95.82	86.12	14.71		
4	- (extended)	-	-	-	89.26	83.60	4.87	92.33	85.25	44.17		
5	✓ (extended)	-	-	-	89.49	83.73	5.08	96.02	86.36	39.74		
	MH-DEOCT		D=2, P=2		D=4, P=3		D=8, P=3					
	CART		Train (%)	Test (%)	Time (s)	Train (%)	Test (%)	Time (s)	Train (%)	Test (%)	Time (s)	
	WS in DE	DE WS	CART WS									
6	-	-	-	81.51	78.14	0.71	89.85	83.57	4.69	96.72	86.36	33.75
7	-	-	✓	81.40	78.23	0.76	89.93	83.57	4.93	96.84	86.42	32.68
8	-	✓	-	81.61	78.18	1.40	90.01	83.58	6.35	96.71	86.42	57.97
9	-	✓	✓	81.63	78.29	1.50	90.03	83.71	6.39	96.93	86.51	55.91
10	✓	✓	-	81.57	78.32	1.45	90.09	83.74	6.48	97.04	86.30	57.48
11	✓	✓	✓	81.64	78.21	1.51	90.24	83.60	6.96	97.30	86.31	68.77

5.3 Performance on large-scale Datasets (millions of samples)

Table 1 presents the performance of MH-DEOCT on three large-scale datasets with millions of samples while all the global optimal methods and LS-OCT failed to give a result with reasonable running time. In general, MH-DEOCT demonstrates improved performance over CART in terms of both training and testing accuracy, with a trade-off in training time.

Table 3: Performance of MH-DEOCT on large-scale datasets (millions of samples)

Dataset	Sample	Feature	Class	Performance	D=2			D=4			D=8	
					CART	MH-DEOCT	CART	MH-DEOCT	CART	MH-DEOCT		
Bitcoin Heist	2,916,697	8	29	Train (%)	98.58	98.58	98.58	98.58	98.61	98.62		
				Test (%)	98.58	98.58	98.58	98.58	98.61	98.62		
				Time (s)	3.64	77.22	5.91	259.98	9.59	1,633.93		
SUSY	5,000,000	18	2	Train (%)	74.46	75.85	76.59	77.79	78.38	79.32		
				Test (%)	74.47	75.84	76.59	77.78	78.34	79.17		
				Time (s)	18.93	164.03	37.32	399.88	75.90	5,100.47		
HIGGS	11,000,000	28	2	Train (%)	63.08	63.49	65.58	66.71	69.47	70.50		
				Test (%)	63.06	63.48	65.55	66.68	69.40	70.38		
				Time (s)	44.52	333.01	82.28	1,049.87	171.65	15,885.24		

5.4 Speedup Analysis: Comparing the GPU and CPU Versions of MH-DEOCT

To facilitate a comprehensive performance evaluation, we conducted an exhaustive assessment of the MH-DEOCT algorithm on both GPU and CPU platforms across 65 diverse datasets, ranging in size from up to 1 million samples. Table 4 summarized results of these evaluations, presenting a quantified speedup factor of 205 on average across all tree depths and datasets. The performance disparity becomes particularly evident with different dataset sizes. For instance, datasets with sample sizes falling within the range of 0-10,000 exhibit a GPU speedup of 46 times compared to the CPU. As the dataset size escalates to the range of 10,000-250,000 samples, the speedup surges to an impressive 805 times. Most strikingly, when confronted with the extensive Htsensor dataset containing 928,991 samples, CPU couldn't produce results within a two-day limit for tree depths of 4 and 8, while the GPU excels by completing the calculations within 60 and 800 seconds, respectively. Additionally, a visual representation of the GPU's performance advantage over dataset size is provided in Figure 7.

Table 4: Speedup of MH-DEOCT on GPU and CPU

Dataset Size	Depth=2	Depth=3	Depth=4	Depth=8	Average on Size
0-10,000	79	56	38	9	46
10,000-250,000	1359	1014	727	121	805
928,991	4761	3671	>2866	>215	-
Average on Depth	351	261	176	33	205

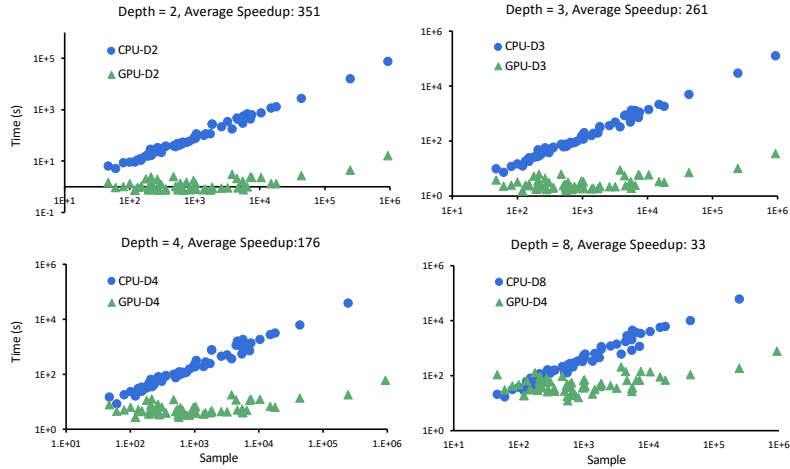


Figure 7: Speedup of MH-DEOCT on GPU and CPU over dataset size in log scale

6 Conclusion

In conclusion, we have proposed MH-DEOCT, a GPU-accelerated moving-horizon differential evolution algorithm for classification trees with continuous features. This approach addresses the limitations of existing methods by incorporating a discrete tree decoding method, a GPU-accelerated implementation, and a moving-horizon strategy for iteratively training shallow subtrees at each node. Our comprehensive evaluation on 68 UCI datasets demonstrates that MH-DEOCT outperforms heuristic methods and achieves a comparable accuracy level to global methods with significantly reduced running time. This performance can be extended to deeper trees and large-scale datasets. This work contributes to the ongoing effort to enhance decision tree training methodologies, offering a promising solution that combines the strengths of both heuristic and global approaches.

Limitation: while our algorithm lacks a theoretical guarantee to reach global optima, its practical applications have demonstrated near-optimal performance, as evidenced by our extensive experiments.

References

- James N. Morgan and John A. Sonquist. Problems in the Analysis of Survey Data, and a Proposal. *Journal of the American Statistical Association*, 58(302), 1963.
- Hyafil Laurent and Ronald L. Rivest. Constructing optimal binary decision trees is NP-complete. *Information processing letters*, 5(1), 1976.
- J. Ross Quinlan. Induction of decision trees. *Machine learning*, 1, 1986.
- J. Ross Quinlan. C 4.5: Programs for machine learning. *The Morgan Kaufmann Series in Machine Learning*, 1993.
- Leo Breiman, Jerome Friedman, Charles J. Stone, and R. A. Olshen. *Classification and Regression Trees*. 1984.
- Dimitris Bertsimas and Jack Dunn. Optimal classification trees. *Machine Learning*, 106(7):1039–1082, 2017.
- Sicco Verwer and Yingqian Zhang. Learning decision trees with flexible constraints and objectives using integer optimization. In *Integration of AI and OR Techniques in Constraint Programming: 14th International Conference, CPAIOR 2017, Padua, Italy, June 5-8, 2017, Proceedings 14*, 2017.
- Sicco Verwer and Yingqian Zhang. Learning optimal classification trees using a binary linear program formulation. In *Proceedings of the AAAI Conference on Artificial Intelligence*, volume 33, 2019.
- Oktay Günlük, Jayant Kalagnanam, Minhan Li, Matt Menickelly, and Katya Scheinberg. Optimal decision trees for categorical data via integer programming. *Journal of Global Optimization*, 81(1), 2021.
- Sina Aghaei, Andrés Gómez, and Phebe Vayanos. Strong Optimal Classification Trees, 2022. URL <http://arxiv.org/abs/2103.15965>.
- Kaixun Hua, Jiayang Ren, and Yankai Cao. A Scalable Deterministic Global Optimization Algorithm for Training Optimal Decision Tree. In *Thirty-Sixth Conference on Neural Information Processing Systems*, 2022.
- Rahul Mazumder, Xiang Meng, and Haoyue Wang. Quant-BnB: A Scalable Branch-and-Bound Method for Optimal Decision Trees with Continuous Features. In *Proceedings of the 39th International Conference on Machine Learning*, 2022.
- Xiyang Hu, Cynthia Rudin, and Margo Seltzer. Optimal sparse decision trees. *Advances in Neural Information Processing Systems*, 32, 2019.
- Gaël Aglin, Siegfried Nijssen, and Pierre Schaus. Learning optimal decision trees using caching branch-and-bound search. In *Proceedings of the AAAI conference on artificial intelligence*, volume 34, pages 3146–3153, 2020.
- Jimmy Lin, Chudi Zhong, Diane Hu, Cynthia Rudin, and Margo Seltzer. Generalized and scalable optimal sparse decision trees. In *International Conference on Machine Learning*, pages 6150–6160. PMLR, 2020.
- Emir Demirović, Anna Lukina, Emmanuel Hebrard, Jeffrey Chan, James Bailey, Christopher Leckie, Kotagiri Ramamohanarao, and Peter J. Stuckey. Murtree: Optimal decision trees via dynamic programming and search. *The Journal of Machine Learning Research*, 23(1), 2022.
- Hayden McTavish, Chudi Zhong, Reto Achermann, Ilias Karimalis, Jacques Chen, Cynthia Rudin, and Margo Seltzer. Fast Sparse Decision Tree Optimization via Reference Ensembles. *Proceedings of the AAAI Conference on Artificial Intelligence*, 36(9), 2022.
- Chan-Sheng Kuo, Tzung-Pei Hong, and Chuen-Lung Chen. Applying genetic programming technique in classification trees. *Soft Computing*, 11(12), 2007.
- Yun-Ju Cho, Hye-Seon Lee, and Chi-Hyuck Jun. Optimization of Decision Tree for Classification Using a Particle Swarm. *Industrial Engineering and Management Systems*, 10(4), 2011.

- Evgeny Dolotov and Nikolai Zolotykh. Evolutionary algorithms for constructing an ensemble of decision trees. In *Analysis of Images, Social Networks and Texts: 8th International Conference*, pages 9–15. Springer, 2020.
- Elif Ersoy, Erinç Albey, and Enis Kayış. A CART-based Genetic Algorithm for Constructing Higher Accuracy Decision Trees:. In *Proceedings of the 9th International Conference on Data Science, Technology and Applications*, Lieusaint - Paris, France, 2020.
- Rafael Rivera-Lopez, Juana Canul-Reich, Efrén Mezura-Montes, and Marco Antonio Cruz-Chávez. Induction of decision trees as classification models through metaheuristics. *Swarm and Evolutionary Computation*, 69, 2022.
- Rainer Storn and Kenneth Price. Differential evolution – a simple and efficient heuristic for global optimization over continuous spaces. *Journal of Global Optimization*, 11(4):341–359, 1997.
- Sreerama Murthy and Steven Salzberg. Lookahead and pathology in decision tree induction. In *Proceedings of the 14th International Joint Conference on Artificial Intelligence-Volume 2*, 1995.
- Ming Dong and Ravi Kothari. Look-ahead based fuzzy decision tree induction. *IEEE Transactions on fuzzy systems*, 9(3), 2001.
- Saher Esmeir and Shaul Markovitch. Lookahead-based algorithms for anytime induction of decision trees. In *Twenty-First International Conference on Machine Learning - ICML '04*, Banff, Alberta, Canada, 2004.
- Michael Roizman and Mark Last. Look-Ahead Mechanism Integration in Decision Tree Induction Models. In Mark Last, Piotr S. Szczepaniak, Zeev Volkovich, and Abraham Kandel, editors, *Advances in Web Intelligence and Data Mining*, Studies in Computational Intelligence. Berlin, Heidelberg, 2006.
- Mark Last and Michael Roizman. Avoiding the Look-Ahead Pathology of Decision Tree Learning. *International Journal of Intelligent Systems*, 28(10), 2013.
- Dheeru Dua and Casey Graff. UCI machine learning repository, 2017.
- Tim Besard, Christophe Foket, and Bjorn De Sutter. Effective extensible programming: Unleashing Julia on GPUs. *IEEE Transactions on Parallel and Distributed Systems*, 2018. ISSN 1045-9219.
- Shane Cook. *CUDA Programming: A Developer's Guide to Parallel Computing with GPUs*. 2012.
- Mohamad Faiz Ahmad, Nor Ashidi Mat Isa, Wei Hong Lim, and Koon Meng Ang. Differential evolution: A recent review based on state-of-the-art works. *Alexandria Engineering Journal*, 61(5):3831–3872, May 2022.
- Ben Sadeghi, Poom Chiarawongse, Kevin Squire, Daniel C. Jones, Andreas Noack, Cédric St-Jean, Rik Huijzer, Roland Schätzle, Ian Butterworth, Yu-Fong Peng, and Anthony Blaom. DecisionTree.jl - A Julia implementation of the CART Decision Tree and Random Forest algorithms, November 2022.
- LLC Interpretable AI. Interpretable ai documentation, 2023. URL <https://www.interpretable.ai>.

Appendix

A Overview of related works

Over the years, **heuristic** techniques have dominated the domain of decision tree learning due to their inherent efficacy and scalability. Algorithms such as CART, proposed by Breiman et al. in 1984 [1], and C4.5, by Quinlan in 1993 [2], are prime examples. These methods initialize with a single node and iteratively expand the tree, often employing post-processing measures to prune the decision trees and minimize overfitting. These classic heuristic methods are deterministic, and once the procedure is completed, they are unable to generate a better solution. To overcome this limitation, a local search method introduced by Bertsimas and Dunn (2017) [3] aims to re-optimize each node by finding best splits at that specific node, while maintaining this node’s original subtrees. It also introduces stochasticity by applying this procedure to multiple initial trees. Demonstrating superior performance compared to CART, this local search method is utilized as a baseline in our research. However, despite their widespread application, these heuristic techniques suffer from a significant drawback: they tend to concentrate solely on individual tree splits, overlooking potential consequences of subsequent splits [3]. As a result, these algorithms risk settling for sub-optimal solutions, which could impair the predictive effectiveness of the decision tree.

In response to the constraints posed by heuristic approaches when dealing with greedy problems, there has been a growing surge in the popularity of the optimal decision tree method. This approach aims to comprehensively explore the entire tree concurrently. Three primary categories of methods have gained prominence: mixed integer programming, dynamic programming, and metaheuristic techniques.

Mixed-integer programming (MIP) methods have recently emerged as powerful tools for constructing optimal decision trees. The fundamental characteristic of these methods is their ability to encode the entire tree by pre-determining the tree depth, establishing variables for each node predicate, and instituting constraints to maintain the tree’s structural integrity. On the frontier of applying MIP to decision tree construction, Bertsimas and Shioda’s work [4] in 2007 stood out, particularly suited for smaller datasets. Their pioneering work paved the way for enhanced MIP formulations by Bertsimas and Dunn (2017) [3] and Verwer and Zhang (2017) [5]. Verwer and Zhang took a significant leap forward in 2019 with the introduction of BinOPT, which optimized the MIP approach by using binary data [6]. This innovation reduced the number of necessary variables and constraints.

While MIP is flexible and capable of integrating various constraints and losses, its inherent complexity often makes it difficult to solve. Among the state-of-the-art solutions addressing the complexity problems, RS-OCT by Hua et al. (2022) [7] has transformed the MIP formulation into a two-stage format with tree structure variables designated as the first-stage variables. RS-OCT argues that branching solely on these first-stage variables is sufficient to ensure convergence. Additionally, they introduced a closed-form lower bound along with two lower bounds based on general-purpose solvers. Meanwhile, Quant-BnB by Mazumder et al. (2022) [8] employs a quantile-based branching and lower bounding strategy, complemented by an efficient single-layer exhaustive search solver. Although these methods offer a theoretical guarantee of reaching the global optimum, they still incur significant computational expenses and are typically limited to shallow decision trees with depths of 2 or 3.

Dynamic programming (DP), a method that breaks problems down into smaller, simpler subproblems, offers a robust solution to constructing optimal decision trees. When applied to decision trees, DP operates on two crucial observations. First, the left and right subtrees stemming from any given node can be optimized separately. This characteristic allows complex tree problems to be fragmented into more manageable subproblems. The second observation highlights overlaps within the tree. This overlap means certain subtrees can be reused during the solution process, making exhaustive searches more efficient through caching techniques. This methodological framework, termed DL8, was initially put forth by Nijssen and Fromont (2007, 2010) [9, 10]. This was further built upon by Aglin et al. (2020) [11] with DL8.5, which combined previous methodologies to optimize misclassification scores while considering tree depth. Building upon the DL8 framework, DL8.5 brought forth innovative bounding techniques. Specifically, the upper bounding method in DL8.5 recalibrated the upper bound of a child node using its parent’s upper bound combined with the optimal value of its sibling. In tandem, DL8.5 also introduced a new lower bound, derived directly from the associated upper bound. Pursuing this trajectory, Demirović et al. (2022) [12] presented MurTree, which aimed to refine misclassification scores while considering constraints on tree depth

and the number of nodes. MurTree came with a slew of enhancements, including a frequency-based solver for depth-two trees, incremental lower bounds, and a caching system tailored for optimal solutions and lower bounds using sub-datasets. These cumulative improvements endowed MurTree with superior scalability compared to its predecessors.

In addition to setting strict limitations on tree depth and nodes, Hu et al. (2019) [13] unveiled an algorithm that harmonizes between misclassifications and tree complexity by incorporating a regularization term into the cost function. Their approach leans heavily on exhaustive search, caching, and establishing a lower bound for misclassifications that's determined by the cost of adding a fresh node to the decision tree. Building on this, Lin et al. (2020) [14] fine-tuned and expanded upon the method, achieving commendable results when the complexity coefficient is set notably high. Based on Lin's work, McTavish et al. (2022) [15] utilized a pre-structured ensemble model to give a more informed estimation regarding binarization techniques, tree dimensions, and lower bounds. Leveraging these insights, their refined algorithm demonstrated marked enhancements in speed and efficiency. However, it's worth noting that these dynamic programming strategies are best suited for binary datasets. Challenges crop up when tackling continuous datasets, such as potential information degradation during binarization, an augmented feature space post-binarization, and escalating computational demands correlating with feature quantity and tree depth.

Meta-Heuristic approaches aim to identify the optimal solution by analyzing the entire tree. While these methods lack a theoretical guarantee of achieving global optimality, numerous applications have demonstrated their proficiency in finding satisfactory solutions. The inception of Meta-Heuristic based decision tree algorithms dates back to the early 1990s [16], and since then, substantial research has been undertaken. Researchers have primarily focused on enhancing performance by addressing two pivotal issues: encoding the decision tree into an individual vector and preserving the tree structure during mutation operations. For the encoding aspect, the prevalent approach is the linear representation, which captures the split feature and thresholds of each tree node in a sequential manner within the individual vector. References [17, 18] detail the ordered sequence of split features in the individual vector while dynamically searching for the corresponding split values. Conversely, [19] focuses on cataloguing the sequence of split thresholds, and [20] encode both the split feature and thresholds concurrently. In terms of mutation operations, there's a trend shifting from mutations based on absolute positions within individual vectors to those determined by relative positions in a decision tree. This includes strategies like node swaps at identical relative positions [21], subtree swaps at the same relative positions [22], and branch swaps sharing the same root node [23].

The foundational metaheuristic approach DEOCT in **our algorithm** is inspired by Meta-Heuristic methods that employ a linear representation for both split features and thresholds. It also uses a direct mutation based on absolute positions, which is a considerably simplified version compared to previous studies. Nonetheless, we've addressed two significant limitations inherent to Meta-Heuristic methods. Firstly, in the context of deeper trees, the performance of Meta-Heuristic methods typically falls short compared to the CART approach when not initialized with a CART warm-start, as confirmed by [24] and corroborated by our ablation study presented in Table 2 of the original paper. Secondly, Meta-Heuristic methods generally exhibit longer run-times relative to greedy techniques because they necessitate evaluating a vast set of potential solutions [20]. To mitigate the first issue, we implemented a moving horizon strategy that focuses on solving a shallow subtree problem. This strategy not only help keep the tree structure but also leverages the strengths of metaheuristics in handling shallow trees. For the second challenge, we introduced a GPU-accelerated version of the decision tree cost evaluation algorithm, complemented by a population-based differential evolution method optimized for GPU parallelism.

A.1 References

- [1] Breiman, L., et al. "Classification and Regression Trees." (1984).
- [2] Quinlan, J. Ross. "C 4.5: Programs for machine learning." The Morgan Kaufmann Series in Machine Learning (1993).
- [3] Bertsimas, Dimitris, and Jack Dunn. "Optimal classification trees." *Machine Learning* 106 (2017): 1039-1082.
- [4] Bertsimas, Dimitris, and Romy Shioda. "Classification and regression via integer optimization." *Operations research* 55.2 (2007): 252-271.

- [5] Verwer, Sicco, and Yingqian Zhang. "Learning decision trees with flexible constraints and objectives using integer optimization." In Proceedings of CPAIOR (2017).
- [6] Verwer, Sicco, and Yingqian Zhang. "Learning optimal classification trees using a binary linear program formulation." In Proceedings of AAAI (2019).
- [7] Hua, Kaixun, Jiayang Ren, and Yankai Cao. "A Scalable Deterministic Global Optimization Algorithm for Training Optimal Decision Tree." In Proceedings of NeurIPS (2022).
- [8] Mazumder, Rahul, Xiang Meng, and Haoyue Wang. "Quant-BnB: A Scalable Branch-and-Bound Method for Optimal Decision Trees with Continuous Features." In Proceedings of ICML (2022).
- [9] Nijssen, Siegfried, and Elisa Fromont. "Mining optimal decision trees from itemset lattices." In Proceedings of SIGKDD (2007).
- [10] Nijssen, Siegfried, and Elisa Fromont. "Optimal constraint-based decision tree induction from itemset lattices." *Data Mining and Knowledge Discovery* 21 (2010): 9-51.
- [11] Aglin, Gaël, Siegfried Nijssen, and Pierre Schaus. "Learning optimal decision trees using caching branch-and-bound search." In Proceedings of AAAI (2020).
- [12] Demirović, Emir, et al. "Murtree: Optimal decision trees via dynamic programming and search." *The Journal of Machine Learning Research* 23.1 (2022): 1169-1215.
- [13] Hu, Xiyang, Cynthia Rudin, and Margo Seltzer. "Optimal sparse decision trees." In Proceedings of NeurIPS (2019).
- [14] Lin, Jimmy, et al. "Generalized and scalable optimal sparse decision trees." In Proceedings of ICML (2020).
- [15] McTavish, Hayden, et al. "Fast sparse decision tree optimization via reference ensembles." In Proceedings of AAAI (2022).
- [16] Sutton, C. "Improving classification trees with simulated annealing." *Computing Science and Statistics: Proceedings of the 23rd Symposium on the Interface*. 1991.
- [17] Cha, Sung-Hyuk, and Charles C. Tappert. "Constructing Binary Decision Trees using Genetic Algorithms." *GEM*. 2008.
- [18] Cha, Sung-Hyuk, and Charles C. Tappert. "A genetic algorithm for constructing compact binary decision trees." *Journal of pattern recognition research* 4.1 (2009): 1-13.
- [19] Omielan, Adam, and Sunil Vadera. "ECCO: A new evolutionary classifier with cost optimisation." *Intelligent Information Processing VI: 7th IFIP TC 12 International Conference* (2012).
- [20] Rivera-Lopez, Rafael, and Juana Canul-Reich. "Construction of near-optimal axis-parallel decision trees using a differential-evolution-based approach." *IEEE Access* 6 (2018): 5548-5563.
- [21] Sörensen, Kenneth, and Gerrit K. Janssens. "Data mining with genetic algorithms on binary trees." *European Journal of Operational Research* 151.2 (2003): 253-264.
- [22] Papagelis, Athanassios, and Dimitrios Kalles. "GA Tree: genetically evolved decision trees." In Proceedings 12th IEEE ICTAI (2000).
- [23] Fu, Zhiwei, et al. "Genetically engineered decision trees: population diversity produces smarter trees." *Operations Research* 51.6 (2003): 894-907.
- [24] Ersoy, Elif, Erinç Albey, and Enis Kayis. "A CART-based Genetic Algorithm for Constructing Higher Accuracy Decision Trees." *DATA*. 2020.

B Differential Evolution and DEOCT algorithms

Algorithm 3 Classic Differential Evolution

- 1: **Input:** The population size N , maximum generation G , mutation factor M , and cross probability CR .
 - 2: **Output:** The best individual \mathbf{s}_{best}^g .
 - 3: Initialize $g \leftarrow 1, \mathcal{S}^g \leftarrow \emptyset$.
 - 4: **for** $r \in 1, \dots, N$ **do**
 - 5: Randomly initialize the individual \mathbf{s}_r^g within the range limits for each variable.
 - 6: $\mathcal{S}^g \leftarrow \mathcal{S}^g \cup \mathbf{s}_r^g$.
 - 7: **end for**
 - 8: Update the best individual, $\mathbf{s}_{best}^g \leftarrow \arg \min_{\mathbf{s}} f(\mathbf{s}_r^g), \mathbf{s}_r^g \in \mathcal{S}^g$.
 - 9: **while** $g \leq$ maximum generation **do**
 - 10: $\mathcal{S}^{g+1} \leftarrow \emptyset$.
 - 11: **for** $r \in 1, \dots, N$ **do**
 - 12: Randomly select two individuals $\mathbf{s}_{r1}^g, \mathbf{s}_{r2}^g$ from \mathcal{S}^g .
 - 13: Generate the mutant vector \mathbf{v}_r^g using Equation (1).
 - 14: Generate the cross vector \mathbf{u}_r^g using Equation (2).
 - 15: Select the better vector \mathbf{s}_r^{g+1} using Equation (3).
 - 16: $\mathcal{S}^{g+1} \leftarrow \mathcal{S}^{g+1} \cup \mathbf{s}_r^{g+1}$.
 - 17: **end for**
 - 18: Update the best individual, $\mathbf{s}_{best}^{g+1} \leftarrow \arg \min_{\mathbf{s}} \{\mathbf{s}_{best}^g, f(\mathbf{s}_r^{g+1})\}, \mathbf{s}_r^{g+1} \in \mathcal{S}^{g+1}$.
 - 19: $g \leftarrow g + 1$.
 - 20: **end while**
-

Algorithm 4 DEOCT

- 1: **Input:** OCT: training set (\mathbf{X}, \mathbf{Y}) , tree depth D , minimum sample size n_{min} , and complexity parameter α . DE: the population size N , maximum generation G , warm-starts \mathcal{S}^0 , mutation factor M , and cross probability CR .
 - 2: **Output:** The best individual \mathbf{s}_{best}^g .
 - 3: Initialize $g \leftarrow 1, \mathcal{S}^g \leftarrow \mathcal{S}^0$.
 - 4: **for** $r \in |\mathcal{S}^0| + 1, \dots, N$ **do**
 - 5: Randomly initialize the individual \mathbf{s}_r^g within the range limits for each variable.
 - 6: $\mathcal{S}^g \leftarrow \mathcal{S}^g \cup \mathbf{s}_r^g$.
 - 7: **end for**
 - 8: $\mathbf{s}_{best}^g \leftarrow \arg \min_{\mathbf{s}} f(\mathbf{s}_r^g), \mathbf{s}_r^g \in \mathcal{S}^g$.
 - 9: **while** $g \leq G$ **do**
 - 10: $\mathcal{S}^{g+1} \leftarrow \emptyset, \mathcal{U}^g \leftarrow \emptyset$.
 - 11: **for** $r \in 1, \dots, N$ **do**
 - 12: Randomly select $\mathbf{s}_{r1}^g, \mathbf{s}_{r2}^g$ from \mathcal{S}^g .
 - 13: Generate the mutant vector \mathbf{v}_r^g using Eqn. 1.
 - 14: Generate the cross vector \mathbf{u}_r^g using Eqn. 2.
 - 15: $\mathcal{U}^g \leftarrow \mathcal{U}^g \cup \mathbf{u}_r^g$.
 - 16: **end for**
 - 17: Evaluate the fitness of each cross vector \mathbf{u}_r^g in \mathcal{U}^g using OCT fitness Algorithm 1.
 - 18: **for** $r \in 1, \dots, N$ **do**
 - 19: Select the individual with better fitness as \mathbf{s}_r^{g+1} from \mathbf{s}_r^g and \mathbf{u}_r^g using Equation (3).
 - 20: $\mathcal{S}^{g+1} \leftarrow \mathcal{S}^{g+1} \cup \mathbf{s}_r^{g+1}$.
 - 21: **end for**
 - 22: $\mathbf{s}_{best}^{g+1} \leftarrow \arg \min_{\mathbf{s}} f(\mathbf{s}_r^{g+1}), \mathbf{s}_r^{g+1} \in \mathcal{S}^{g+1}$.
 - 23: $g \leftarrow g + 1$.
 - 24: **end while**
-

C Results of hyperparameter tuning with validation sets

In this section, we delve into the results of hyperparameter tuning with validation sets, as showcased in Table 5. This involved a comparative analysis of our algorithm, MH-DEOCT, with CART and IAI-OCT. It's noteworthy that IAI-OCT is a commercial OCT package developed by LLC Interpretable AI (Bertsimas and Dunn, 2017; Interpretable AI, 2023).

In the IAI-OCT package, the complexity parameter α is automatically adjusted using a training-validation-retraining procedure. This function is intrinsic to the package and cannot be disabled. As a result, IAI-OCT was excluded from the comparison in Table 1. Instead, we used a self-implemented version named LS-OCT for the comparison. The running time of our implementation is slower than IAI-OCT, likely because IAI-OCT has been fully optimized for speed as a commercial software product. Nevertheless, both LS-OCT and IAI-OCT demonstrate a similar accelerated growth pattern in speed as the sample size increases (as shown in Figure 5). Due to licensing restrictions, IAI-OCT was run on a personal laptop with an AMD 5800H CPU, which has similar sequential performance capabilities to the server used for other tests (in GeekBench 6 for single-core performance, the laptop is scored 1750 and the server is scored 1650).

For our proposed algorithm, MH-DEOCT, we adjusted the complexity parameter α utilizing the same training-validation-retraining procedure as the IAI-OCT package. In comparison, CART requires tuning of an analogous parameter, termed "purity_thresh", during the pruning operation to efficiently control the complexity of the tree structure. For both MH-DEOCT and CART, we examined 21 parameter values uniformly selected from their parameter domains to identify the optimal parameter value. In terms of the datasets, we divided 65 datasets, up to 1 million samples, into training, validation, and testing subsets following a 50%-25%-25% ratio. This partitioning was repeated ten times, each iteration utilizing a unique random seed. The hyperparameter tuning process was conducted for each partitioned dataset, and the reported results represent the average of all 650 experiments (10 partitions for each of the 65 datasets).

The results in Table 5 demonstrate that hyperparameter tuning consistently enhances the testing accuracy of all algorithms compared to their non-tuned versions. Specifically, the testing accuracy of the tuned MH-DEOCT improves on average by 1.37% relative to its non-tuned counterpart, albeit at the cost of a slight 1.29% decrease in training accuracy. Moreover, when compared to tuned CART and IAI-OCT, MH-DEOCT exhibits superior performance in testing accuracy by an average of 1.92% and 0.80%, respectively. Additionally, MH-DEOCT maintains a higher training accuracy than the other two algorithms.

Table 5: Average accuracy of hyperparameter tuning with validation sets on 65 datasets within 1 million samples

Performance	Depth	$\alpha = 0$			With Tuning		
		CART	LS-OCT	MH-DEOCT	CART	IAI-OCT	MH-DEOCT
Train (%)	2	79.41	81.47	81.64	78.93	80.77	81.25
	3	84.30	86.04	86.82	83.30	85.54	86.26
	4	87.62	88.87	90.24	86.00	88.21	89.19
	8	95.67	96.26	97.30	92.11	92.84	94.57
Test (%)	2	76.91	78.19	78.21	77.43	78.13	78.85
	3	80.45	81.57	81.78	81.16	82.10	82.71
	4	82.42	83.32	83.60	83.22	84.23	84.81
	8	85.78	85.80	86.31	87.03	87.54	87.73
Time (s)	2	0.03	140.34	1.51	3.25	31.18	29.46
	3	0.05	231.98	3.58	2.12	69.28	69.56
	4	0.06	366.77	6.96	2.56	136.52	127.38
	8	0.12	869.29	68.77	4.05	613.60	973.11

D Comparison with global methods requiring binary datasets

We conducted a comprehensive benchmarking of our approach using the state-of-the-art global optimal dynamic programming method, GOSDT-Guesses (2022) [1], which is tailored to binary features. To accommodate continuous features in our evaluation, we employed two binarization techniques: MDLP [2] and Guess [1]. For the Guess binarization, we opted for the most extensive setting from the reference GBDT model in [1] ($n_{est} = 50, max_{depth} = 2$) to minimize potential data loss during conversion. Our evaluation encompassed 64 datasets, each with fewer than 250,000 samples. The HTSensor dataset (928,991 samples) was excluded due to its lengthy conversion time (over two hours) and the incompatibility of all global methods to process its binarized version. MH-DEOCT employed the same parameters as detailed in our original paper. Notably, GOSDT (2022) failed to generate results for 8 of the 64 binarized datasets. To ensure a fair comparison, we considered only the average results from the remaining 56 datasets, as summarized in Table 6.

Table 6: Comparison of continuous and binary features, dynamic programming and our algorithm on 63 datasets (Continuous datasets have better average train and test accuracy; MH-DEOCT obtains higher accuracy on continuous datasets than GOSDT on binarized datasets.)

Performance	Dataset Type	# Features [Mean (Max)]	Depth=2			
			CART	Quant-BnB (Global)	GOSDT (2022, Global)	MH-DEOCT (Ours)
Train (%)	Continuous	20.1 (73)	80.68	83.17	-	82.93
	MDLP-Binarized	76.1 (1003)	78.45	80.36	80.36	80.22
	Guess-Binarized	30.4 (103)	79.07	82.00	82.00	81.90
Test (%)	Continuous	20.1 (73)	77.93	79.43	-	79.42
	MDLP-Binarized	76.1 (1003)	76.20	78.29	78.28	78.11
	Guess-Binarized	30.4 (103)	77.33	78.75	78.75	78.63
Time (s)	Continuous	20.1 (73)	0.01	1.76	-	1.77
	MDLP-Binarized	76.1 (1003)	0.02	49.12	6.91	3.41
	Guess-Binarized	30.4 (103)	0.01	3.23	4.33	2.11

* GOSDT was unable to produce results for 7 out of 64 datasets when binarized using MDLP and for 1 out of 64 datasets when binarized using Guess. For an fair comparison, we present the average results from the 56 out of 64 datasets where GOSDT successfully generated outcomes.

D.1 Comparison of Continuous and Binarized Datasets

While full binarization methods, such as one-hot encoding, offer consistent search spaces for splits between continuous and corresponding binary datasets, they significantly inflate the feature count. Across the aforementioned 64 datasets, the original average feature count was 20.1, which soared to an average of 4060 post-binarization, with a maximum of 124,968. Handling such vast binary features poses challenges for current global optimal solvers. For context, the largest reported managed binary feature count, 9460 by DL8.5 [2], was derived from 19 continuous features with 1151 samples. Furthermore, full binarization leads to substantial increases in storage requirements; for example, a dataset with 17,898 samples grew from 3MB to approximately 9GB after conversion, presenting challenges in addressing real-world large-scale problems.

As a solution to reduce binarized features, various methods have been proposed. Guess [1] derives thresholds from pre-trained boosted decision tree models, MDLP [3] applies the minimum description length principle, and Bucketization [2, 4] avoids splitting between consecutive observations. However, Bucketization’s accuracy loss has been documented by [5]. In our assessments, we evaluated MDLP-binarized, Guess-binarized, and original continuous datasets. As depicted in Table 6, Quant-BnB consistently achieves global optima across all three datasets. It’s worth noting that the accuracy of the continuous datasets is notably higher compared to both the MDLP and Guess binarized versions, emphasizing the potential information loss when converting numerical features to binary, especially when dataset size management is a priority.

D.2 Comparison of GOSDT-Guesses and MH-DEOCT

The comparison presented in Table 6 underscores that our algorithm achieves results comparable to the global optimal solutions provided by GOSDT-Guesses on binary datasets. Comparing continuous with binarized datasets, MH-DEOCT consistently delivers superior accuracy on continuous datasets in comparison to the optimal results of GOSDT-Guess on the corresponding binarized datasets. Additionally, Appendix D.2 provides results for two datasets with sample sizes exceeding 10,000 over various tree depths. It demonstrates that GOSDT-Guesses encounters challenges in obtaining optimal

solutions within a reasonable time for larger datasets and deeper trees (e.g., it failed to produce results within a 4-hour limit for depth=8 in two datasets in the table). In contrast, our algorithm adeptly handles these challenges, efficiently solving problems with larger datasets (up to 11,000,000 samples) and deeper trees, setting a precedent in the literature.

Table 7: Comparison of MH-DEOCT and GOSDT (2022) on Guess-Binarized datasets with different tree depth (GOSDT is slower and failed to solve deep trees and datasets large than 245,057 samples, while our algorithm can solve depth=8 trees with up to 11,000,000 samples)

Dataset	Sample	# Feature (Original/Guess)	Class	Performance	Depth = 2			Depth = 4			Depth = 8		
					CART	GOSDT-Guesses	MH-DEOCT	CART	GOSDT-Guesses	MH-DEOCT	CART	GOSDT-Guesses	MH-DEOCT
Eeg	14,980	14 / 103	2	Train (%)	63.02	66.95	66.95	70.01	74.70	72.62	77.64	OoT	78.01
				Test (%)	62.36	66.42	66.42	68.78	73.55	71.21	75.50	OoT	75.59
				Time (s)	0.03	4.64	3.73	0.07	1542	21.33	0.11	OoT	312
Skin-seg	245,057	3 / 63	2	Train (%)	90.71	92.70	91.97	97.43	98.16	98.06	99.29	OoT	99.33
				Test (%)	90.67	92.60	91.89	97.38	98.18	98.02	99.27	OoT	99.31
				Time (s)	0.64	90.21	11.3	0.97	1881	42.14	1.16	OoT	508

* OoT: Out of 4-hour Time limit.

* For datasets of larger sizes (e.g., ranging from 928,991 to 11,000,000 samples), the binarization process requires over two hours, rendering it unsuitable even as a preprocessing step. However, our algorithm is capable of effectively handling datasets containing up to 11,000,000 samples.

[1] McTavish, Hayden, et al. "Fast sparse decision tree optimization via reference ensembles." AAAI. 2022.

[2] Demirović, Emir, et al. "Murtree: Optimal decision trees via dynamic programming and search." JMLR 23.1 (2022): 1169-1215.

[3] Verwer, Sicco, and Yingqian Zhang. "Learning optimal classification trees using a binary linear program formulation." AAAI. 2019.

[4] Aglin, Gaël, Siegfried Nijssen, and Pierre Schaus. "Learning optimal decision trees using caching branch-and-bound search." AAAI. 2020.

[5] Lin, Jimmy, et al. "Generalized and scalable optimal sparse decision trees." ICML. 2020.

E Detailed experiment results with $\alpha = 0$ in Table 1

In this section, we expand upon the experiment results presented in Table 1 by providing a more detailed analysis for each of the 65 datasets. We have documented the average training and testing accuracy, as well as the training time for each dataset based on 10 random splits. These performance metrics offer valuable insight into the stability and efficiency of the models and algorithms employed in our study. To facilitate easier comprehension, the results are presented in a tabular format, with each row corresponding to a dataset and columns representing the average training accuracy, testing accuracy, and training time. By examining these comprehensive results, readers can better understand the strengths and limitations of the methods used, as well as their applicability to various data conditions.

In these compared methods, LS-OCT is a local-search heuristic method providing node-by-node polishing on the result of CART and other warm-starts Bertsimas and Dunn (2017). We use 100 warm-start solutions in LS-OCT, including one CART solution and 99 random generated solutions. It should be noted that LS-OCT was unable to produce a result for the Htsensor dataset, which contains 928,991 samples, at Depth=8 within a 24-hour timeframe. Therefore, this particular result is not included in the subsequent tables. In addition, the global optimality of the methods Quant-BnB and RS-OCT can be inferred from their training times. With a time limit of four hours for Quant-BnB and RS-OCT, any training time less than these limits indicates that a global optimal solution has been achieved.

E.1 Training accuracy (%) on 65 datasets within 1 million samples

Table 8: Depth=2 average training accuracy (%) on 65 datasets with 10 random splits within 1 million samples

Dataset	Sample	Feature	Class	Depth=2							
				CART	LS-OCT	Quant-BnB	RS-OCT	DEOCT	MH-DEOCT	DEOCT (Long)	MH-DEOCT (Long)
Soybean-small	47	35	4	100.00	100.00	100.00	100.00	100.00	100.00	100.00	100.00
Echocardiogram	61	11	2	100.00	100.00	100.00	100.00	100.00	100.00	100.00	100.00
Hepatitis	80	19	2	95.00	95.50	96.67	96.67	96.00	96.00	96.17	96.33

Table 8 continued from previous page

Dataset	Sample	Feature	Class	Depth=2							
				CART	LS-OCT	Quant-BnB	RS-OCT	DEOCT	MH-DEOCT	DEOCT (Long)	MH-DEOCT (Long)
Fertility	100	9	2	87.73	89.47	90.13	90.13	90.13	90.13	90.00	90.00
Acute-inflammations-1	120	6	2	91.44	100.00	100.00	100.00	100.00	100.00	100.00	100.00
Acute-inflammations-2	120	6	2	100.00	100.00	100.00	100.00	100.00	100.00	100.00	100.00
Hayes-roth	132	5	3	58.38	62.63	63.43	63.43	63.43	63.43	63.43	63.43
Iris	150	4	3	96.16	96.25	96.25	96.25	96.16	96.16	96.16	96.25
Teaching-assistant-evaluation	151	5	3	52.57	55.13	56.28	56.28	56.19	56.19	56.28	56.28
Wine	178	13	3	95.56	97.59	97.67	97.67	97.59	97.67	97.67	97.67
Breast-cancer-prognostic	194	31	2	79.05	83.45	84.46	82.91	83.38	83.72	83.85	84.12
Parkinsons	195	23	2	92.67	95.82	96.37	96.37	94.73	94.86	95.14	95.21
Connectionist-bench-sonar	208	60	2	78.72	83.27	85.45	83.78	84.23	84.23	84.42	84.68
Image-segmentation	210	19	7	57.32	58.47	58.85	58.85	58.41	58.41	58.66	58.66
Seeds	210	7	3	92.48	94.84	95.10	95.10	93.38	93.63	93.63	94.27
Glass	214	9	6	66.69	67.81	68.06	68.06	67.88	68.00	68.00	68.06
Thyroid-disease-new-thyroid	215	5	3	93.60	96.96	97.02	97.02	96.40	96.46	96.83	96.96
Congressional-voting-records	232	16	2	96.67	96.67	96.67	96.67	96.67	96.67	96.67	96.67
Spectf-heart	267	22	2	80.85	80.85	80.85	80.85	80.85	80.85	80.85	80.85
Spectf-heart	267	44	2	81.55	86.30	87.75	83.00	86.40	87.20	87.35	87.40
Cylinder-bands	277	39	2	71.01	73.82	76.33	76.33	75.27	75.70	75.89	75.89
Heart-disease-Cleveland	282	13	5	61.47	62.42	63.08	62.99	63.03	63.03	63.03	63.03
Haberman-survival	306	3	2	77.21	78.78	79.34	79.35	79.08	79.21	79.34	79.34
Ionosphere	351	34	2	90.72	91.22	91.41	84.87	91.14	91.29	91.29	91.33
Dermatology	358	34	6	73.13	77.28	77.35	77.35	77.35	77.35	77.35	77.35
Thoracic-surgery	470	16	2	85.48	86.02	86.22	86.05	86.02	86.11	86.19	86.19
Body	507	5	2	90.16	92.37	93.00	93.00	92.18	92.45	92.76	92.76
Climate-model-crashes	540	20	2	91.73	93.78	94.12	93.70	93.83	93.98	94.00	94.02
Monks-problems-3	554	6	2	96.43	96.43	96.43	96.43	96.43	96.43	96.43	96.43
Monks-problems-1	556	6	2	74.00	77.72	77.75	77.75	77.72	77.72	77.72	77.75
Breast-cancer-diagnosi	569	30	2	93.90	96.06	96.43	95.94	96.27	96.29	96.34	96.34
Indian-liver-patient	579	10	2	71.22	74.29	75.09	74.72	74.77	74.86	75.02	75.02
Monks-problems-2	600	6	2	65.78	65.82	65.82	65.82	65.82	65.82	65.82	65.82
Balance-scale	625	4	3	68.59	72.56	72.74	72.74	72.74	72.74	72.74	72.74
Credit-approval	653	15	2	86.61	87.01	87.34	87.18	87.24	87.26	87.30	87.30
Breast-cancer	683	9	2	93.30	96.54	96.80	96.80	96.50	96.62	96.80	96.80
Blood-transfusion	748	4	2	76.58	78.09	78.43	78.43	78.34	78.40	78.43	78.43
Mammographic-mass	830	5	2	83.55	84.95	85.19	85.19	84.87	84.97	85.19	85.19
Tic-tac-toe-endgame	958	9	2	70.01	70.24	70.24	70.24	70.24	70.24	70.24	70.24
Connectionist-bench	990	13	11	28.49	32.63	32.76	32.76	32.60	32.76	32.76	32.76
Statlog-project-German-credit	1,000	20	2	72.16	74.29	74.68	74.51	74.68	74.68	74.68	74.68
Concrete	1,030	8	3	62.67	65.92	65.98	65.98	65.85	65.96	65.87	65.96
Qsar-biodegradation	1,055	41	2	78.29	80.64	81.19	81.19	80.72	80.76	80.76	80.76
Banknote-authentication	1,372	4	2	89.94	92.77	92.88	92.88	92.52	92.59	92.66	92.75
Contraceptive-method-choice	1,473	9	3	47.43	53.92	54.32	54.32	53.56	54.12	54.32	54.32
Car-evaluation	1,728	6	4	77.93	77.93	77.93	78.02	77.93	77.93	77.93	77.93
Ozone-level-detection-eight	1,847	72	2	93.21	94.07	94.44	93.80	93.90	94.15	94.14	94.19
Ozone-level-detection-one	1,848	72	2	96.98	97.24	97.46	97.20	97.17	97.24	97.37	97.38
Seismic-bumps	2,584	18	2	93.43	93.64	93.75	93.47	93.59	93.62	93.64	93.64
Chess-king-rook-versus-king-pawn	3,196	36	2	75.43	85.10	87.14	87.14	86.95	86.95	84.03	87.14
Thyroidann	3,772	21	3	97.90	97.90	97.90	97.72	97.90	97.90	97.90	97.90
Statloglansat	4,435	36	6	64.81	68.76	68.95	65.40	68.92	68.95	68.95	68.95
Spambase	4,601	57	2	85.06	87.01	87.31	85.94	87.17	87.31	87.00	87.18
Wall-following-robot-2	5,456	2	4	93.92	93.95	93.95	93.95	93.94	93.94	93.94	93.94
Pageblock	5,473	10	5	95.09	95.38	95.38	95.38	95.38	95.38	95.38	95.38
Optical-recognition	5,620	62	10	35.48	38.40	38.47	36.93	38.45	38.45	38.40	38.40
Statlog-project-landsat-satellite	6,435	36	6	64.02	67.95	68.07	65.05	68.05	68.07	68.05	68.07
Thyroid-disease-ann-thyroid	7,200	21	3	97.56	97.56	97.56	97.25	97.56	97.56	97.56	97.56
Pendigits	7,494	16	10	39.09	39.84	39.90	39.90	39.85	39.90	39.88	39.90
Avila	10,430	10	12	52.49	53.97	54.08	53.51	53.73	53.75	53.76	53.79
Eeg	14,980	14	2	62.84	65.66	66.97	66.52	65.49	65.70	66.57	66.94
Htru	17,898	8	2	97.73	97.93	97.94	97.88	97.82	97.83	97.84	97.84
Shuttle	43,500	9	7	93.86	94.33	95.40	95.40	94.18	94.48	94.78	94.78
Skinsegmentation	245,057	3	2	90.67	92.65	92.68	92.67	92.68	92.68	92.68	92.68
Htsensor	928,991	11	3	58.14	59.86	59.87	59.62	59.87	59.87	59.85	59.85
Average Training Accuracy (%)				79.41	81.47	81.86	81.42	81.56	81.64	81.66	81.75

Table 9: Depth=2 training accuracy standard deviation (%) on 65 datasets with 10 random splits within 1 million samples

Dataset	Sample	Feature	Class	Depth=2							
				CART	LS-OCT	Quant-BnB	RS-OCT	DEOCT	MH-DEOCT	DEOCT (Long)	MH-DEOCT (Long)
Soybean-small	47	35	4	0.00	0.00	0.00	0.00	0.00	0.00	0.00	0.00
Echocardiogram	61	11	2	0.00	0.00	0.00	0.00	0.00	0.00	0.00	0.00
Hepatitis	80	19	2	2.94	2.94	1.92	1.92	2.51	2.51	2.49	2.33
Fertility	100	9	2	2.33	1.93	1.43	1.43	1.43	1.43	1.69	1.69
Acute-inflammations-1	120	6	2	1.18	0.00	0.00	0.00	0.00	0.00	0.00	0.00
Acute-inflammations-2	120	6	2	0.00	0.00	0.00	0.00	0.00	0.00	0.00	0.00
Hayes-roth	132	5	3	1.89	2.13	1.56	1.56	1.56	1.56	1.56	1.56
Iris	150	4	3	1.04	1.18	1.18	1.18	1.04	1.04	1.04	1.18
Teaching-assistant-evaluation	151	5	3	3.21	2.05	1.68	1.68	1.73	1.73	1.68	1.68
Wine	178	13	3	2.64	0.85	0.75	0.75	0.85	0.75	0.75	0.75
Breast-cancer-prognostic	194	31	2	2.95	1.11	0.71	0.96	1.07	0.87	0.87	0.57
Parkinsons	195	23	2	1.94	0.82	0.65	0.65	0.97	0.81	0.68	0.79
Connectionist-bench-sonar	208	60	2	2.67	1.72	0.86	1.42	1.39	1.39	1.51	1.26
Image-segmentation	210	19	7	1.80	1.37	1.62	1.62	1.56	1.56	1.57	1.57
Seeds	210	7	3	1.50	0.56	0.67	0.67	1.21	1.08	1.08	0.79
Glass	214	9	6	2.32	1.92	1.87	2.18	1.75	1.81	1.86	1.87
Thyroid-disease-new-thyroid	215	5	3	3.19	0.99	1.05	1.05	1.16	1.10	1.32	1.11

Table 9 continued from previous page

Dataset	Sample	Feature	Class	Depth=2							
				CART	LS-OCT	Quant-BnB	RS-OCT	DEOCT	MH-DEOCT	DEOCT (Long)	MH-DEOCT (Long)
Congressional-voting-records	232	16	2	0.71	0.71	0.71	0.71	0.71	0.71	0.71	0.71
Spectf-heart	267	22	2	1.47	1.47	1.47	1.47	1.47	1.47	1.47	1.47
Spectf-heart	267	44	2	2.49	1.09	1.21	2.19	0.99	1.49	1.18	1.20
Cylinder-bands	277	39	2	2.39	1.85	0.91	0.34	1.22	0.82	0.77	0.77
Heart-disease-Cleveland	282	13	5	1.72	1.26	1.39	1.39	1.30	1.30	1.30	1.30
Haberman-survival	306	3	2	1.76	1.07	1.09	1.09	1.12	1.05	1.09	1.09
Ionosphere	351	34	2	1.19	1.22	1.14	1.84	1.01	1.05	1.05	1.13
Dermatology	358	34	6	4.82	1.32	1.29	1.29	1.29	1.29	1.29	1.29
Thoracic-surgery	470	16	2	1.07	0.83	0.78	0.86	0.82	0.83	0.77	0.77
Body	507	5	2	1.83	0.69	0.63	0.63	0.95	0.68	0.69	0.69
Climate-model-crashes	540	20	2	0.66	0.61	0.62	0.50	0.56	0.61	0.55	0.54
Monks-problems-3	554	6	2	0.48	0.48	0.48	0.48	0.48	0.48	0.48	0.48
Monks-problems-1	556	6	2	1.24	0.91	0.89	0.89	0.89	0.89	0.89	0.89
Breast-cancer-diagnosti	569	30	2	1.38	0.50	0.43	0.56	0.37	0.35	0.34	0.34
Indian-liver-patient	579	10	2	1.26	1.02	1.10	1.12	1.25	1.20	1.14	1.14
Monks-problems-2	600	6	2	1.24	1.20	1.20	1.20	1.20	1.20	1.20	1.20
Balance-scale	625	4	3	2.39	0.81	0.65	0.65	0.65	0.65	0.65	0.65
Credit-approval	653	15	2	0.81	0.77	0.78	0.78	0.75	0.79	0.75	0.75
Breast-cancer	683	9	2	0.76	0.45	0.40	0.40	0.48	0.48	0.40	0.40
Blood-transfusion	748	4	2	1.25	1.12	1.08	1.08	1.08	1.08	1.08	1.08
Mammographic-mass	830	5	2	0.91	0.63	0.55	0.55	0.83	0.74	0.55	0.55
Tic-tac-toe-endgame	958	9	2	0.88	0.70	0.70	0.70	0.70	0.70	0.70	0.70
Connectionist-bench	990	13	11	1.64	0.54	0.46	0.45	0.57	0.46	0.46	0.46
Statlog-project-German-credit	1,000	20	2	1.94	0.67	0.79	0.66	0.79	0.79	0.79	0.79
Concrete	1,030	8	3	2.18	1.14	1.09	1.28	1.07	1.07	1.04	1.07
Qsar-biodegradation	1,055	41	2	1.01	0.54	0.81	1.03	0.76	0.70	0.70	0.70
Banknote-authentication	1,372	4	2	0.31	0.42	0.35	0.35	0.68	0.70	0.60	0.49
Contraceptive-method-choice	1,473	9	3	0.66	1.15	0.84	0.84	1.18	0.78	0.84	0.84
Car-evaluation	1,728	6	4	0.52	0.52	0.52	0.51	0.52	0.52	0.52	0.52
Ozone-level-detection-eight	1,847	72	2	0.36	0.41	0.35	0.44	0.37	0.35	0.44	0.41
Ozone-level-detection-one	1,848	72	2	0.20	0.19	0.14	0.18	0.22	0.19	0.16	0.15
Seismic-bumps	2,584	18	2	0.15	0.14	0.14	0.16	0.19	0.19	0.16	0.16
Chess-king-rook-versus-king-pawn	3,196	36	2	0.46	3.76	0.39	3.64	0.80	0.80	3.66	0.39
Thyroidann	3,772	21	3	0.15	0.15	0.15	0.30	0.15	0.15	0.15	0.15
Statloglansat	4,435	36	6	0.60	0.30	0.22	0.15	0.23	0.22	0.22	0.22
Spambase	4,601	57	2	1.95	0.52	0.19	0.42	0.44	0.19	0.71	0.42
Wall-following-robot-2	5,456	2	4	0.18	0.18	0.18	0.18	0.17	0.17	0.17	0.17
Pageblock	5,473	10	5	0.49	0.17	0.16	0.16	0.16	0.16	0.16	0.16
Optical-recognition	5,620	62	10	0.52	0.40	0.39	0.86	0.41	0.41	0.42	0.42
Statlog-project-landsat-satellite	6,435	36	6	0.41	0.31	0.37	0.63	0.40	0.37	0.40	0.37
Thyroid-disease-ann-thyroid	7,200	21	3	0.11	0.11	0.11	0.35	0.11	0.11	0.11	0.11
Pendigits	7,494	16	10	0.33	0.24	0.22	0.10	0.25	0.24	0.24	0.24
Avila	10,430	10	12	0.36	0.35	0.29	0.34	0.31	0.32	0.31	0.31
Eeg	14,980	14	2	0.42	0.76	0.16	0.14	0.59	0.65	0.65	0.20
Htru	17,898	8	2	0.07	0.07	0.06	0.03	0.07	0.07	0.06	0.07
Shuttle	43,500	9	7	0.04	0.57	0.04	0.05	0.36	0.35	0.25	0.25
Skinsegmentation	245,057	3	2	0.04	0.04	0.04	0.04	0.04	0.04	0.04	0.04
Htsensor	928,991	11	3	0.02	0.03	0.02	0.03	0.03	0.03	0.03	0.03
Average Training Accuracy STD (%)				1.22	0.83	0.68	0.79	0.76	0.73	0.78	0.70

Table 10: Depth=3 average training accuracy (%) on 65 datasets with 10 random splits within 1 million samples

Dataset	Sample	Feature	Class	Depth=3							
				CART	LS-OCT	Quant-BnB	DEOCT	MH-DEOCT	DEOCT (Long)	MH-DEOCT (Long)	
Soybean-small	47	35	4	100.00	100.00	-	100.00	100.00	100.00	100.00	100.00
Echocardiogram	61	11	2	100.00	100.00	100.00	100.00	100.00	100.00	100.00	100.00
Hepatitis	80	19	2	97.50	97.83	100.00	98.33	99.00	99.33	99.33	99.33
Fertility	100	9	2	90.40	91.73	93.87	92.80	92.93	93.73	94.27	94.27
Acute-inflammations-1	120	6	2	100.00	100.00	100.00	100.00	100.00	100.00	100.00	100.00
Acute-inflammations-2	120	6	2	100.00	100.00	100.00	100.00	100.00	100.00	100.00	100.00
Hayes-roth	132	5	3	64.04	70.61	75.56	72.53	72.83	73.43	74.04	74.04
Iris	150	4	3	97.14	98.21	99.82	98.21	98.21	98.75	99.20	99.20
Teaching-assistant-evaluation	151	5	3	61.06	64.16	67.96	67.61	68.14	68.50	68.50	68.50
Wine	178	13	3	98.42	99.70	100.00	99.85	99.92	99.85	99.85	99.85
Breast-cancer-prognostic	194	31	2	84.46	87.36	92.57	87.64	90.07	90.07	90.68	90.68
Parkinsons	195	23	2	97.95	98.84	100.00	99.11	99.59	99.73	99.79	99.79
Connectionist-bench-sonar	208	60	2	88.33	89.29	95.51	91.41	92.82	93.27	93.59	93.59
Image-segmentation	210	19	7	79.75	84.20	-	84.84	86.50	87.58	88.15	88.15
Seeds	210	7	3	94.65	97.01	98.73	96.50	96.62	97.58	97.83	97.83
Glass	214	9	6	74.81	77.44	80.50	77.00	78.56	79.00	79.94	79.94
Thyroid-disease-new-thyroid	215	5	3	98.26	98.82	99.75	98.76	98.88	99.19	99.25	99.25
Congressional-voting-records	232	16	2	97.07	97.47	97.93	97.47	97.47	97.70	97.70	97.70
Spectf-heart	267	22	2	82.05	82.60	83.80	82.80	82.90	82.95	83.20	83.20
Spectf-heart	267	44	2	85.40	88.80	93.60	88.95	91.05	91.20	91.85	91.85
Cylinder-bands	277	39	2	74.20	77.20	-	79.37	81.74	82.13	83.00	83.00
Heart-disease-Cleveland	282	13	5	65.21	66.21	70.24	68.10	68.29	68.53	68.58	68.58
Haberman-survival	306	3	2	79.08	80.35	82.53	81.53	81.57	82.18	82.23	82.23
Ionosphere	351	34	2	92.17	93.99	-	93.65	94.03	94.30	94.79	94.79
Dermatology	358	34	6	85.60	88.25	90.90	89.78	90.04	90.34	90.34	90.34
Thoracic-surgery	470	16	2	86.36	86.88	88.64	87.13	87.67	87.78	88.01	88.01
Body	507	5	2	93.74	95.58	96.58	95.76	96.42	96.34	96.53	96.53
Climate-model-crashes	540	20	2	94.07	95.28	96.64	95.31	95.65	95.98	96.27	96.27
Monks-problems-3	554	6	2	96.48	96.48	98.94	96.58	96.58	96.58	96.58	96.58
Monks-problems-1	556	6	2	78.20	87.34	88.87	85.66	86.52	87.17	87.70	87.70
Breast-cancer-diagnosti	569	30	2	96.97	97.75	98.97	97.75	97.93	98.26	98.43	98.43

Table 10 continued from previous page

Dataset	Sample	Feature	Class	Depth=3						
				CART	LS-OCT	Quant-BnB	DEOCT	MH-DEOCT	DEOCT (Long)	MH-DEOCT (Long)
Indian-liver-patient	579	10	2	72.51	75.90	79.08	76.43	77.72	78.09	78.41
Monks-problems-2	600	6	2	66.53	67.60	68.53	68.33	68.33	68.38	68.38
Balance-scale	625	4	3	75.94	77.24	78.76	78.57	78.59	78.61	78.61
Credit-approval	653	15	2	87.08	87.93	89.61	88.49	88.79	88.79	88.88
Breast-cancer	683	9	2	97.11	97.50	97.97	97.75	97.87	97.99	97.99
Blood-transfusion	748	4	2	79.73	80.20	81.68	81.07	81.19	81.46	81.48
Mammographic-mass	830	5	2	85.27	85.55	86.30	86.01	86.09	86.19	86.19
Tic-tac-toe-endgame	958	9	2	71.84	76.53	77.74	77.10	77.35	77.35	77.37
Connectionist-bench	990	13	11	41.68	45.22	48.65	46.29	46.74	47.47	48.15
Statlog-project-German-credit	1,000	20	2	75.15	76.24	77.57	77.07	77.28	77.60	77.72
Concrete	1,030	8	3	69.07	71.65	74.12	72.40	72.72	72.77	72.97
Qsar-biodegradation	1,055	41	2	82.77	83.92	86.47	84.83	85.22	85.37	85.56
Banknote-authentication	1,372	4	2	95.74	97.31	98.48	97.29	97.95	98.17	98.45
Contraceptive-method-choice	1,473	9	3	52.40	56.44	58.28	57.53	57.79	57.76	57.79
Car-evaluation	1,728	6	4	78.99	81.28	81.93	81.76	82.03	82.04	82.04
Ozone-level-detection-eight	1,847	72	2	93.23	94.32	95.52	94.27	94.77	94.87	95.21
Ozone-level-detection-one	1,848	72	2	97.10	97.40	98.14	97.40	97.65	97.63	97.82
Seismic-bumps	2,584	18	2	93.51	93.78	-	93.72	93.90	93.86	94.00
Chess-king-rook-versus-king-pawn	3,196	36	2	90.60	92.93	94.02	90.60	90.60	90.93	91.90
Thyroidann	3,772	21	3	99.38	99.38	101.91	99.40	99.40	99.40	99.40
Statloglansat	4,435	36	6	79.88	81.97	84.00	83.79	84.00	84.10	84.11
Spambase	4,601	57	2	87.66	90.30	90.21	90.25	90.34	90.28	90.28
Wall-following-robot-2	5,456	2	4	99.97	100.00	100.00	99.99	99.99	99.99	99.99
Pageblock	5,473	10	5	95.99	96.39	96.98	96.36	96.42	96.47	96.69
Optical-recognition	5,620	62	10	56.43	59.76	62.94	59.47	59.79	59.96	60.09
Statlog-project-landsat-satellite	6,435	36	6	79.26	81.57	83.64	83.18	83.59	83.66	83.69
Thyroid-disease-ann-thyroid	7,200	21	3	99.14	99.15	99.20	99.17	99.17	99.17	99.17
Pendigits	7,494	16	10	62.60	66.68	68.79	66.72	66.95	68.10	68.22
Avila	10,430	10	12	54.04	58.15	58.36	57.20	57.41	57.37	57.42
Eg	14,980	14	2	66.70	68.86	71.06	69.02	69.51	69.62	69.95
Htru	17,898	8	2	97.84	98.00	98.09	97.99	98.03	98.04	98.04
Shuttle	43,500	9	7	99.65	99.79	99.88	99.79	99.82	99.80	99.86
Skinsegmentation	245,057	3	2	96.54	96.62	96.83	96.66	96.66	96.66	96.67
Htsensor	928,991	11	3	64.50	67.75	65.49	67.49	67.75	67.73	67.76
Average Training Accuracy (%)				84.30	86.04	87.37	86.43	86.82	87.03	87.23

Table 11: Depth=3 training accuracy standard deviation (%) on 65 datasets with 10 random splits within 1 million samples

Dataset	Sample	Feature	Class	Depth=3						
				CART	LS-OCT	Quant-BnB	DEOCT	MH-DEOCT	DEOCT (Long)	MH-DEOCT (Long)
Soybean-small	47	35	4	0.00	0.00	-	0.00	0.00	0.00	0.00
Echocardiogram	61	11	2	0.00	0.00	0.00	0.00	0.00	0.00	0.00
Hepatitis	80	19	2	2.39	1.93	0.00	1.57	1.17	0.86	0.86
Fertility	100	9	2	2.87	1.64	2.23	1.43	1.26	1.78	1.99
Acute-inflammations-1	120	6	2	0.00	0.00	0.00	0.00	0.00	0.00	0.00
Acute-inflammations-2	120	6	2	0.00	0.00	0.00	0.00	0.00	0.00	0.00
Hayes-roth	132	5	3	1.79	2.49	2.19	2.60	2.75	2.24	2.02
Iris	150	4	3	0.82	0.60	0.40	0.60	0.60	0.96	0.89
Teaching-assistant-evaluation	151	5	3	5.84	2.65	2.76	2.29	2.36	2.44	2.44
Wine	178	13	3	1.68	0.39	0.00	0.32	0.24	0.32	0.32
Breast-cancer-prognostic	194	31	2	2.61	1.43	0.68	1.01	1.35	0.96	1.27
Parkinsons	195	23	2	1.91	0.73	0.00	0.73	0.48	0.35	0.33
Connectionist-bench-sonar	208	60	2	1.88	1.57	0.64	1.71	1.34	1.06	1.13
Image-segmentation	210	19	7	5.39	2.73	-	2.16	2.89	1.54	1.54
Seeds	210	7	3	1.21	0.95	0.45	1.09	1.04	0.99	0.96
Glass	214	9	6	3.41	1.40	1.12	2.16	1.79	1.72	1.49
Thyroid-disease-new-thyroid	215	5	3	1.20	0.85	0.34	0.77	0.64	0.59	0.49
Congressional-voting-records	232	16	2	0.79	0.73	0.66	0.73	0.73	0.54	0.54
Spect-heart	267	22	2	1.30	0.99	0.97	0.82	1.02	1.04	1.14
Spectf-heart	267	44	2	3.38	1.09	0.96	1.09	1.52	1.40	1.03
Cylinder-bands	277	39	2	3.43	1.69	-	1.04	1.11	0.76	1.45
Heart-disease-Cleveland	282	13	5	2.19	1.88	1.27	2.05	1.90	1.80	1.86
Haberman-survival	306	3	2	1.17	1.09	0.98	0.87	0.87	0.89	0.94
Ionosphere	351	34	2	1.40	0.86	-	1.13	0.88	0.91	0.95
Dermatology	358	34	6	4.29	2.87	1.31	1.09	1.47	1.17	1.17
Thoracic-surgery	470	16	2	1.21	0.95	0.67	0.82	0.99	0.86	0.95
Body	507	5	2	0.64	0.74	0.32	0.67	0.50	0.64	0.62
Climate-model-crashes	540	20	2	0.74	0.80	0.54	0.60	0.57	0.61	0.63
Monks-problems-3	554	6	2	0.57	0.57	0.37	0.54	0.54	0.54	0.54
Monks-problems-1	556	6	2	5.34	1.64	1.00	0.67	1.61	1.90	2.25
Breast-cancer-diagnosti	569	30	2	0.87	0.37	0.21	0.46	0.40	0.34	0.38
Indian-liver-patient	579	10	2	1.67	1.19	1.21	1.14	1.20	1.15	1.34
Monks-problems-2	600	6	2	1.09	1.09	0.90	0.81	0.81	0.87	0.87
Balance-scale	625	4	3	0.65	0.81	0.65	0.73	0.74	0.69	0.69
Credit-approval	653	15	2	0.86	0.86	0.67	0.52	0.62	0.61	0.57
Breast-cancer	683	9	2	0.51	0.33	0.17	0.31	0.30	0.24	0.24
Blood-transfusion	748	4	2	0.77	0.55	0.85	0.80	0.73	0.72	0.69
Mammographic-mass	830	5	2	0.67	0.49	0.60	0.53	0.58	0.56	0.56
Tic-tac-toe-endgame	958	9	2	1.26	0.48	0.58	0.90	0.62	0.47	0.47
Connectionist-bench	990	13	11	1.52	0.90	0.62	1.16	1.52	1.36	0.90
Statlog-project-German-credit	1,000	20	2	2.08	0.99	0.74	0.75	0.63	0.79	0.77
Concrete	1,030	8	3	2.08	0.93	0.32	0.82	0.76	0.65	0.71
Qsar-biodegradation	1,055	41	2	1.48	0.68	0.40	0.96	0.87	1.05	1.03
Banknote-authentication	1,372	4	2	0.47	0.34	0.15	0.59	0.46	0.50	0.17
Contraceptive-method-choice	1,473	9	3	1.44	0.64	0.72	0.66	0.55	0.58	0.55

Table 11 continued from previous page

Dataset	Sample	Feature	Class	Depth=3						
				CART	LS-OCT	Quant-BnB	DEOCT	MH-DEOCT	DEOCT (Long)	MH-DEOCT (Long)
Car-evaluation	1,728	6	4	0.53	0.66	0.32	0.48	0.27	0.28	0.28
Ozone-level-detection-eight	1,847	72	2	0.38	0.46	0.30	0.28	0.37	0.39	0.42
Ozone-level-detection-one	1,848	72	2	0.25	0.17	0.14	0.17	0.24	0.19	0.16
Seismic-bumps	2,584	18	2	0.14	0.17	-	0.13	0.15	0.15	0.12
Chess-king-rook-versus-king-pawn	3,196	36	2	0.31	1.65	0.33	0.31	0.31	1.29	1.82
Thyroidann	3,772	21	3	0.09	0.09	5.57	0.09	0.09	0.09	0.09
Statloglansat	4,435	36	6	0.30	0.64	0.30	0.49	0.39	0.38	0.37
Spambase	4,601	57	2	0.75	0.35	0.54	0.44	0.40	0.33	0.33
Wall-following-robot-2	5,456	2	4	0.07	0.00	0.00	0.05	0.04	0.05	0.04
Pageblock	5,473	10	5	0.30	0.13	0.12	0.06	0.18	0.21	0.32
Optical-recognition	5,620	62	10	1.16	1.18	0.33	0.54	0.43	0.27	0.32
Statlog-project-landsat-satellite	6,435	36	6	0.36	0.39	0.20	0.37	0.30	0.21	0.18
Thyroid-disease-ann-thyroid	7,200	21	3	0.08	0.07	0.07	0.06	0.06	0.06	0.06
Pendigits	7,494	16	10	0.47	1.24	0.17	0.86	0.95	0.68	0.73
Avila	10,430	10	12	0.60	0.46	0.35	0.35	0.29	0.50	0.44
Eeg	14,980	14	2	0.55	0.53	0.18	0.34	0.52	0.55	0.54
Htru	17,898	8	2	0.10	0.08	0.04	0.08	0.08	0.07	0.08
Shuttle	43,500	9	7	0.01	0.01	0.01	0.01	0.04	0.02	0.03
Skinsegmentation	245,057	3	2	0.02	0.03	0.02	0.02	0.02	0.02	0.05
Htsensor	928,991	11	3	0.03	0.03	0.02	0.35	0.03	0.05	0.02
Average Training Accuracy STD (%)				1.28	0.83	0.63	0.73	0.73	0.70	0.71

Table 12: Depth=4,8 average training accuracy (%) on 65 datasets with 10 random splits within 1 million samples

Dataset	Sample	Feature	Class	Depth=4					Depth=8						
				CART	LS-OCT	DEOCT	MH-DEOCT	DEOCT (Long)	MH-DEOCT (Long)	CART	LS-OCT	DEOCT	MH-DEOCT	DEOCT (Long)	MH-DEOCT (Long)
Soybean-small	47	35	4	100.00	100.00	100.00	100.00	100.00	100.00	100.00	100.00	100.00	100.00	100.00	100.00
Echocardiogram	61	11	2	100.00	100.00	100.00	100.00	100.00	100.00	100.00	100.00	100.00	100.00	100.00	100.00
Hepatitis	80	19	2	99.50	99.50	99.50	99.83	100.00	100.00	100.00	100.00	100.00	100.00	100.00	100.00
Fertility	100	9	2	93.60	94.13	94.93	96.13	96.53	97.20	98.67	99.20	98.89	98.89	98.93	98.93
Acute-inflammations-1	120	6	2	100.00	100.00	100.00	100.00	100.00	100.00	100.00	100.00	100.00	100.00	100.00	100.00
Acute-inflammations-2	120	6	2	100.00	100.00	100.00	100.00	100.00	100.00	100.00	100.00	100.00	100.00	100.00	100.00
Hayes-roth	132	5	3	74.24	76.57	78.69	81.82	84.75	86.16	93.94	95.56	94.28	96.97	96.57	98.79
Iris	150	4	3	99.46	99.64	99.82	99.82	99.82	99.91	100.00	100.00	100.00	100.00	100.00	100.00
Teaching-assistant-evaluation	151	5	3	67.70	69.56	72.48	74.25	75.22	75.75	89.23	88.85	89.23	92.48	89.23	92.21
Wine	178	13	3	99.70	100.00	99.92	100.00	100.00	100.00	99.87	100.00	100.00	100.00	100.00	100.00
Breast-cancer-prognostic	194	31	2	88.72	90.81	90.47	95.00	93.11	95.54	98.65	99.46	98.87	100.00	98.78	99.86
Parkinsons	195	23	2	99.59	99.59	99.86	100.00	100.00	100.00	100.00	100.00	100.00	100.00	100.00	100.00
Connectionist-bench-sonar	208	60	2	93.85	94.23	94.74	97.56	96.86	98.59	99.79	100.00	99.79	100.00	99.79	100.00
Image-segmentation	210	19	7	91.27	93.63	94.27	96.11	96.50	97.20	99.79	100.00	99.79	99.89	99.87	99.87
Seeds	210	7	3	97.52	98.28	98.09	98.22	98.92	99.24	100.00	100.00	100.00	100.00	100.00	100.00
Glass	214	9	6	82.00	84.38	84.81	87.81	87.63	89.00	99.27	99.44	99.27	99.58	99.38	99.88
Thyroid-disease-new-thyroid	215	5	3	99.13	99.63	99.63	99.75	99.88	99.88	99.90	100.00	99.90	100.00	99.90	99.88
Congressional-voting-records	232	16	2	97.93	97.99	98.62	98.97	99.20	99.31	100.00	99.94	100.00	100.00	100.00	100.00
Spect-heart	267	22	2	83.75	84.45	85.80	86.05	86.50	86.70	92.33	92.60	92.33	92.83	92.70	93.40
Spectf-heart	267	44	2	88.20	91.25	90.80	94.65	93.15	95.90	97.92	98.45	97.92	100.00	98.30	99.80
Cylinder-bands	277	39	2	79.47	80.63	82.37	88.21	85.99	89.23	95.33	95.31	95.33	99.76	95.65	99.90
Heart-disease-Cleveland	282	13	5	71.37	72.09	73.18	74.36	74.79	75.97	97.55	97.63	97.71	97.71	97.55	97.82
Haberman-survival	306	3	2	80.48	81.97	82.79	83.89	84.89	85.02	87.85	89.61	87.85	91.19	89.17	92.93
Ionosphere	351	34	2	94.75	95.93	95.70	96.31	96.88	97.30	99.68	99.85	99.68	99.94	99.70	99.92
Dermatology	358	34	6	92.46	93.92	95.19	95.37	95.75	95.78	99.44	99.40	99.44	99.56	99.48	99.55
Thoracic-surgery	470	16	2	87.53	87.98	87.98	89.09	88.86	89.72	92.61	92.22	92.61	94.22	92.84	95.34
Body	507	5	2	96.76	97.24	97.84	98.29	98.37	98.47	99.91	100.00	99.91	100.00	99.91	99.95
Climate-model-crashes	540	20	2	96.07	96.59	96.62	97.48	97.11	97.95	99.92	99.93	99.92	100.00	99.92	100.00
Monks-problems-3	554	6	2	98.87	98.87	98.87	98.87	98.87	98.87	98.96	99.01	99.04	99.04	99.13	99.13
Monks-problems-1	556	6	2	81.77	95.08	93.12	93.50	96.04	97.58	96.32	100.00	100.00	100.00	100.00	100.00
Breast-cancer-diagnosti	569	30	2	98.19	98.52	98.57	98.92	99.11	99.27	100.00	100.00	100.00	100.00	100.00	100.00
Indian-liver-patient	579	10	2	74.22	77.72	78.23	81.96	80.48	82.37	82.76	84.65	82.91	95.12	84.01	97.14
Monks-problems-2	600	6	2	69.42	70.16	71.56	71.98	72.44	72.51	99.41	99.71	99.48	99.96	99.96	100.00
Balance-scale	625	4	3	80.11	82.26	84.19	84.68	84.79	84.85	95.58	95.45	95.58	95.58	95.73	95.85
Credit-approval	653	15	2	88.67	89.28	90.08	90.90	90.86	91.37	95.74	96.11	95.77	97.82	95.74	98.90
Breast-cancer	683	9	2	97.70	97.91	98.24	98.50	98.67	98.77	99.74	99.82	99.74	99.90	99.74	99.96
Blood-transfusion	748	4	2	80.41	81.14	82.26	82.62	82.80	82.85	86.30	86.49	86.36	88.32	86.88	89.45
Mammographic-mass	830	5	2	85.71	86.09	86.82	87.04	87.28	87.38	89.39	89.73	89.47	90.97	89.71	91.93
Tic-tac-toe-endgame	958	9	2	77.51	81.25	82.74	85.35	85.00	85.65	95.26	95.77	95.26	99.72	95.26	99.89
Connectionist-bench	990	13	11	54.58	58.81	59.12	60.80	60.35	61.99	94.61	95.61	94.70	97.21	95.74	98.46
Statlog-project-German-credit	1,000	20	2	76.71	77.53	78.81	80.09	79.75	80.29	87.40	88.01	87.40	94.60	87.40	95.47
Concrete	1,030	8	3	75.54	77.51	78.58	79.55	79.20	79.86	94.26	95.04	94.34	96.98	95.03	97.69
Qsar-biodegradation	1,055	41	2	85.50	86.62	87.21	88.33	88.24	88.98	94.71	95.22	94.73	97.70	95.12	98.36
Banknote-authentication	1,372	4	2	97.76	99.17	99.49	99.55	99.56	99.68	99.98	100.00	99.98	100.00	99.98	100.00
Contraceptive-method-choice	1,473	9	3	57.32	57.86	58.63	60.27	59.76	60.57	65.66	66.01	65.88	75.94	67.52	77.63
Car-evaluation	1,728	6	4	83.80	85.57	86.42	86.53	86.98	86.98	96.82	96.91	96.99	97.56	96.94	97.30
Ozone-level-detection-eight	1,847	72	2	94.48	94.96	94.74	95.88	95.20	96.24	98.58	98.77	98.58	99.46	98.58	99.29
Ozone-level-detection-one	1,848	72	2	97.48	97.73	97.65	97.99	97.81	98.32	99.12	99.39	99.15	99.69	99.32	99.75
Seismic-bumps	2,584	18	2	93.82	94.08	93.98	94.32	94.15	94.55	96.04	96.20	96.04	96.78	96.04	96.89
Chess-king-rook-versus-king-pawn	3,196	36	2	94.19	94.35	94.19	94.19	94.19	94.21	98.50	98.42	98.50	98.56	98.51	98.51
Thyroidann	3,772	21	3	99.70	99.70	99.72	99.73	99.73	99.73	99.99	100.00	100.00	100.00	100.00	100.00
Statloglansat	4,435	36	6	83.02	85.03	85.66	86.10	86.55	86.63	93.38	94.06	93.38	94.94	94.40	95.38
Spambase	4,601	57	2	90.77	91.50	91.78	91.97	92.05	92.25	95.21	95.59	95.44	95.85	95.76	96.36
Wall-following-robot-2	5,456	2	4	99.97	100.00	99.99	99.99	99.99	99.99	99.95	100.00	99.98	99.98	99.97	99.98
Pageblock	5,473	10	5	96.74	96.94	97.04	97.28	97.42	97.51	98.65	98.86	98.65	99.17	98.89	99.37
Optical-recognition	5,620	62	10	72.76	74.51	75.37	76.82	76.51	77.27	96.60	96.65	96.61	97.70	96.94	98.06
Statlog-project-landsat-satellite	6,435	36	6	82.18	84.38	84.82	85.45	85.73	85.87	92.37	93.23	92.37	93.76	93.44	94.29
Thyroid-disease-ann-thyroid	7,200	21	3	99.53	99.53	99.54	99.54	99.56	99.57	99.96	99.98	99.97	99.97	99.99	99.99
Pendigits	7,494	16	10	80.86	82.88	83.27	83.79	84.41	84.99	97.96	98.24	97.97	98.76	98.32	99.07

Table 12 continued from previous page

Dataset	Sample	Feature	Class	Depth=4				Depth=8							
				CART	LS-OCT	DEOCT	MH-DEOCT	DEOCT (Long)	MH-DEOCT (Long)	CART	LS-OCT	DEOCT	MH-DEOCT	DEOCT (Long)	MH-DEOCT (Long)
Avila	10,430	10	12	57.24	60.33	60.98	61.34	61.33	61.59	76.77	79.84	77.97	81.81	79.37	84.60
Eeg	14,980	14	2	70.12	71.94	72.36	73.37	72.87	74.01	79.31	81.93	80.50	86.72	82.30	88.07
Htru	17,898	8	2	97.94	98.11	98.15	98.22	98.24	98.26	98.66	98.74	98.66	98.89	98.71	99.03
Shuttle	43,500	9	7	99.83	99.92	99.94	99.94	99.95	99.95	100.00	100.00	100.00	100.00	100.00	100.00
Skinsegmentation	245,057	3	2	97.42	98.41	98.81	98.82	98.94	98.94	99.50	99.75	99.80	99.95	99.85	99.96
Htsensor	928,991	11	3	68.66	70.89	71.28	72.21	71.37	72.75	83.57	-	84.61	92.85	86.85	94.35
Average Training Accuracy (%)				87.62	88.87	89.33	90.24	90.26	90.80	95.67	96.26	95.82	97.30	96.14	97.66

Table 13: Depth=4,8 training accuracy standard deviation (%) on 65 datasets with 10 splits within 1 million samples

Dataset	Sample	Feature	Class	Depth=4				Depth=8							
				CART	LS-OCT	DEOCT	MH-DEOCT	DEOCT (Long)	MH-DEOCT (Long)	CART	LS-OCT	DEOCT	MH-DEOCT	DEOCT (Long)	MH-DEOCT (Long)
Soybean-small	47	35	4	0.00	0.00	0.00	0.00	0.00	0.00	0.00	0.00	0.00	0.00	0.00	0.00
Echocardiogram	61	11	2	0.00	0.00	0.00	0.00	0.00	0.00	0.00	0.00	0.00	0.00	0.00	0.00
Hepatitis	80	19	2	0.81	0.76	0.81	0.53	0.00	0.00	0.00	0.00	0.00	0.00	0.00	0.00
Fertility	100	9	2	2.16	1.71	1.51	1.47	1.43	1.17	1.17	0.69	1.00	0.92	0.60	0.60
Acute-inflammations-1	120	6	2	0.00	0.00	0.00	0.00	0.00	0.00	0.00	0.00	0.00	0.00	0.00	0.00
Acute-inflammations-2	120	6	2	0.00	0.00	0.00	0.00	0.00	0.00	0.00	0.00	0.00	0.00	0.00	0.00
Hayes-roth	132	5	3	1.45	2.66	2.79	3.63	2.45	2.13	1.64	1.09	2.09	1.01	0.90	1.32
Iris	150	4	3	0.62	0.44	0.38	0.38	0.38	0.28	0.00	0.00	0.00	0.00	0.00	0.00
Teaching-assistant-evaluation	151	5	3	6.12	3.07	3.13	2.45	2.28	2.33	5.10	4.07	3.93	1.75	4.50	2.37
Wine	178	13	3	0.53	0.00	0.24	0.00	0.00	0.00	0.24	0.00	0.00	0.00	0.00	0.00
Breast-cancer-prognostic	194	31	2	2.51	1.18	1.08	1.24	0.94	0.91	1.36	0.89	1.26	0.00	1.38	0.30
Parkinsons	195	23	2	0.48	0.45	0.29	0.00	0.00	0.00	0.00	0.00	0.00	0.00	0.00	0.00
Connectionist-bench-sonar	208	60	2	2.27	2.13	2.00	1.44	1.46	0.73	0.31	0.00	0.33	0.00	0.35	0.00
Image-segmentation	210	19	7	3.74	1.87	1.88	1.06	1.09	1.51	0.54	0.00	0.52	0.24	0.28	0.28
Seeds	210	7	3	0.92	0.64	0.67	0.59	0.67	0.59	0.20	0.00	0.60	0.00	0.00	0.00
Glass	214	9	6	2.18	2.45	2.92	0.94	1.74	2.40	0.79	0.55	0.61	0.29	0.77	0.28
Thyroid-disease-new-thyroid	215	5	3	0.73	0.41	0.43	0.43	0.26	0.26	0.30	0.00	0.32	0.00	0.28	0.28
Congressional-voting-records	232	16	2	0.73	0.59	0.40	0.53	0.40	0.45	0.18	0.18	0.00	0.00	0.00	0.00
Spect-heart	267	22	2	1.30	1.08	0.79	0.83	0.88	0.98	1.45	1.35	0.98	0.69	1.04	1.08
Spectf-heart	267	44	2	2.28	1.17	1.21	2.06	1.06	1.71	1.81	1.69	1.99	0.00	1.82	0.27
Cylinder-bands	277	39	2	2.60	1.90	1.71	1.61	1.12	1.42	2.78	2.79	2.96	0.24	2.98	0.22
Heart-disease-Cleveland	282	13	5	2.35	2.42	1.75	1.98	1.56	2.07	1.17	1.09	0.97	0.88	0.79	1.04
Haberman-survival	306	3	2	1.44	1.03	1.15	1.39	0.75	0.74	2.73	2.49	2.59	1.88	2.42	2.03
Ionosphere	351	34	2	1.33	0.80	0.93	0.72	0.71	0.85	0.38	0.27	0.29	0.14	0.32	0.17
Dermatology	358	34	6	4.57	2.29	0.92	0.71	0.44	0.47	0.31	0.26	0.31	0.33	0.33	0.31
Thoracic-surgery	470	16	2	1.20	0.90	0.91	0.91	0.84	0.86	1.53	1.47	1.28	1.22	1.50	1.43
Body	507	5	2	0.87	0.66	0.46	0.59	0.65	0.70	0.18	0.00	0.14	0.00	0.14	0.12
Climate-model-crashes	540	20	2	0.86	0.53	0.49	0.42	0.44	0.35	0.17	0.17	0.13	0.00	0.14	0.00
Monks-problems-3	554	6	2	0.30	0.29	0.30	0.30	0.30	0.30	0.28	0.27	0.26	0.24	0.22	0.22
Monks-problems-1	556	6	2	4.06	2.05	0.48	1.11	2.00	0.41	3.25	0.00	0.00	0.00	0.00	0.00
Breast-cancer-diagnosti	569	30	2	0.60	0.30	0.37	0.48	0.24	0.23	0.07	0.00	0.00	0.00	0.00	0.00
Indian-liver-patient	579	10	2	1.31	1.49	1.07	1.83	1.15	1.63	2.38	1.30	2.80	1.88	1.96	1.19
Monks-problems-2	600	6	2	0.91	0.83	0.44	0.52	0.42	0.43	2.63	0.91	0.71	0.08	0.10	0.00
Balance-scale	625	4	3	1.67	0.85	0.98	0.65	0.60	0.71	0.87	0.87	0.50	0.46	0.54	0.36
Credit-approval	653	15	2	0.98	0.65	0.50	0.53	0.59	0.60	1.58	1.38	2.19	0.61	1.57	0.37
Breast-cancer	683	9	2	0.39	0.28	0.26	0.31	0.29	0.35	0.19	0.19	0.20	0.15	0.22	0.09
Blood-transfusion	748	4	2	0.79	0.71	0.72	0.75	0.60	0.62	0.90	1.00	1.12	1.09	0.72	1.92
Mammographic-mass	830	5	2	0.73	0.55	0.49	0.53	0.70	0.61	0.69	0.65	0.68	1.20	1.03	0.92
Tic-tac-toe-endgame	958	9	2	1.36	0.92	0.71	0.74	0.90	0.53	0.97	0.83	1.03	0.11	1.09	0.12
Connectionist-bench	990	13	11	2.07	1.22	1.31	1.73	0.98	0.87	1.01	0.99	1.11	0.96	1.13	0.45
Statlog-project-German-credit	1,000	20	2	2.16	1.49	0.82	0.46	0.76	0.68	0.99	1.14	1.03	0.51	0.33	2.13
Concrete	1,030	8	3	1.51	1.09	0.97	0.63	0.67	0.66	1.27	0.95	1.15	0.86	1.21	0.75
Qsar-biodegradation	1,055	41	2	1.34	1.14	0.67	0.64	0.78	0.66	1.59	1.55	2.02	0.37	1.76	0.54
Banknote-authentication	1,372	4	2	1.13	0.36	0.10	0.08	0.15	0.16	0.07	0.00	0.04	0.00	0.04	0.00
Contraceptive-method-choice	1,473	9	3	0.71	0.64	0.87	0.73	0.60	0.54	1.18	1.26	1.20	0.67	0.98	0.93
Car-evaluation	1,728	6	4	0.48	0.87	0.55	0.54	0.55	0.55	0.40	0.39	0.29	0.42	0.22	0.05
Ozone-level-detection-eight	1,847	72	2	0.44	0.35	0.43	0.49	0.35	0.30	0.56	0.50	0.60	0.24	0.67	0.32
Ozone-level-detection-one	1,848	72	2	0.37	0.23	0.24	0.22	0.17	0.29	0.45	0.43	0.45	0.23	0.36	0.16
Seismic-bumps	2,584	18	2	0.23	0.20	0.17	0.17	0.17	0.20	0.38	0.37	0.37	0.58	0.33	0.28
Chess-king-rook-versus-king-pawn	3,196	36	2	0.25	0.28	0.25	0.25	0.25	0.26	0.15	0.15	0.09	0.12	0.10	0.10
Thyroidann	3,772	21	3	0.06	0.06	0.05	0.05	0.05	0.06	0.01	0.01	0.00	0.00	0.00	0.00
Statloglansat	4,435	36	6	0.55	0.68	0.52	0.61	0.59	0.52	0.42	0.35	0.43	0.38	0.45	0.25
Spambase	4,601	57	2	0.25	0.26	0.37	0.31	0.26	0.36	0.69	0.45	0.24	0.33	0.30	0.30
Wall-following-robot-2	5,456	2	4	0.07	0.00	0.05	0.04	0.05	0.04	0.07	0.00	0.06	0.05	0.07	0.05
Pageblock	5,473	10	5	0.12	0.09	0.13	0.18	0.19	0.16	0.12	0.07	0.11	0.17	0.05	0.08
Optical-recognition	5,620	62	10	0.79	0.79	0.70	0.63	0.61	0.54	0.21	0.26	0.14	0.19	0.15	0.18
Statlog-project-landsat-satellite	6,435	36	6	0.70	0.53	0.43	0.24	0.36	0.34	0.38	0.35	0.34	0.39	0.33	0.31
Thyroid-disease-ann-thyroid	7,200	21	3	0.04	0.04	0.04	0.04	0.06	0.06	0.04	0.03	0.03	0.03	0.03	0.03
Pendigits	7,494	16	10	0.42	0.68	0.55	0.29	0.35	0.70	0.26	0.19	0.24	0.20	0.25	0.13
Avila	10,430	10	12	0.63	0.39	0.33	0.37	0.32	0.39	1.32	0.87	1.15	2.38	0.84	2.73
Eeg	14,980	14	2	1.04	0.55	0.45	0.57	0.49	0.60	0.93	0.67	0.88	0.92	0.93	0.47
Htru	17,898	8	2	0.09	0.06	0.09	0.08	0.07	0.07	0.10	0.09	0.09	0.09	0.11	0.11
Shuttle	43,500	9	7	0.02	0.03	0.01	0.01	0.01	0.01	0.02	0.00	0.02	0.00	0.00	0.00
Skinsegmentation	245,057	3	2	0.02	0.10	0.08	0.07	0.01	0.01	0.02	0.03	0.03	0.01	0.01	0.01
Htsensor	928,991	11	3	0.03	0.07	0.19	0.23	0.27	0.16	0.10	-	0.52	1.38	0.31	1.39
Average Training Accuracy STD (%)				1.12	0.80	0.70	0.67	0.59	0.59	0.78	0.59	0.67	0.41	0.60	0.45

E.2 Testing accuracy (%) on 65 datasets within 1 million samples

Table 14: Depth=2 average testing accuracy (%) on 65 datasets with 10 random splits within 1 million samples

Dataset	Sample	Feature	Class	Depth=2							
				CART	LS-OCT	Quant-BnB	RS-OCT	DEOCT	MH-DEOCT	DEOCT (Long)	MH-DEOCT (Long)
Soybean-small	47	35	4	98.33	98.33	98.33	100.00	98.33	100.00	98.33	100.00
Echocardiogram	61	11	2	96.25	96.25	97.50	97.50	95.63	98.13	95.63	97.50
Hepatitis	80	19	2	81.00	80.50	78.00	81.00	80.50	79.50	80.00	78.50
Fertility	100	9	2	88.80	84.00	84.40	85.60	86.00	86.40	85.20	86.00
Acute-inflamations-1	120	6	2	92.33	100.00	100.00	100.00	100.00	100.00	100.00	100.00
Acute-inflamations-2	120	6	2	100.00	100.00	99.67	100.00	100.00	100.00	100.00	100.00
Hayes-roth	132	5	3	46.06	46.06	51.21	51.21	50.30	50.30	50.61	50.61
Iris	150	4	3	95.00	94.47	93.95	93.95	95.00	94.47	95.00	93.95
Teaching-assistant-evaluation	151	5	3	38.95	45.26	43.95	45.79	47.63	45.26	47.11	45.26
Wine	178	13	3	87.33	91.56	90.67	91.11	91.11	90.89	90.44	90.89
Breast-cancer-prognostic	194	31	2	71.60	69.80	69.40	69.40	67.80	66.80	69.20	68.40
Parkinsons	195	23	2	87.14	88.16	90.61	92.25	87.76	87.14	86.53	87.96
Connectionist-bench-sonar	208	60	2	69.23	68.65	72.50	70.58	71.73	71.92	69.42	71.15
Image-segmentation	210	19	7	50.00	50.57	47.55	47.55	47.74	46.60	46.60	46.60
Seeds	210	7	3	88.87	89.43	89.62	89.62	87.74	88.49	87.74	88.30
Glass	214	9	6	60.74	61.85	61.11	62.59	61.30	60.93	60.56	61.11
Thyroid-disease-new-thyroid	215	5	3	87.59	91.11	92.04	92.04	90.00	90.37	91.48	91.67
Congressional-voting-records	232	16	2	97.93	97.93	97.93	97.93	97.93	97.93	97.93	97.93
Spect-heart	267	22	2	75.07	75.07	75.07	75.07	75.07	75.07	75.07	75.07
Spectf-heart	267	44	2	74.93	74.33	72.24	72.24	74.48	73.43	73.43	73.13
Cylinder-bands	277	39	2	59.29	62.00	62.57	62.57	63.29	63.43	62.29	62.00
Heart-disease-Cleveland	282	13	5	56.34	55.21	53.38	53.52	54.08	53.94	53.80	53.80
Haberman-survival	306	3	2	72.73	72.21	72.86	72.86	73.51	73.12	73.38	73.51
Ionosphere	351	34	2	89.20	88.86	86.48	85.68	87.73	87.84	88.52	88.41
Dermatology	358	34	6	71.11	75.89	75.56	75.56	76.11	75.67	76.11	75.67
Thoracic-surgery	470	16	2	85.59	85.00	83.98	83.98	84.83	84.92	83.98	84.58
Body	507	5	2	88.35	89.92	89.92	89.92	88.66	88.66	89.45	89.53
Climate-model-crashes	540	20	2	90.67	91.11	90.89	91.19	90.96	91.48	91.70	91.63
Monks-problems-3	554	6	2	96.26	96.26	96.26	96.26	96.26	96.26	96.26	96.26
Monks-problems-1	556	6	2	76.55	76.76	76.62	76.76	76.62	76.62	76.69	76.69
Breast-cancer-diagnosti	569	30	2	90.91	93.01	93.36	93.78	93.22	93.22	93.71	93.78
Indian-liver-patient	579	10	2	72.41	70.69	69.45	70.41	70.41	70.90	70.14	70.21
Monks-problems-2	600	6	2	65.33	64.20	64.20	64.20	64.20	64.20	64.20	64.20
Balance-scale	625	4	3	65.16	68.73	68.54	68.54	68.54	68.54	68.54	68.54
Credit-approval	653	15	2	86.16	85.73	85.61	85.12	85.79	85.79	85.49	85.61
Breast-cancer	683	9	2	91.99	95.85	96.49	96.49	96.02	96.37	96.49	96.49
Blood-transfusion	748	4	2	72.78	75.19	73.37	73.64	73.96	73.42	74.17	74.17
Mammographic-mass	830	5	2	81.88	82.98	83.08	83.12	82.60	83.08	83.08	83.08
Tic-tac-toe-endgame	958	9	2	69.37	67.38	67.38	67.38	67.04	67.38	67.04	67.38
Connectionist-bench	990	13	11	27.22	31.69	32.06	32.06	31.21	31.49	32.22	32.02
Statlog-project-German-credit	1,000	20	2	71.12	71.40	72.64	72.96	72.72	72.56	72.72	72.56
Concrete	1,030	8	3	60.27	62.13	62.64	62.33	62.95	62.91	63.49	63.02
Qsar-biodegradation	1,055	41	2	75.27	78.64	77.84	77.84	78.86	78.64	78.60	78.71
Banknote-authentication	1,372	4	2	88.69	91.43	91.22	91.37	91.37	91.25	91.52	91.72
Contraceptive-method-choice	1,473	9	3	46.80	54.99	54.88	55.04	53.63	54.74	54.80	54.80
Car-evaluation	1,728	6	4	77.31	77.31	77.31	77.36	77.31	77.31	77.31	77.31
Ozone-level-detection-eight	1,847	72	2	92.64	92.68	92.55	92.23	92.62	92.42	92.38	92.36
Ozone-level-detection-one	1,848	72	2	96.69	96.28	96.30	96.34	96.49	96.49	96.34	96.39
Seismic-bumps	2,584	18	2	93.39	93.19	93.02	93.28	93.11	93.10	93.08	93.11
Chess-king-rook-versus-king-pawn	3,196	36	2	75.58	84.44	86.26	86.26	85.89	85.89	83.28	86.26
Thyroidann	3,772	21	3	97.91	97.91	97.89	97.58	97.91	97.91	97.91	97.91
Statloglansat	4,435	36	6	64.17	68.20	68.43	66.00	68.34	68.34	68.34	68.34
Spambase	4,601	57	2	84.27	86.77	86.93	85.07	86.81	86.89	86.45	86.69
Wall-following-robot-2	5,456	2	4	94.05	94.09	94.06	94.09	94.07	94.07	94.07	94.07
Pageblock	5,473	10	5	94.82	95.22	95.19	95.00	95.23	95.22	95.22	95.22
Optical-recognition	5,620	62	10	34.37	37.38	37.33	35.87	37.59	37.59	38.06	38.08
Statlog-project-landsat-satellite	6,435	36	6	63.80	67.31	67.49	65.35	67.17	67.49	67.20	67.48
Thyroid-disease-ann-thyroid	7,200	21	3	97.50	97.50	97.48	97.17	97.50	97.50	97.50	97.50
Pendigits	7,494	16	10	38.51	39.39	39.12	39.12	38.62	38.86	39.13	38.86
Avila	10,430	10	12	52.63	54.20	54.38	53.93	53.78	53.84	53.78	53.85
Eeg	14,980	14	2	62.41	65.18	66.60	66.42	65.05	65.31	66.15	66.69
Htru	17,898	8	2	97.75	97.85	97.83	97.94	97.73	97.74	97.76	97.77
Shuttle	43,500	9	7	94.00	94.45	95.54	95.54	94.28	94.46	94.69	94.69
Skinsegmentation	245,057	3	2	90.72	92.68	92.70	92.69	92.70	92.70	92.70	92.70
Htsensor	928,991	11	3	58.07	59.89	59.90	59.65	59.88	59.88	59.87	59.87
Average Testing Accuracy (%)				76.91	78.19	78.20	78.23	78.20	78.21	78.15	78.27

Table 15: Depth=2 testing accuracy standard deviation (%) on 65 datasets with 10 random splits within 1 million samples

Dataset	Sample	Feature	Class	Depth=2							
				CART	LS-OCT	Quant-BnB	RS-OCT	DEOCT	MH-DEOCT	DEOCT (Long)	MH-DEOCT (Long)
Soybean-small	47	35	4	3.51	3.51	5.27	0.00	5.27	0.00	5.27	0.00
Echocardiogram	61	11	2	3.23	3.23	3.23	3.29	3.02	3.02	3.02	3.23
Hepatitis	80	19	2	7.75	8.32	7.89	8.10	8.96	8.64	6.67	9.14
Fertility	100	9	2	7.00	9.61	7.41	6.31	7.83	7.11	6.81	7.60
Acute-inflamations-1	120	6	2	3.53	0.00	0.00	0.00	0.00	0.00	0.00	0.00
Acute-inflamations-2	120	6	2	0.00	0.00	1.05	0.00	0.00	0.00	0.00	0.00
Hayes-roth	132	5	3	5.68	9.24	5.61	8.90	6.73	6.73	5.35	5.35
Iris	150	4	3	3.15	4.01	3.73	3.34	3.15	2.90	3.15	3.73
Teaching-assistant-evaluation	151	5	3	10.87	8.67	9.37	6.70	7.89	5.38	7.69	5.66
Wine	178	13	3	6.38	3.44	3.44	2.96	3.63	3.84	3.78	3.84
Breast-cancer-prognostic	194	31	2	5.32	4.57	3.27	2.99	2.57	3.29	2.86	3.24
Parkinsons	195	23	2	2.16	5.51	3.07	2.85	3.47	5.27	2.40	2.96
Connectionist-bench-sonar	208	60	2	6.47	4.54	5.59	5.59	3.40	3.53	4.84	6.78

Table 15 continued from previous page

Dataset	Sample	Feature	Class	Depth=2							
				CART	LS-OCT	Quant-BnB	RS-OCT	DEOCT	MH-DEOCT	DEOCT (Long)	MH-DEOCT (Long)
Image-segmentation	210	19	7	6.05	5.02	6.64	7.47	6.66	6.66	6.29	6.29
Seeds	210	7	3	4.91	2.84	2.04	3.38	3.90	3.38	4.20	3.65
Glass	214	9	6	6.04	5.53	5.38	6.34	6.08	6.26	6.11	6.23
Thyroid-disease-new-thyroid	215	5	3	5.24	5.51	3.39	3.40	5.25	5.30	3.51	4.39
Congressional-voting-records	232	16	2	2.12	2.12	2.12	2.12	2.12	2.12	2.12	2.12
Spect-heart	267	22	2	4.40	4.40	4.40	3.95	4.40	4.40	4.40	4.40
Spectf-heart	267	44	2	4.38	5.06	5.23	4.23	5.14	5.21	4.76	4.93
Cylinder-bands	277	39	2	4.96	5.44	3.00	3.03	4.26	4.58	3.58	4.22
Heart-disease-Cleveland	282	13	5	4.88	3.68	4.62	4.40	4.51	4.70	4.59	4.59
Haberman-survival	306	3	2	3.30	2.68	2.70	3.01	2.46	2.94	2.75	2.82
Ionosphere	351	34	2	4.36	4.72	6.12	5.20	5.40	5.62	4.50	4.63
Dermatology	358	34	6	8.78	4.13	4.09	5.11	4.03	4.04	4.03	4.04
Thoracic-surgery	470	16	2	2.59	2.12	2.57	2.44	1.81	1.73	1.98	1.82
Body	507	5	2	2.87	3.52	3.54	3.24	3.37	3.28	3.18	3.17
Climate-model-crashes	540	20	2	1.98	2.52	1.75	2.11	2.12	1.22	2.03	1.95
Monks-problems-3	554	6	2	1.43	1.43	1.43	1.43	1.43	1.43	1.43	1.43
Monks-problems-1	556	6	2	3.72	2.58	2.57	2.58	2.57	2.57	2.61	2.61
Breast-cancer-diagnosti	569	30	2	3.09	2.68	1.52	1.91	1.84	1.84	1.92	1.38
Indian-liver-patient	579	10	2	3.66	3.86	3.44	3.04	3.96	4.31	4.06	4.02
Monks-problems-2	600	6	2	3.71	4.26	4.26	4.26	4.26	4.26	4.26	4.26
Balance-scale	625	4	3	4.25	2.57	1.95	2.05	1.95	1.95	1.95	1.95
Credit-approval	653	15	2	2.42	2.93	2.44	2.57	2.74	2.32	2.54	2.25
Breast-cancer	683	9	2	1.68	1.86	1.35	1.35	1.76	1.45	1.35	1.35
Blood-transfusion	748	4	2	2.86	3.37	2.71	2.84	3.10	2.77	3.61	3.61
Mammographic-mass	830	5	2	1.91	1.82	1.96	1.96	1.43	1.43	1.96	1.96
Tic-tac-toe-endgame	958	9	2	2.67	1.63	1.63	1.63	1.35	1.63	1.35	1.63
Connectionist-bench	990	13	11	2.72	2.70	2.15	1.99	2.76	2.13	2.18	2.16
Statlog-project-German-credit	1,000	20	2	3.31	3.08	2.63	2.25	2.75	2.94	2.74	2.93
Concrete	1,030	8	3	3.64	4.10	4.45	4.28	3.62	3.44	3.64	3.44
Qsar-biodegradation	1,055	41	2	3.22	3.03	2.74	40.51	3.03	2.70	2.70	2.74
Banknote-authentication	1,372	4	2	1.05	1.18	0.97	1.01	0.72	0.79	0.99	1.05
Contraceptive-method-choice	1,473	9	3	1.95	2.19	2.40	2.36	2.82	2.90	2.39	2.39
Car-evaluation	1,728	6	4	1.56	1.56	1.56	1.61	1.56	1.56	1.56	1.56
Ozone-level-detection-eight	1,847	72	2	1.08	1.45	1.03	1.53	1.49	1.54	1.16	1.05
Ozone-level-detection-one	1,848	72	2	0.62	0.86	0.45	0.48	0.64	0.70	0.59	0.60
Seismic-bumps	2,584	18	2	0.46	0.61	0.45	0.46	0.59	0.62	0.64	0.61
Chess-king-rook-versus-king-pawn	3,196	36	2	1.39	3.54	1.17	3.80	1.45	1.45	3.82	1.17
Thyroidann	3,772	21	3	0.46	0.46	0.43	0.35	0.46	0.46	0.46	0.46
Statloglansat	4,435	36	6	1.30	0.74	0.71	0.68	0.71	0.68	0.67	0.67
Spambase	4,601	57	2	2.70	0.76	0.68	1.35	0.81	0.65	1.25	0.98
Wall-following-robot-2	5,456	2	4	0.58	0.55	0.56	0.55	0.58	0.58	0.58	0.58
Pageblock	5,473	10	5	0.66	0.65	0.63	0.60	0.63	0.64	0.64	0.64
Optical-recognition	5,620	62	10	0.84	1.07	1.10	1.40	1.32	1.33	1.05	1.06
Statlog-project-landsat-satellite	6,435	36	6	1.10	1.22	1.12	1.13	0.87	1.12	0.86	1.13
Thyroid-disease-ann-thyroid	7,200	21	3	0.33	0.33	0.35	0.50	0.33	0.33	0.33	0.33
Pendigits	7,494	16	10	0.83	0.89	1.45	1.03	1.20	1.23	1.20	1.23
Avila	10,430	10	12	1.13	0.83	0.85	0.56	0.96	1.00	1.00	0.87
Eg	14,980	14	2	0.75	1.09	0.54	0.59	0.96	1.01	0.75	0.60
Htru	17,898	8	2	0.25	0.21	0.20	0.11	0.20	0.20	0.24	0.24
Shuttle	43,500	9	7	0.12	0.51	0.12	0.16	0.32	0.32	0.30	0.30
Skinsegmentation	245,057	3	2	0.12	0.13	0.13	0.13	0.13	0.13	0.13	0.13
Htsensor	928,991	11	3	0.06	0.08	0.07	0.07	0.07	0.07	0.09	0.09
Average Testing Accuracy STD (%)				3.01	2.87	2.63	3.16	2.69	2.58	2.60	2.56

Table 16: Depth=3 average testing accuracy (%) on 65 datasets with 10 random splits within 1 million samples

Dataset	Sample	Feature	Class	Depth=3						
				CART	LS-OCT	Quant-BnB	DEOCT	MH-DEOCT	DEOCT (Long)	MH-DEOCT (Long)
Soybean-small	47	35	4	98.33	98.33	-	98.33	100.00	98.33	100.00
Echocardiogram	61	11	2	96.25	96.25	100.00	98.13	96.25	96.88	98.13
Hepatitis	80	19	2	81.00	78.00	80.00	79.50	81.00	80.00	80.00
Fertility	100	9	2	82.80	82.80	80.80	80.80	81.20	82.40	80.40
Acute-inflammations-1	120	6	2	99.33	99.33	100.00	100.00	99.00	100.00	100.00
Acute-inflammations-2	120	6	2	100.00	100.00	100.00	100.00	100.00	100.00	99.67
Hayes-roth	132	5	3	53.33	50.91	52.73	53.94	54.55	53.64	52.42
Iris	150	4	3	95.79	95.79	95.26	96.32	96.05	95.79	96.05
Teaching-assistant-evaluation	151	5	3	46.84	52.11	58.95	56.05	57.89	57.11	57.63
Wine	178	13	3	88.89	92.89	93.33	90.89	91.78	92.67	92.22
Breast-cancer-prognostic	194	31	2	70.40	71.40	68.00	69.00	71.20	66.80	69.00
Parkinsons	195	23	2	89.39	91.02	98.78	91.02	90.61	91.63	91.84
Connectionist-bench-sonar	208	60	2	70.19	69.62	76.15	70.77	71.15	74.62	73.65
Image-segmentation	210	19	7	75.66	80.57	-	76.04	77.36	76.60	78.68
Seeds	210	7	3	87.36	90.00	90.57	88.68	89.43	90.94	91.32
Glass	214	9	6	62.78	63.15	70.00	62.59	66.67	65.74	66.30
Thyroid-disease-new-thyroid	215	5	3	92.41	92.22	91.48	92.59	92.41	92.22	91.85
Congressional-voting-records	232	16	2	97.24	97.24	94.14	97.07	97.07	96.38	96.38
Spect-heart	267	22	2	74.03	74.18	72.24	74.18	73.88	73.28	73.13
Spectf-heart	267	44	2	74.18	73.43	70.75	73.28	71.94	73.88	72.54
Cylinder-bands	277	39	2	60.86	65.57	-	62.86	66.57	65.57	64.57
Heart-disease-Cleveland	282	13	5	56.06	55.77	51.83	53.38	52.54	52.96	52.82
Haberman-survival	306	3	2	72.34	72.21	71.43	71.56	71.17	70.00	70.26
Ionosphere	351	34	2	89.77	88.41	-	88.41	88.41	86.36	86.02
Dermatology	358	34	6	81.67	86.89	87.56	89.00	88.89	88.33	88.78
Thoracic-surgery	470	16	2	83.56	83.47	81.69	83.39	83.73	83.64	83.39
Body	507	5	2	89.06	93.07	92.76	91.81	91.81	90.24	91.10

Table 16 continued from previous page

Dataset	Sample	Feature	Class	Depth=3						
				CART	LS-OCT	Quant-BnB	DEOCT	MH-DEOCT	DEOCT (Long)	MH-DEOCT (Long)
Climate-model-crashes	540	20	2	89.78	90.30	91.41	91.19	91.48	90.59	90.00
Monks-problems-3	554	6	2	96.12	96.12	98.85	95.83	95.83	95.83	95.83
Monks-problems-1	556	6	2	78.71	86.04	88.78	82.01	84.17	84.75	84.75
Breast-cancer-diagnosti	569	30	2	92.87	94.27	93.57	93.85	94.69	94.13	93.92
Indian-liver-patient	579	10	2	70.55	71.45	69.93	69.24	69.93	68.62	68.97
Monks-problems-2	600	6	2	61.40	59.40	55.87	57.80	57.53	57.20	57.33
Balance-scale	625	4	3	69.62	72.80	71.72	72.87	72.80	72.23	72.04
Credit-approval	653	15	2	85.30	85.37	83.66	84.63	84.51	84.63	84.70
Breast-cancer	683	9	2	95.67	95.91	96.26	96.20	96.02	95.38	95.79
Blood-transfusion	748	4	2	76.95	77.43	77.22	77.75	77.65	77.70	77.43
Mammographic-mass	830	5	2	83.13	82.36	82.02	82.55	81.92	82.45	82.12
Tic-tac-toe-endgame	958	9	2	68.58	73.46	71.17	72.92	73.00	72.96	72.92
Connectionist-bench	990	13	11	39.03	39.15	43.95	41.81	42.02	41.49	43.63
Statlog-project-German-credit	1,000	20	2	73.76	73.32	75.20	74.36	73.76	74.28	73.80
Concrete	1,030	8	3	66.05	66.98	71.32	67.91	69.07	68.10	68.37
Qsar-biodegradation	1,055	41	2	78.41	79.58	82.27	80.38	81.29	81.25	81.74
Banknote-authentication	1,372	4	2	95.16	96.12	97.49	96.50	96.68	96.47	97.17
Contraceptive-method-choice	1,473	9	3	51.73	56.12	56.91	55.96	56.26	56.37	56.83
Car-evaluation	1,728	6	4	79.70	79.63	81.06	80.37	80.16	80.28	80.28
Ozone-level-detection-eight	1,847	72	2	92.62	92.10	92.64	92.49	92.36	92.34	92.21
Ozone-level-detection-one	1,848	72	2	96.28	96.28	94.94	96.43	96.10	96.32	96.08
Seismic-bumps	2,584	18	2	93.11	92.88	-	92.94	92.91	92.79	92.71
Chess-king-rook-versus-king-pawn	3,196	36	2	89.89	92.44	93.16	89.89	89.89	90.28	91.41
Thyroidann	3,772	21	3	99.25	99.26	99.17	99.25	99.25	99.24	99.24
Statloglansat	4,435	36	6	78.68	80.58	82.96	82.48	82.53	82.69	82.59
Spambase	4,601	57	2	86.84	89.52	89.66	89.39	89.61	89.32	89.30
Wall-following-robot-2	5,456	2	4	99.96	100.00	99.93	99.98	99.97	99.98	99.97
Pageblock	5,473	10	5	95.95	96.08	96.54	96.15	96.27	96.03	96.17
Optical-recognition	5,620	62	10	56.57	58.35	59.98	58.67	58.97	59.44	59.64
Statlog-project-landsat-satellite	6,435	36	6	78.45	80.56	82.96	82.31	82.70	82.80	82.80
Thyroid-disease-ann-thyroid	7,200	21	3	99.07	99.07	98.93	99.09	99.09	99.09	99.09
Pendigits	7,494	16	10	62.52	66.53	67.76	66.46	66.63	67.98	68.07
Avila	10,430	10	12	54.01	57.96	58.56	56.92	57.30	57.10	57.11
Eeg	14,980	14	2	65.85	68.21	69.95	68.11	68.73	68.84	69.17
Htru	17,898	8	2	97.80	97.88	97.92	97.88	97.88	97.89	97.90
Shuttle	43,500	9	7	99.64	99.78	99.84	99.79	99.80	99.80	99.83
Skinsegmentation	245,057	3	2	96.48	96.59	96.84	96.58	96.59	96.58	96.62
Htsensor	928,991	11	3	64.43	67.69	65.47	67.44	67.71	67.69	67.72
Average Testing Accuracy (%)				80.45	81.57	81.90	81.48	81.78	81.64	81.74

Table 17: Depth=3 testing accuracy standard deviation (%) on 65 datasets with 10 random splits within 1 million samples

Dataset	Sample	Feature	Class	Depth=3						
				CART	LS-OCT	Quant-BnB	DEOCT	MH-DEOCT	DEOCT (Long)	MH-DEOCT (Long)
Soybean-small	47	35	4	3.51	3.51	-	5.27	0.00	5.27	0.00
Echocardiogram	61	11	2	3.23	3.23	0.00	3.02	6.04	4.42	3.02
Hepatitis	80	19	2	7.38	8.56	6.12	7.25	4.59	5.77	4.71
Fertility	100	9	2	8.65	5.35	9.96	10.12	8.01	9.28	8.10
Acute-inflamations-1	120	6	2	2.11	2.11	0.00	0.00	3.16	0.00	0.00
Acute-inflamations-2	120	6	2	0.00	0.00	0.00	0.00	0.00	0.00	1.05
Hayes-roth	132	5	3	5.38	10.08	11.26	7.67	8.08	9.48	9.04
Iris	150	4	3	3.33	3.96	4.32	2.83	3.77	3.96	3.97
Teaching-assistant-evaluation	151	5	3	13.06	8.30	10.29	10.31	8.13	7.85	8.18
Wine	178	13	3	6.79	3.44	2.72	4.38	4.45	5.03	4.83
Breast-cancer-prognostic	194	31	2	5.15	4.62	6.32	5.60	5.59	5.18	6.13
Parkinsons	195	23	2	3.82	4.43	2.74	3.75	3.22	4.13	4.61
Connectionist-bench-sonar	208	60	2	6.92	6.71	3.99	4.23	4.97	3.72	4.35
Image-segmentation	210	19	7	6.32	3.09	-	4.71	5.90	6.43	6.60
Seeds	210	7	3	3.33	3.21	4.81	3.77	4.38	4.94	4.38
Glass	214	9	6	4.57	4.90	5.46	6.34	8.28	6.00	6.40
Thyroid-disease-new-thyroid	215	5	3	4.57	4.08	3.10	4.36	3.65	3.68	2.79
Congressional-voting-records	232	16	2	2.02	2.18	3.36	2.00	2.00	1.90	1.90
Spect-heart	267	22	2	4.83	5.27	5.54	6.10	6.61	8.01	7.99
Spectf-heart	267	44	2	3.59	4.03	4.03	4.69	3.57	3.54	3.93
Cylinder-bands	277	39	2	5.64	5.53	-	5.39	4.82	3.46	5.55
Heart-disease-Cleveland	282	13	5	6.86	6.41	7.68	6.17	6.90	6.94	7.49
Haberman-survival	306	3	2	3.92	3.01	0.92	3.94	3.66	4.48	4.48
Ionosphere	351	34	2	5.25	4.38	-	3.78	3.66	4.01	3.17
Dermatology	358	34	6	7.34	5.41	3.88	3.49	3.19	3.68	3.37
Thoracic-surgery	470	16	2	3.25	3.00	1.54	3.20	3.17	3.77	3.67
Body	507	5	2	3.65	2.19	1.96	3.15	2.86	2.60	2.92
Climate-model-crashes	540	20	2	2.09	1.99	1.44	1.33	1.79	3.00	3.19
Monks-problems-3	554	6	2	1.70	1.70	1.09	1.62	1.62	1.62	1.62
Monks-problems-1	556	6	2	5.01	4.22	2.99	2.56	3.81	2.60	2.51
Breast-cancer-diagnosti	569	30	2	2.08	1.54	1.88	1.27	1.62	1.65	1.84
Indian-liver-patient	579	10	2	4.37	3.38	3.86	3.58	4.15	4.02	3.94
Monks-problems-2	600	6	2	3.02	3.49	2.84	2.37	2.46	2.66	2.67
Balance-scale	625	4	3	3.30	2.15	1.32	2.25	2.23	1.54	1.84
Credit-approval	653	15	2	2.94	2.32	2.42	2.65	2.62	2.62	2.51
Breast-cancer	683	9	2	0.84	1.77	1.21	1.49	1.40	1.69	1.72
Blood-transfusion	748	4	2	2.59	2.62	5.10	3.07	3.12	1.84	2.03
Mammographic-mass	830	5	2	1.37	2.26	2.32	2.27	2.03	2.00	2.02
Tic-tac-toe-endgame	958	9	2	2.91	2.09	0.75	1.48	1.91	1.51	1.51
Connectionist-bench	990	13	11	4.24	3.06	1.10	2.27	2.27	3.35	2.64
Statlog-project-German-credit	1,000	20	2	2.60	3.03	3.96	2.66	2.10	3.57	3.53

Table 17 continued from previous page

Dataset	Sample	Feature	Class	Depth=3						
				CART	LS-OCT	Quant-BnB	DEOCT	MH-DEOCT	DEOCT (Long)	MH-DEOCT (Long)
Concrete	1,030	8	3	3.79	2.69	1.53	2.28	2.16	2.04	2.17
Qsar-biodegradation	1,055	41	2	2.77	2.58	2.64	1.94	2.21	1.80	2.32
Banknote-authentication	1,372	4	2	0.52	0.93	0.44	0.74	0.65	0.83	0.89
Contraceptive-method-choice	1,473	9	3	3.47	2.78	2.39	1.74	1.99	1.79	1.64
Car-evaluation	1,728	6	4	1.59	1.24	0.96	1.70	1.39	1.28	1.28
Ozone-level-detection-eight	1,847	72	2	1.12	1.47	1.47	1.40	1.27	1.14	1.18
Ozone-level-detection-one	1,848	72	2	0.83	0.71	0.36	0.55	0.46	0.74	0.62
Seismic-bumps	2,584	18	2	0.35	0.61	-	0.49	0.49	0.67	0.70
Chess-king-rook-versus-king-pawn	3,196	36	2	0.92	1.74	0.98	0.92	0.92	0.62	1.77
Thyroidann	3,772	21	3	0.28	0.27	0.37	0.25	0.25	0.24	0.24
Statloglansat	4,435	36	6	1.48	1.53	1.31	1.28	1.22	1.44	1.33
Spambase	4,601	57	2	0.76	0.83	1.17	0.79	0.64	0.84	0.84
Wall-following-robot-2	5,456	2	4	0.08	0.00	0.05	0.07	0.09	0.07	0.09
Pageblock	5,473	10	5	0.33	0.27	0.54	0.26	0.30	0.42	0.47
Optical-recognition	5,620	62	10	1.61	2.28	1.10	0.83	0.95	1.23	1.24
Statlog-project-landsat-satellite	6,435	36	6	0.68	0.92	0.60	0.90	0.58	0.60	0.60
Thyroid-disease-ann-thyroid	7,200	21	3	0.17	0.17	0.21	0.18	0.18	0.18	0.18
Pendigits	7,494	16	10	1.77	2.17	0.56	1.11	1.38	1.27	1.32
Avila	10,430	10	12	0.82	1.12	0.58	1.38	1.50	0.89	0.94
Eeg	14,980	14	2	0.83	0.84	0.77	0.71	0.78	0.71	0.81
Htru	17,898	8	2	0.24	0.24	0.21	0.23	0.26	0.25	0.23
Shuttle	43,500	9	7	0.05	0.04	0.02	0.04	0.05	0.04	0.04
Skinsegmentation	245,057	3	2	0.04	0.11	0.06	0.04	0.04	0.04	0.10
Htsensor	928,991	11	3	0.08	0.07	0.06	0.40	0.07	0.06	0.06
Average Testing Accuracy STD (%)				3.05	2.80	2.51	2.72	2.70	2.78	2.73

Table 18: Depth=4,8 average testing accuracy (%) on 65 datasets with 10 random splits within 1 million samples

Dataset	Sample	Feature	Class	Depth=4					Depth=8						
				CART	LS-OCT	DEOCT	MH-DEOCT	DEOCT (Long)	MH-DEOCT (Long)	CART	LS-OCT	DEOCT	MH-DEOCT	DEOCT (Long)	MH-DEOCT (Long)
Soybean-small	47	35	4	98.33	98.33	98.33	98.33	98.33	100.00	98.33	98.33	95.83	100.00	93.33	100.00
Echocardiogram	61	11	2	96.25	96.25	96.25	96.25	95.00	96.25	96.25	96.25	87.50	93.75	85.00	95.00
Hepatitis	80	19	2	81.00	81.00	81.00	82.50	81.00	79.00	81.50	81.50	80.00	80.83	80.00	83.00
Fertility	100	9	2	84.40	84.40	83.60	80.40	82.40	80.80	79.20	74.80	82.67	84.00	80.00	87.20
Acute-inflammations-1	120	6	2	99.33	99.33	100.00	100.00	100.00	100.00	99.33	99.33	100.00	100.00	100.00	100.00
Acute-inflammations-2	120	6	2	100.00	100.00	100.00	100.00	100.00	100.00	100.00	100.00	100.00	100.00	100.00	100.00
Hayes-roth	132	5	3	61.82	60.00	58.18	59.39	65.76	65.45	78.79	69.70	76.77	69.19	72.12	65.45
Iris	150	4	3	96.05	95.00	95.53	95.53	95.53	96.32	96.05	96.05	96.49	95.61	95.79	97.89
Teaching-assistant-evaluation	151	5	3	49.21	55.00	54.74	56.32	55.00	57.63	60.53	60.53	64.04	62.72	66.32	64.21
Wine	178	13	3	89.78	91.56	89.33	91.11	88.89	88.89	89.78	90.00	88.89	90.37	89.33	88.89
Breast-cancer-prognostic	194	31	2	68.60	68.00	67.80	70.00	70.40	68.20	68.20	68.80	68.00	69.00	67.20	65.20
Parkinsons	195	23	2	89.80	89.59	90.41	89.80	91.22	89.80	90.00	89.80	92.52	91.50	92.65	90.20
Connectionist-bench-sonar	208	60	2	72.69	72.69	70.19	73.27	71.15	71.92	73.08	73.08	74.68	71.47	74.23	68.85
Image-segmentation	210	19	7	83.58	83.96	84.72	83.40	84.91	83.02	87.17	87.17	87.74	85.53	86.79	83.40
Seeds	210	7	3	90.00	91.70	91.13	90.57	92.08	90.00	92.08	92.26	90.88	89.62	92.08	89.43
Glass	214	9	6	68.70	67.78	68.89	67.59	67.59	69.26	69.63	69.26	70.99	68.52	71.11	69.63
Thyroid-disease-new-thyroid	215	5	3	91.48	91.85	92.22	91.11	91.85	91.85	92.04	91.85	92.28	90.12	92.22	89.63
Congressional-voting-records	232	16	2	96.03	96.03	97.59	96.03	95.86	95.52	95.34	95.34	96.26	95.69	95.52	94.83
Spect-heart	267	22	2	73.43	76.72	77.16	75.97	74.78	75.07	75.82	74.48	75.87	75.12	76.12	78.21
Spectf-heart	267	44	2	75.22	72.24	73.28	73.28	71.64	73.28	73.13	72.69	74.38	71.39	74.63	73.73
Cylinder-bands	277	39	2	63.71	65.57	65.71	67.57	66.57	67.14	65.43	65.57	65.48	66.43	68.29	63.71
Heart-disease-Cleveland	282	13	5	55.63	53.24	55.49	56.90	56.76	58.73	51.55	51.27	52.35	52.35	52.96	54.65
Haberman-survival	306	3	2	70.13	69.48	69.61	70.13	68.44	69.09	66.36	65.45	67.10	67.53	68.83	67.79
Ionosphere	351	34	2	87.50	87.50	87.61	87.16	87.05	87.84	87.27	86.59	88.64	86.74	88.18	85.00
Dermatology	358	34	6	88.44	92.44	92.00	92.89	92.89	92.89	95.22	94.89	94.44	93.89	93.78	92.89
Thoracic-surgery	470	16	2	83.56	83.05	83.73	82.97	82.63	82.80	81.44	81.10	81.07	80.65	80.51	81.02
Body	507	5	2	91.73	92.20	91.65	92.36	92.91	92.99	92.36	92.36	93.31	92.91	93.54	93.86
Climate-model-crashes	540	20	2	91.33	91.33	91.04	91.33	90.22	90.37	90.89	90.89	90.99	90.12	90.22	91.70
Monks-problems-3	554	6	2	99.06	99.06	99.06	99.06	99.06	99.06	97.70	97.27	97.48	97.72	96.98	96.83
Monks-problems-1	556	6	2	78.20	93.74	90.86	92.01	95.54	96.98	90.58	100.00	100.00	100.00	100.00	100.00
Breast-cancer-diagnosi	569	30	2	94.27	93.78	93.78	94.13	93.15	92.59	93.29	93.22	94.17	93.24	93.71	93.15
Indian-liver-patient	579	10	2	68.90	69.17	68.76	69.24	69.72	69.79	66.62	65.66	67.24	67.01	68.41	66.07
Monks-problems-2	600	6	2	59.73	58.87	60.47	59.60	59.13	58.47	95.33	98.00	96.89	98.56	98.93	98.67
Balance-scale	625	4	3	74.33	78.09	80.32	78.66	78.03	77.58	76.24	77.20	75.80	75.80	76.31	75.29
Credit-approval	653	15	2	84.15	85.00	85.49	84.15	86.71	85.98	83.17	82.80	83.43	82.93	82.80	81.59
Breast-cancer	683	9	2	95.61	96.02	95.61	95.67	95.38	95.56	94.50	94.50	95.32	95.22	95.09	95.67
Blood-transfusion	748	4	2	76.20	76.84	77.65	75.94	75.94	75.78	73.48	74.01	74.06	74.78	74.12	72.83
Mammographic-mass	830	5	2	81.97	82.02	81.88	81.35	81.73	81.11	79.09	78.89	78.04	78.77	78.17	78.75
Tic-tac-toe-endgame	958	9	2	76.17	80.21	78.88	83.04	81.63	82.38	86.62	87.67	86.81	97.50	87.58	97.58
Connectionist-bench	990	13	11	48.39	52.54	51.69	52.50	51.69	52.90	76.90	77.26	78.29	78.23	77.98	77.98
Statlog-project-German-credit	1,000	20	2	73.16	73.32	73.92	72.40	73.36	73.40	71.84	71.20	72.80	71.40	73.44	69.76
Concrete	1,030	8	3	69.22	71.32	71.63	72.13	72.56	71.63	81.09	80.85	80.68	81.59	80.16	81.32
Qsar-biodegradation	1,055	41	2	80.57	81.82	82.01	83.03	82.46	82.27	81.17	81.55	82.51	82.07	84.85	81.36
Banknote-authentication	1,372	4	2	96.41	97.55	98.51	98.51	98.31	98.28	98.31	98.34	98.74	98.59	98.89	98.89
Contraceptive-method-choice	1,473	9	3	55.58	56.48	57.15	56.10	56.15	56.42	53.82	53.17	53.34	51.99	53.88	52.63
Car-evaluation	1,728	6	4	83.03	85.19	85.79	85.51	85.74	85.74	96.27	96.27	96.57	96.45	96.67	95.97
Ozone-level-detection-eight	1,847	72	2	92.34	92.29	92.49	92.19	92.42	92.32	91.39	91.67	91.23	91.45	91.21	90.43
Ozone-level-detection-one	1,848	72	2	96.19	95.95	95.89	96.23	96.30	96.08	95.11	95.04	95.17	94.88	95.28	94.46
Seismic-bumps	2,584	18	2	93.00	92.65	92.72	92.72	92.62	92.79	91.41	90.94	91.56	91.02	91.95	91.11
Chess-king-rook-versus-king-pawn	3,196	36	2	93.78	93.80	93.78	93.78	93.78	93.80	98.37	98.37	98.31	98.39	98.35	98.35
Thyroidann	3,772	21	3	99.47	99.49	99.50	99.48	99.52	99.51	99.80	99.80	99.81	99.75	99.77	99.77
Statloglansat	4,435	36	6	81.25	82.84	83.33	83.64	84.13	84.17	85.28	85.86	85.65	86.70	86.11	86.08
Spambase	4,601	57	2	89.75	90.10	90.32	90.70	90.87	90.87	91.74	91.76	91.92	91.89	91.92	91.61
Wall-following-robot-2	5,456	2	4	99.96	100.00	99.98	99.98	99.98	99.98	99.96	100.00	99.96	99.96	99.96	99.96
Pageblock	5,473	10	5	96.49	96.35	96.57	96.68	96.82	96.97	96.82	96.71	96.99	96.99	96.84	96.67

Table 18 continued from previous page

Dataset	Sample	Feature	Class	Depth=4					Depth=8						
				CART	LS-OCT	DEOCT	MH-DEOCT	DEOCT (Long)	MH-DEOCT (Long)	CART	LS-OCT	DEOCT	MH-DEOCT	DEOCT (Long)	MH-DEOCT (Long)
Optical-recognition	5,620	62	10	71.67	73.30	73.94	75.52	74.93	75.82	90.12	90.15	90.32	90.21	90.38	90.42
Statlog-project-landsat-satellite	6,435	36	6	81.35	82.67	83.39	83.80	84.02	84.26	86.13	86.13	86.42	86.24	86.77	86.08
Thyroid-disease-ann-thyroid	7,200	21	3	99.40	99.40	99.41	99.38	99.41	99.40	99.59	99.61	99.56	99.60	99.60	99.60
Pendigits	7,494	16	10	80.39	81.58	82.42	82.68	83.63	84.11	95.01	95.04	94.72	95.16	94.76	95.51
Avila	10,430	10	12	56.58	59.87	60.46	60.82	60.73	60.86	74.87	77.00	75.11	78.88	76.23	82.42
Eeg	14,980	14	2	69.30	71.16	71.19	72.06	71.58	73.00	76.30	78.43	77.64	81.79	78.37	82.79
Htru	17,898	8	2	97.83	97.92	98.02	97.98	98.00	97.91	97.75	97.66	97.72	97.73	97.74	97.60
Shuttle	43,500	9	7	99.80	99.89	99.92	99.92	99.92	99.93	99.95	99.96	99.96	99.95	99.96	99.96
Skinsegmentation	245,057	3	2	97.37	98.39	98.80	98.80	98.92	98.92	99.49	99.73	99.77	99.92	99.83	99.93
Htsensor	928,991	11	3	68.60	70.86	71.22	72.16	71.30	72.67	83.58	-	84.63	92.78	86.83	94.29
Average Testing Accuracy (%)				82.42	83.32	83.45	83.60	83.63	83.74	85.78	85.80	86.12	86.31	86.17	86.26

Table 19: Depth=4,8 testing accuracy standard deviation (%) on 65 datasets with 10 random splits within 1 million samples

Dataset	Sample	Feature	Class	Depth=4					Depth=8						
				CART	LS-OCT	DEOCT	MH-DEOCT	DEOCT (Long)	MH-DEOCT (Long)	CART	LS-OCT	DEOCT	MH-DEOCT	DEOCT (Long)	MH-DEOCT (Long)
Soybean-small	47	35	4	3.51	3.51	5.27	3.51	5.00	0.00	3.51	3.51	6.97	0.00	10.87	0.00
Echocardiogram	61	11	2	3.23	3.23	3.23	4.37	6.73	6.04	3.23	3.23	9.68	7.91	19.06	8.15
Hepatitis	80	19	2	6.99	6.99	5.68	4.86	7.00	4.59	6.69	6.69	3.16	2.04	3.54	5.46
Fertility	100	9	2	6.65	5.80	6.65	8.32	8.80	9.39	7.00	10.84	7.00	8.39	7.48	12.70
Acute-inflammations-1	120	6	2	2.11	2.11	0.00	0.00	0.00	0.00	2.11	2.11	0.00	0.00	0.00	0.00
Acute-inflammations-2	120	6	2	0.00	0.00	0.00	0.00	0.00	0.00	0.00	0.00	0.00	0.00	0.00	0.00
Hayes-roth	132	5	3	4.33	6.19	7.26	9.81	11.34	8.35	6.23	12.29	7.82	17.92	3.95	12.96
Iris	150	4	3	3.10	4.20	3.73	3.73	3.54	2.83	3.10	3.10	2.15	2.72	2.35	2.20
Teaching-assistant-evaluation	151	5	3	11.17	5.47	5.08	7.25	5.32	8.63	6.56	6.91	6.15	4.22	5.06	3.00
Wine	178	13	3	4.94	5.11	4.29	4.80	4.33	5.34	4.94	4.83	5.07	6.23	5.31	5.67
Breast-cancer-prognostic	194	31	2	4.99	4.42	7.21	5.16	4.27	5.69	4.47	4.54	6.32	5.76	6.72	6.26
Parkinsons	195	23	2	3.33	3.53	4.20	4.19	3.77	4.41	3.11	3.04	2.47	3.96	1.83	1.71
Connectionist-bench-sonar	208	60	2	3.82	4.13	5.68	5.08	6.72	4.17	5.66	5.66	6.01	6.92	6.61	11.16
Image-segmentation	210	19	7	5.34	7.29	6.56	5.02	5.40	5.34	5.54	5.54	4.74	5.02	5.17	5.88
Seeds	210	7	3	3.09	3.47	4.08	4.62	3.46	2.82	3.75	3.82	4.20	5.17	5.40	5.60
Glass	214	9	6	4.23	6.37	4.60	6.66	3.99	5.40	5.47	5.25	4.17	4.38	4.26	4.26
Thyroid-disease-new-thyroid	215	5	3	4.02	4.20	3.79	3.98	4.16	3.72	4.46	4.29	1.39	1.91	2.75	2.48
Congressional-voting-records	232	16	2	2.82	2.82	2.33	2.58	3.79	4.16	2.82	2.82	2.29	2.61	3.78	3.86
Spect-heart	267	22	2	4.92	4.52	5.59	5.56	4.35	5.45	4.49	3.95	5.93	5.14	6.76	3.59
Spectf-heart	267	44	2	3.32	2.46	4.42	5.05	3.66	3.18	5.50	5.93	6.07	3.33	6.76	4.03
Cylinder-bands	277	39	2	6.64	4.69	7.00	4.90	3.90	4.04	5.46	5.49	5.45	2.96	3.41	5.94
Heart-disease-Cleveland	282	13	5	5.64	5.78	6.06	4.84	6.21	5.19	2.50	2.41	3.01	3.01	2.92	6.48
Haberman-survival	306	3	2	4.20	3.31	3.88	3.57	1.54	2.58	4.95	4.79	5.61	5.98	4.40	2.13
Ionosphere	351	34	2	3.86	3.71	3.53	3.97	3.34	3.03	3.11	4.69	2.49	3.91	2.49	2.71
Dermatology	358	34	6	7.20	2.71	2.33	2.58	3.07	3.28	1.89	1.97	2.11	2.79	1.69	2.30
Thoracic-surgery	470	16	2	4.36	4.57	3.39	2.60	3.22	3.92	3.18	3.27	3.46	3.65	2.68	1.95
Body	507	5	2	2.47	2.24	2.07	1.78	1.83	1.80	2.52	2.57	1.91	1.80	2.04	2.69
Climate-model-crashes	540	20	2	2.66	2.26	2.41	1.64	2.01	2.59	2.54	2.54	1.90	2.46	1.69	1.42
Monks-problems-3	554	6	2	0.90	0.90	0.90	0.90	0.85	0.90	1.11	1.55	0.99	1.24	0.94	1.31
Monks-problems-1	556	6	2	4.75	4.00	2.12	3.47	3.21	0.82	7.82	0.00	0.00	0.00	0.00	0.00
Breast-cancer-diagnosti	569	30	2	1.74	1.93	2.71	2.26	1.87	1.69	1.72	1.81	1.69	1.57	1.40	1.15
Indian-liver-patient	579	10	2	4.13	4.23	4.62	4.41	3.54	4.60	3.07	2.13	1.21	4.88	3.14	3.21
Monks-problems-2	600	6	2	4.47	4.75	2.69	3.77	3.18	4.30	6.92	2.15	1.87	1.86	2.03	2.05
Balance-scale	625	4	3	2.57	4.06	4.22	2.99	2.47	2.44	3.21	2.88	3.69	3.69	4.35	5.00
Credit-approval	653	15	2	2.99	3.46	2.57	2.63	1.87	1.91	2.56	1.84	2.74	3.68	2.49	2.09
Breast-cancer	683	9	2	1.21	1.67	1.39	1.70	1.18	1.24	1.66	1.66	1.33	1.54	1.35	0.78
Blood-transfusion	748	4	2	2.88	3.05	2.83	2.56	2.71	3.41	3.15	2.76	3.44	1.77	1.72	1.58
Mammographic-mass	830	5	2	2.55	1.79	1.43	1.78	2.29	1.83	1.80	2.13	1.92	3.73	2.94	3.07
Tic-tac-toe-endgame	958	9	2	2.37	2.06	2.17	2.41	3.17	1.96	2.74	2.90	3.22	1.42	3.55	1.62
Connectionist-bench	990	13	11	3.62	2.74	3.15	2.34	3.37	2.44	4.45	3.80	4.94	2.87	5.32	3.00
Statlog-project-German-credit	1,000	20	2	2.69	3.26	2.56	2.32	2.23	2.01	2.69	2.63	2.95	4.69	2.39	3.62
Concrete	1,030	8	3	2.62	2.79	2.88	3.03	2.44	2.81	2.29	2.67	2.87	2.67	2.35	2.18
Qsar-biodegradation	1,055	41	2	2.99	1.96	1.88	2.47	2.18	3.11	2.89	2.65	4.17	1.14	1.93	2.22
Banknote-authentication	1,372	4	2	1.22	0.90	0.71	0.75	0.92	0.90	0.79	0.78	0.63	1.08	0.56	0.32
Contraceptive-method-choice	1,473	9	3	2.11	1.80	2.11	1.88	1.51	1.73	2.02	2.06	2.54	1.50	1.00	1.48
Car-evaluation	1,728	6	4	1.71	1.40	1.56	1.52	1.26	1.33	1.00	1.01	0.61	0.70	0.26	0.42
Ozone-level-detection-eight	1,847	72	2	1.06	0.95	1.28	1.29	1.13	0.98	1.35	1.23	1.39	0.90	1.56	1.14
Ozone-level-detection-one	1,848	72	2	0.92	1.03	0.99	0.63	0.72	0.77	1.01	0.87	1.30	1.53	1.46	0.87
Seismic-bumps	2,584	18	2	0.61	0.37	0.52	0.54	0.51	0.80	0.81	0.99	0.97	0.92	0.22	0.56
Chess-king-rook-versus-king-pawn	3,196	36	2	0.74	0.63	0.74	0.74	0.70	0.75	0.37	0.37	0.23	0.31	0.21	0.21
Thyroidann	3,772	21	3	0.19	0.22	0.21	0.23	0.17	0.18	0.11	0.11	0.12	0.14	0.14	0.14
Statloglansat	4,435	36	6	1.61	1.06	1.09	1.38	1.14	1.62	0.88	0.88	0.74	0.69	0.75	0.71
Spambase	4,601	57	2	1.05	0.89	0.80	0.88	0.69	0.53	0.45	0.49	1.03	0.89	1.04	1.27
Wall-following-robot-2	5,456	2	4	0.08	0.00	0.07	0.07	0.07	0.07	0.08	0.00	0.09	0.09	0.10	0.12
Pageblock	5,473	10	5	0.31	0.28	0.30	0.45	0.38	0.23	0.37	0.35	0.25	0.41	0.31	0.38
Optical-recognition	5,620	62	10	1.08	1.08	0.62	1.19	1.29	0.89	1.00	0.81	0.84	0.63	0.86	0.64
Statlog-project-landsat-satellite	6,435	36	6	1.06	0.55	0.29	0.74	0.82	0.73	0.53	0.62	0.52	0.93	0.70	1.10
Thyroid-disease-ann-thyroid	7,200	21	3	0.13	0.13	0.12	0.12	0.10	0.11	0.10	0.10	0.12	0.12	0.02	0.02
Pendigits	7,494	16	10	1.09	1.00	1.07	1.55	0.79	1.18	0.71	0.58	0.67	0.73	0.36	0.28
Avila	10,430	10	12	1.46	1.02	1.20	0.92	1.15	1.46	1.80	1.32	1.51	3.10	1.70	2.32
Eeg	14,980	14	2	1.31	0.61	0.89	0.63	1.06	0.71	0.91	0.57	0.81	0.79	1.18	0.78

E.3 Training time (s) on 65 datasets within 1 million samples

Table 20: Depth=2 average training time (s) on 65 datasets with 10 random splits within 1 million samples

Dataset	Sample	Feature	Class	Depth=2							
				CART	LS-OCT	Quant-BnB	RS-OCT	DEOCT	MH-DEOCT	DEOCT (Long)	MH-DEOCT (Long)
Soybean-small	47	35	4	0.00	1.33	0.13	13.96	0.58	1.17	7.15	14.32
Echocardiogram	61	11	2	0.00	0.42	0.07	18.22	0.37	0.74	3.96	7.96
Hepatitis	80	19	2	0.00	0.90	0.09	163.05	0.48	0.97	5.66	11.34
Fertility	100	9	2	0.00	0.66	0.06	169.94	0.38	0.75	4.15	8.28
Acute-inflammations-1	120	6	2	0.00	1.01	0.04	18.40	0.47	1.51	4.42	9.48
Acute-inflammations-2	120	6	2	0.00	0.43	0.02	13.92	0.37	0.79	3.88	8.13
Hayes-roth	132	5	3	0.00	0.43	0.01	180.25	0.38	0.75	4.14	8.30
Iris	150	4	3	0.00	0.38	0.06	113.50	0.37	0.73	4.02	8.05
Teaching-assistant-evaluation	151	5	3	0.00	0.60	0.03	818.03	0.37	0.74	4.10	8.23
Wine	178	13	3	0.00	1.74	0.09	60.96	0.45	0.90	5.15	10.27
Breast-cancer-prognostic	194	31	2	0.00	4.37	0.66	14,400.00	0.51	1.03	5.72	11.51
Parkinsons	195	23	2	0.00	2.93	0.17	3,690.96	0.49	0.99	5.61	11.25
Connectionist-bench-sonar	208	60	2	0.00	10.46	1.30	14,400.00	0.64	1.28	7.69	15.48
Image-segmentation	210	19	7	0.00	2.74	0.37	3,977.34	0.52	1.05	6.36	12.86
Seeds	210	7	3	0.00	1.02	0.13	96.44	0.40	0.80	4.48	8.91
Glass	214	9	6	0.00	1.55	0.10	2,047.54	0.44	0.87	5.08	10.19
Thyroid-disease-new-thyroid	215	5	3	0.00	0.81	0.07	48.86	0.38	0.76	4.16	8.32
Congressional-voting-records	232	16	2	0.00	2.64	0.06	129.65	0.41	0.83	4.63	9.43
Spect-heart	267	22	2	0.00	3.85	0.11	3,721.09	0.46	0.92	5.26	10.57
Spectf-heart	267	44	2	0.00	8.40	2.00	14,400.00	0.64	1.31	8.45	16.98
Cylinder-bands	277	39	2	0.00	8.48	0.74	14,400.00	0.60	1.20	7.44	15.04
Heart-disease-Cleveland	282	13	5	0.00	2.30	0.20	14,400.00	0.49	0.97	5.89	11.80
Haberman-survival	306	3	2	0.00	0.58	0.03	373.15	0.36	0.71	3.77	7.57
Ionosphere	351	34	2	0.00	7.31	0.47	14,400.00	0.50	1.02	5.94	11.91
Dermatology	358	34	6	0.00	8.76	0.28	1,353.78	0.70	1.41	9.03	18.13
Thoracic-surgery	470	16	2	0.00	5.32	0.22	14,400.00	0.44	0.88	5.16	10.26
Body	507	5	2	0.00	1.88	0.04	297.18	0.38	0.75	4.18	8.43
Climate-model-crashes	540	20	2	0.00	6.13	0.42	14,400.00	0.49	1.00	5.66	11.36
Monks-problems-3	554	6	2	0.00	1.97	0.02	35.91	0.39	0.77	4.25	8.48
Monks-problems-1	556	6	2	0.00	2.02	0.05	183.85	0.38	0.76	4.29	8.58
Breast-cancer-diagnosti	569	30	2	0.00	9.70	0.43	14,400.00	0.67	1.36	8.32	16.63
Indian-liver-patient	579	10	2	0.00	3.43	0.27	14,400.00	0.40	0.80	4.57	9.11
Monks-problems-2	600	6	2	0.00	2.14	0.03	3,284.51	0.38	0.76	4.21	8.44
Balance-scale	625	4	3	0.00	1.49	0.02	724.59	0.41	0.82	4.69	9.42
Credit-approval	653	15	2	0.00	6.53	0.19	14,400.00	0.48	0.97	5.73	11.40
Breast-cancer	683	9	2	0.00	4.39	0.17	1,026.01	0.42	0.83	4.80	9.61
Blood-transfusion	748	4	2	0.00	1.78	0.03	6,466.31	0.39	0.78	4.42	8.84
Mammographic-mass	830	5	2	0.00	2.43	0.14	650.45	0.39	0.77	4.42	8.84
Tic-tac-toe-endgame	958	9	2	0.00	6.18	0.13	14,025.29	0.45	0.89	5.12	10.24
Connectionist-bench	990	13	11	0.00	9.75	0.41	1,998.87	0.74	1.49	9.61	19.24
Statlog-project-German-credit	1,000	20	2	0.00	13.82	0.35	14,400.00	0.46	0.92	4.96	9.93
Concrete	1,030	8	3	0.00	6.04	0.23	14,400.00	0.50	1.00	5.63	11.25
Qsar-biodegradation	1,055	41	2	0.00	30.26	1.49	14,400.00	0.99	1.99	14.00	28.05
Banknote-authentication	1,372	4	2	0.00	3.19	0.03	418.48	0.44	0.89	5.12	10.12
Contraceptive-method-choice	1,473	9	3	0.00	7.72	0.14	14,400.00	0.50	0.99	5.77	11.64
Car-evaluation	1,728	6	4	0.00	7.61	0.09	716.82	0.53	1.06	6.75	13.54
Ozone-level-detection-eight	1,847	72	2	0.01	94.77	17.34	14,400.00	1.24	2.50	16.29	32.80
Ozone-level-detection-one	1,848	72	2	0.01	98.30	18.85	14,400.00	1.23	2.44	15.89	31.48
Seismic-bumps	2,584	18	2	0.00	31.26	1.41	14,400.00	0.59	1.17	6.90	13.84
Chess-king-rook-versus-king-pawn	3,196	36	2	0.00	82.10	0.50	13,501.16	0.87	1.76	11.19	22.87
Thyroidann	3,772	21	3	0.00	56.68	0.43	14,400.00	0.77	1.54	10.78	21.59
Statloglansat	4,435	36	6	0.01	126.49	4.93	14,400.00	1.00	2.02	12.42	24.91
Spambase	4,601	57	2	0.01	185.26	11.75	14,400.00	1.22	2.43	16.75	33.19
Wall-following-robot-2	5,456	2	4	0.00	9.06	0.12	172.53	0.51	1.03	6.30	12.61
Pageblock	5,473	10	5	0.01	37.29	0.69	14,400.00	0.67	1.36	7.78	15.58
Optical-recognition	5,620	62	10	0.01	256.19	13.51	14,400.00	1.54	3.06	18.32	36.56
Statlog-project-landsat-satellite	6,435	36	6	0.01	185.52	6.79	14,400.00	1.03	2.09	12.97	26.14
Thyroid-disease-ann-thyroid	7,200	21	3	0.00	113.41	0.74	14,400.00	0.82	1.65	11.45	22.97
Pendigits	7,494	16	10	0.01	93.16	2.94	5,525.77	1.11	2.26	14.19	28.41
Avila	10,430	10	12	0.02	82.06	1.58	14,400.00	1.13	2.29	13.76	27.62
Eeg	14,980	14	2	0.02	147.57	2.88	14,400.00	0.66	1.33	7.55	15.00
Htru	17,898	8	2	0.03	85.85	1.66	14,400.00	0.63	1.33	6.94	13.94
Shuttle	43,500	9	7	0.02	246.47	2.33	2,569.28	1.34	2.74	17.58	35.19
Skinsegmentation	245,057	3	2	0.05	496.70	2.69	14,400.00	2.12	4.38	26.31	52.81
Htsensor	928,991	11	3	1.85	6,485.88	89.31	14,400.00	6.60	16.00	64.08	130.88
Average Training Time (s)				0.03	140.34	2.96	7,701.63	0.72	1.51	8.54	17.17

* RS-OCT with training time larger than 14400s is recorded as 14400s in Table 20.

Table 21: Depth=2 training time standard deviation (s) on 65 datasets with 10 random splits within 1 million samples

Dataset	Sample	Feature	Class	Depth=2							
				CART	LS-OCT	Quant-BnB	RS-OCT	DEOCT	MH-DEOCT	DEOCT (Long)	MH-DEOCT (Long)
Soybean-small	47	35	4	0.00	0.02	0.01	14.72	0.02	0.03	0.22	0.42
Echocardiogram	61	11	2	0.00	0.03	0.01	18.88	0.01	0.02	0.10	0.22
Hepatitis	80	19	2	0.00	0.01	0.01	94.06	0.01	0.02	0.16	0.44
Fertility	100	9	2	0.00	0.01	0.01	119.81	0.00	0.01	0.06	0.13
Acute-inflammations-1	120	6	2	0.00	0.03	0.10	19.02	0.27	0.02	0.29	0.04
Acute-inflammations-2	120	6	2	0.00	0.01	0.00	14.67	0.01	0.20	0.01	0.20
Hayes-roth	132	5	3	0.00	0.01	0.00	57.16	0.01	0.02	0.07	0.14
Iris	150	4	3	0.00	0.01	0.00	75.20	0.00	0.00	0.06	0.10

Table 21 continued from previous page

Dataset	Sample	Feature	Class	Depth=2							
				CART	LS-OCT	Quant-BnB	RS-OCT	DEOCT	MH-DEOCT	DEOCT (Long)	MH-DEOCT (Long)
Teaching-assistant-evaluation	151	5	3	0.00	0.00	0.00	251.98	0.00	0.01	0.07	0.11
Wine	178	13	3	0.00	0.02	0.01	25.38	0.01	0.01	0.11	0.16
Breast-cancer-prognostic	194	31	2	0.00	0.09	0.19	39.29	0.01	0.02	0.26	0.70
Parkinsons	195	23	2	0.00	0.08	0.03	4103.50	0.02	0.05	0.46	1.07
Connectionist-bench-sonar	208	60	2	0.00	0.11	0.15	37.76	0.06	0.12	0.68	1.45
Image-segmentation	210	19	7	0.00	0.03	0.05	2518.47	0.02	0.03	0.36	0.76
Seeds	210	7	3	0.00	0.01	0.00	18.98	0.01	0.01	0.07	0.16
Glass	214	9	6	0.00	0.02	0.03	512.17	0.01	0.02	0.12	0.26
Thyroid-disease-new-thyroid	215	5	3	0.00	0.02	0.00	28.02	0.00	0.01	0.09	0.17
Congressional-voting-records	232	16	2	0.00	0.15	0.00	85.82	0.00	0.00	0.01	0.02
Spectf-heart	267	22	2	0.00	0.04	0.04	2129.95	0.00	0.01	0.01	0.04
Spectf-heart	267	44	2	0.00	0.14	0.26	34.02	0.03	0.04	0.32	0.50
Cylinder-bands	277	39	2	0.00	0.08	0.06	25.91	0.05	0.11	0.68	1.40
Heart-disease-Cleveland	282	13	5	0.00	0.03	0.01	30.02	0.01	0.01	0.10	0.22
Haberman-survival	306	3	2	0.00	0.05	0.00	75.41	0.01	0.02	0.07	0.15
Ionosphere	351	34	2	0.00	0.09	0.11	19.25	0.04	0.07	0.45	0.84
Dermatology	358	34	6	0.00	0.71	0.01	276.95	0.01	0.02	0.27	0.57
Thoracic-surgery	470	16	2	0.00	0.04	0.02	26.23	0.01	0.02	0.36	0.65
Body	507	5	2	0.00	0.02	0.01	97.73	0.01	0.02	0.08	0.21
Climate-model-crashes	540	20	2	0.00	0.28	0.16	40.51	0.00	0.01	0.15	0.28
Monks-problems-3	554	6	2	0.00	0.07	0.00	20.32	0.00	0.01	0.03	0.04
Monks-problems-1	556	6	2	0.00	0.02	0.00	57.94	0.00	0.00	0.03	0.04
Breast-cancer-diagnosti	569	30	2	0.00	0.74	0.10	24.12	0.01	0.01	0.05	0.08
Indian-liver-patient	579	10	2	0.00	0.08	0.01	27.86	0.01	0.02	0.19	0.34
Monks-problems-2	600	6	2	0.00	0.06	0.00	441.25	0.00	0.01	0.08	0.13
Balance-scale	625	4	3	0.00	0.03	0.01	68.34	0.01	0.01	0.08	0.15
Credit-approval	653	15	2	0.00	0.59	0.01	76.15	0.01	0.03	0.43	0.76
Breast-cancer	683	9	2	0.00	0.09	0.01	269.51	0.00	0.01	0.03	0.05
Blood-transfusion	748	4	2	0.00	0.01	0.00	1822.45	0.01	0.01	0.08	0.18
Mammographic-mass	830	5	2	0.00	0.04	0.00	106.91	0.00	0.01	0.05	0.07
Tic-tac-toe-endgame	958	9	2	0.00	0.04	0.01	881.32	0.01	0.02	0.15	0.31
Connectionist-bench	990	13	11	0.00	0.66	0.01	412.90	0.01	0.01	0.15	0.25
Statlog-project-German-credit	1,000	20	2	0.00	0.61	0.06	21.94	0.01	0.02	0.05	0.08
Concrete	1,030	8	3	0.00	0.07	0.02	703.02	0.01	0.03	0.21	0.46
Qsar-biodegradation	1,055	41	2	0.00	0.40	0.04	32.98	0.01	0.01	0.19	0.19
Banknote-authentication	1,372	4	2	0.00	0.02	0.00	81.79	0.01	0.02	0.08	0.17
Contraceptive-method-choice	1,473	9	3	0.00	0.06	0.00	24.46	0.00	0.01	0.13	0.34
Car-evaluation	1,728	6	4	0.00	0.12	0.00	138.74	0.00	0.00	0.01	0.03
Ozone-level-detection-eight	1,847	72	2	0.00	2.15	1.37	50.91	0.01	0.02	0.98	1.86
Ozone-level-detection-one	1,848	72	2	0.00	1.57	1.99	36.87	0.03	0.07	1.40	3.00
Seismic-bumps	2,584	18	2	0.00	0.52	0.17	18.97	0.01	0.02	0.25	0.61
Chess-king-rook-versus-king-pawn	3,196	36	2	0.00	4.98	0.13	2106.88	0.03	0.06	0.65	0.64
Thyroidann	3,772	21	3	0.00	0.63	0.08	14.79	0.00	0.00	0.03	0.04
Statloglansat	4,435	36	6	0.00	1.82	0.17	0.00	0.01	0.02	0.19	0.52
Spambase	4,601	57	2	0.00	11.33	1.43	53.45	0.09	0.15	1.47	2.39
Wall-following-robot-2	5,456	2	4	0.00	0.08	0.01	69.83	0.00	0.01	0.01	0.02
Pageblock	5,473	10	5	0.00	0.62	0.03	0.00	0.00	0.01	0.07	0.13
Optical-recognition	5,620	62	10	0.00	12.52	0.82	280.43	0.03	0.03	0.07	0.11
Statlog-project-landsat-satellite	6,435	36	6	0.00	7.84	0.74	52.69	0.01	0.02	0.41	0.90
Thyroid-disease-ann-thyroid	7,200	21	3	0.00	1.31	0.06	20.23	0.00	0.01	0.04	0.17
Pendigits	7,494	16	10	0.00	0.79	0.21	706.03	0.01	0.01	0.08	0.24
Avila	10,430	10	12	0.00	1.31	0.11	20.33	0.01	0.03	0.20	0.44
Eeg	14,980	14	2	0.00	8.64	0.24	35.31	0.02	0.05	0.31	0.35
Htrlu	17,898	8	2	0.00	2.89	0.63	22.59	0.01	0.02	0.07	0.13
Shuttle	43,500	9	7	0.00	2.83	0.09	437.29	0.01	0.02	0.28	0.55
Skinsegmentation	245,057	3	2	0.01	6.03	0.18	20.38	0.16	0.16	0.15	0.18
Htsensor	928,991	11	3	0.06	160.86	3.64	0.00	0.08	0.16	0.28	0.63
Average Training Time STD (s)				0.00	3.61	0.21	306.92	0.02	0.03	0.23	0.43

Table 22: Depth=3 average training time (s) on 65 datasets with 10 random splits within 1 million samples

Dataset	Sample	Feature	Class	Depth=3						
				CART	LS-OCT	Quant-BnB	DEOCT	MH-DEOCT	DEOCT (Long)	MH-DEOCT (Long)
Soybean-small	47	35	4	0.00	2.56	-	0.85	2.86	11.47	37.16
Echocardiogram	61	11	2	0.00	0.73	13.43	0.54	1.50	6.66	17.89
Hepatitis	80	19	2	0.00	1.66	8.33	0.70	2.23	8.94	27.76
Fertility	100	9	2	0.00	0.89	0.49	0.54	1.80	6.64	21.88
Acute-inflammations-1	120	6	2	0.00	1.30	5.89	0.53	2.20	22.02	40.91
Acute-inflammations-2	120	6	2	0.00	0.73	0.31	0.52	1.56	6.29	18.54
Hayes-roth	132	5	3	0.00	0.78	0.31	0.52	1.74	6.57	21.60
Iris	150	4	3	0.00	0.71	1.23	0.51	1.71	6.44	20.77
Teaching-assistant-evaluation	151	5	3	0.00	0.92	7.27	0.54	1.85	6.84	22.37
Wine	178	13	3	0.00	2.41	19.57	0.65	2.19	8.28	26.77
Breast-cancer-prognostic	194	31	2	0.00	8.05	439.81	0.77	2.60	9.75	32.18
Parkinsons	195	23	2	0.00	5.79	55.49	0.74	2.39	9.48	29.71
Connectionist-bench-sonar	208	60	2	0.00	15.34	1,285.24	1.07	3.58	14.68	47.53
Image-segmentation	210	19	7	0.00	4.94	-	0.86	2.83	11.31	36.42
Seeds	210	7	3	0.00	2.06	5.91	0.58	1.96	7.27	23.41
Glass	214	9	6	0.00	2.29	18.61	0.70	2.28	8.72	27.98
Thyroid-disease-new-thyroid	215	5	3	0.00	1.20	1.45	0.53	1.84	6.77	22.15
Congressional-voting-records	232	16	2	0.00	3.85	0.38	0.61	2.05	7.49	24.83
Spectf-heart	267	22	2	0.00	7.25	5.06	0.69	2.30	8.53	27.79
Spectf-heart	267	44	2	0.00	15.62	3,436.81	0.99	3.23	13.68	43.45
Cylinder-bands	277	39	2	0.00	12.86	-	0.94	3.06	12.42	39.33
Heart-disease-Cleveland	282	13	5	0.00	4.18	30.93	0.77	2.48	9.67	30.56

Table 22 continued from previous page

Dataset	Sample	Feature	Class	Depth=3						
				CART	LS-OCT	Quant-BnB	DEOCT	MH-DEOCT	DEOCT (Long)	MH-DEOCT (Long)
Haberman-survival	306	3	2	0.00	1.03	6.93	0.48	1.67	5.95	19.67
Ionosphere	351	34	2	0.00	13.69	-	0.77	2.46	10.39	32.41
Dermatology	358	34	6	0.00	14.85	25.00	1.11	3.47	15.30	46.65
Thoracic-surgery	470	16	2	0.00	7.79	38.82	0.65	2.19	8.24	26.98
Body	507	5	2	0.00	2.71	4.38	0.55	1.86	6.97	22.32
Climate-model-crashes	540	20	2	0.00	11.07	249.42	0.73	2.37	9.21	29.00
Monks-problems-3	554	6	2	0.00	3.53	0.23	0.55	1.86	6.78	21.97
Monks-problems-1	556	6	2	0.00	3.88	0.27	0.54	1.70	6.73	21.36
Breast-cancer-diagnosti	569	30	2	0.00	22.00	335.73	0.99	3.13	13.50	40.65
Indian-liver-patient	579	10	2	0.00	5.88	191.96	0.61	2.03	7.56	24.41
Monks-problems-2	600	6	2	0.00	3.81	9.88	0.55	1.86	6.96	22.38
Balance-scale	625	4	3	0.00	2.76	0.44	0.68	2.14	8.25	25.21
Credit-approval	653	15	2	0.00	10.96	107.77	0.71	2.31	8.87	28.06
Breast-cancer	683	9	2	0.00	7.72	4.60	0.61	2.02	7.61	24.18
Blood-transfusion	748	4	2	0.00	3.24	6.03	0.56	1.85	6.85	22.07
Mammographic-mass	830	5	2	0.00	4.34	1.55	0.57	1.91	7.10	22.66
Tic-tac-toe-endgame	958	9	2	0.00	8.84	0.45	0.68	2.18	8.59	26.81
Connectionist-bench	990	13	11	0.01	15.86	108.51	1.27	3.80	16.35	47.84
Statlog-project-German-credit	1,000	20	2	0.00	24.09	146.78	0.74	2.36	8.97	27.81
Concrete	1,030	8	3	0.00	8.39	148.22	0.74	2.35	9.82	29.34
Qsar-biodegradation	1,055	41	2	0.00	59.47	17,481.80	1.48	4.32	19.30	55.41
Banknote-authentication	1,372	4	2	0.00	5.82	2.46	0.65	2.09	8.22	25.06
Contraceptive-method-choice	1,473	9	3	0.00	13.66	3.61	0.78	2.42	10.51	30.67
Car-evaluation	1,728	6	4	0.00	13.92	0.32	0.87	2.65	11.74	34.94
Ozone-level-detection-eight	1,847	72	2	0.02	171.59	14,417.64	2.01	6.10	25.42	78.51
Ozone-level-detection-one	1,848	72	2	0.02	189.05	14,419.85	2.00	5.86	25.01	76.27
Seismic-bumps	2,584	18	2	0.00	61.42	-	0.87	2.81	11.81	36.20
Chess-king-rook-versus-king-pawn	3,196	36	2	0.00	127.17	6.22	1.19	3.48	16.35	50.77
Thyroidann	3,772	21	3	0.00	77.38	60.40	1.17	2.91	15.57	37.78
Statloglansat	4,435	36	6	0.01	172.36	8,863.18	1.73	5.26	20.49	65.28
Spambase	4,601	57	2	0.01	354.01	14,392.94	2.04	6.22	26.07	80.09
Wall-following-robot-2	5,456	2	4	0.00	14.43	24.72	0.83	2.42	10.42	30.09
Pageblock	5,473	10	5	0.01	49.82	633.29	1.09	3.33	13.74	42.05
Optical-recognition	5,620	62	10	0.02	462.87	14,400.99	2.77	8.80	35.75	110.97
Statlog-project-landsat-satellite	6,435	36	6	0.02	269.82	12,531.62	1.77	5.45	20.77	66.56
Thyroid-disease-ann-thyroid	7,200	21	3	0.00	147.43	80.72	1.25	3.31	16.48	42.81
Pendigits	7,494	16	10	0.01	134.10	3,408.29	1.87	5.76	24.36	74.51
Avila	10,430	10	12	0.02	119.99	3,206.35	1.98	5.88	25.86	74.49
Eeg	14,980	14	2	0.02	209.97	9,505.80	1.04	3.34	12.90	41.12
Htru	17,898	8	2	0.04	142.70	8,110.32	0.96	3.11	11.39	35.73
Shuttle	43,500	9	7	0.03	420.43	85.46	2.49	7.15	31.48	88.66
Skinsegmentation	245,057	3	2	0.06	883.94	256.81	3.68	10.08	46.48	122.65
Htsensor	928,991	11	3	2.70	10,704.60	3,647.36	11.12	34.35	109.58	300.86
Average Training Time (s)				0.05	231.98	2,204.39	1.15	3.58	14.46	43.14

Table 23: Depth=3 training time standard deviation (s) on 65 datasets with 10 random splits within 1 million samples

Dataset	Sample	Feature	Class	Depth=3						
				CART	LS-OCT	Quant-BnB	DEOCT	MH-DEOCT	DEOCT (Long)	MH-DEOCT (Long)
Soybean-small	47	35	4	0.00	0.03	-	0.01	0.04	0.59	1.58
Echocardiogram	61	11	2	0.00	0.01	5.87	0.01	0.13	0.33	1.36
Hepatitis	80	19	2	0.00	0.02	3.59	0.01	0.17	0.31	2.27
Fertility	100	9	2	0.00	0.01	0.02	0.00	0.12	0.21	0.90
Acute-inflammations-1	120	6	2	0.00	0.01	12.60	0.03	0.19	5.88	6.98
Acute-inflammations-2	120	6	2	0.00	0.02	0.04	0.01	0.18	0.22	2.08
Hayes-roth	132	5	3	0.00	0.01	0.04	0.01	0.15	0.23	0.77
Iris	150	4	3	0.00	0.01	0.11	0.01	0.15	0.24	1.68
Teaching-assistant-evaluation	151	5	3	0.00	0.01	13.06	0.01	0.02	0.29	1.06
Wine	178	13	3	0.00	0.02	5.73	0.02	0.05	0.46	1.32
Breast-cancer-prognostic	194	31	2	0.00	0.14	64.21	0.01	0.05	0.50	1.22
Parkinsons	195	23	2	0.00	0.08	22.61	0.03	0.09	0.68	2.15
Connectionist-bench-sonar	208	60	2	0.00	0.54	252.37	0.03	0.16	0.98	3.42
Image-segmentation	210	19	7	0.00	0.04	-	0.01	0.02	0.43	0.96
Seeds	210	7	3	0.00	0.02	1.54	0.01	0.02	0.28	0.88
Glass	214	9	6	0.00	0.03	1.85	0.01	0.02	0.36	1.29
Thyroid-disease-new-thyroid	215	5	3	0.00	0.02	0.43	0.01	0.03	0.23	0.91
Congressional-voting-records	232	16	2	0.00	0.03	0.22	0.01	0.03	0.24	0.83
Spect-heart	267	22	2	0.00	0.03	10.19	0.01	0.03	0.28	1.01
Spectf-heart	267	44	2	0.00	0.16	169.44	0.03	0.23	1.16	2.96
Cylinder-bands	277	39	2	0.00	1.39	-	0.04	0.13	0.46	2.15
Heart-disease-Cleveland	282	13	5	0.00	0.04	7.34	0.01	0.02	0.35	1.04
Haberman-survival	306	3	2	0.00	0.01	13.43	0.01	0.02	0.21	0.78
Ionosphere	351	34	2	0.00	1.19	-	0.04	0.29	0.88	2.09
Dermatology	358	34	6	0.00	0.16	0.64	0.01	0.06	0.46	1.23
Thoracic-surgery	470	16	2	0.00	0.08	9.47	0.01	0.06	0.39	1.74
Body	507	5	2	0.00	0.03	0.56	0.01	0.02	0.32	1.17
Climate-model-crashes	540	20	2	0.00	0.05	87.57	0.01	0.15	0.31	0.95
Monks-problems-3	554	6	2	0.00	0.04	0.03	0.01	0.01	0.25	0.89
Monks-problems-1	556	6	2	0.00	0.48	0.23	0.01	0.18	0.30	1.50
Breast-cancer-diagnosti	569	30	2	0.00	2.39	79.16	0.01	0.05	0.72	1.47
Indian-liver-patient	579	10	2	0.00	0.08	6.87	0.01	0.02	0.30	0.94
Monks-problems-2	600	6	2	0.00	0.06	13.18	0.01	0.02	0.34	1.16
Balance-scale	625	4	3	0.00	0.02	0.29	0.25	0.55	0.34	0.99
Credit-approval	653	15	2	0.00	1.38	8.59	0.01	0.05	0.31	0.95
Breast-cancer	683	9	2	0.00	0.09	0.12	0.01	0.02	0.27	0.78

Table 23 continued from previous page

Dataset	Sample	Feature	Class	Depth=3						
				CART	LS-OCT	Quant-BnB	DEOCT	MH-DEOCT	DEOCT (Long)	MH-DEOCT (Long)
Blood-transfusion	748	4	2	0.00	0.03	0.17	0.01	0.01	0.20	0.81
Mammographic-mass	830	5	2	0.00	0.07	0.07	0.00	0.01	0.20	0.73
Tic-tac-toe-endgame	958	9	2	0.00	0.07	0.24	0.01	0.03	0.31	0.90
Connectionist-bench	990	13	11	0.00	0.18	6.66	0.01	0.02	0.36	1.12
Statlog-project-German-credit	1,000	20	2	0.00	0.27	15.32	0.02	0.06	0.33	1.47
Concrete	1,030	8	3	0.00	0.06	9.63	0.01	0.04	0.27	1.11
Qsar-biodegradation	1,055	41	2	0.00	0.95	2211.82	0.09	0.23	1.03	2.41
Banknote-authentication	1,372	4	2	0.00	0.10	0.81	0.01	0.03	0.20	0.80
Contraceptive-method-choice	1,473	9	3	0.00	0.83	0.13	0.01	0.02	0.42	0.90
Car-evaluation	1,728	6	4	0.00	0.66	0.03	0.01	0.12	0.44	1.13
Ozone-level-detection-eight	1,847	72	2	0.00	6.81	9.24	0.05	0.17	1.14	3.92
Ozone-level-detection-one	1,848	72	2	0.00	8.69	11.37	0.03	0.36	0.82	3.26
Seismic-bumps	2,584	18	2	0.00	0.57	-	0.02	0.07	0.36	1.49
Chess-king-rook-versus-king-pawn	3,196	36	2	0.00	14.73	0.03	0.01	0.32	0.45	5.77
Thyroidann	3,772	21	3	0.00	0.65	14.10	0.03	0.07	0.68	1.71
Statloglansat	4,435	36	6	0.00	1.71	709.05	0.02	0.06	0.65	1.76
Spambase	4,601	57	2	0.00	4.51	24.00	0.11	0.31	1.60	5.21
Wall-following-robot-2	5,456	2	4	0.00	0.11	11.91	0.01	0.26	0.34	3.37
Pageblock	5,473	10	5	0.00	1.28	118.94	0.01	0.04	0.51	1.87
Optical-recognition	5,620	62	10	0.00	43.50	0.56	0.01	0.04	0.82	2.60
Statlog-project-landsat-satellite	6,435	36	6	0.00	21.97	1080.92	0.03	0.04	0.50	1.54
Thyroid-disease-ann-thyroid	7,200	21	3	0.00	4.48	9.12	0.01	0.27	0.29	3.37
Pendigits	7,494	16	10	0.00	1.70	318.50	0.01	0.04	0.50	1.49
Avila	10,430	10	12	0.00	1.70	251.06	0.01	0.09	0.70	2.23
Eeg	14,980	14	2	0.00	1.91	602.58	0.01	0.05	0.70	1.92
Htru	17,898	8	2	0.00	4.56	676.16	0.01	0.03	0.46	1.39
Shuttle	43,500	9	7	0.00	2.74	25.77	0.02	0.05	0.60	1.66
Skinsegmentation	245,057	3	2	0.01	4.61	33.31	0.16	0.16	0.70	1.97
Htsensor	928,991	11	3	0.06	151.85	14.67	0.07	0.22	1.97	3.71
Average Training Time STD (s)				0.00	4.46	115.79	0.02	0.10	0.58	1.80

Table 24: Depth=4.8 average training time (s) on 65 datasets with 10 random splits within 1 million samples

Dataset	Sample	Feature	Class	Depth=4					Depth=8						
				CART	LS-OCT	DEOCT	MH-DEOCT	DEOCT (Long)	MH-DEOCT (Long)	CART	LS-OCT	DEOCT	MH-DEOCT	DEOCT (Long)	MH-DEOCT (Long)
Soybean-small	47	35	4	0.00	3.41	1.25	5.24	16.13	67.17	0.00	32.19	11.17	27.57	115.10	310.61
Echocardiogram	61	11	2	0.00	1.20	0.82	2.68	10.64	32.77	0.00	13.06	8.10	19.11	96.74	207.36
Hepatitis	80	19	2	0.00	2.43	1.01	4.20	13.15	54.07	0.00	25.56	7.32	19.76	90.78	266.78
Fertility	100	9	2	0.00	1.61	0.82	3.51	10.29	44.63	0.00	17.39	7.15	21.82	81.86	282.83
Acute-inflammations-1	120	6	2	0.00	1.72	0.82	3.29	24.83	53.59	0.00	14.02	11.42	19.58	108.14	176.26
Acute-inflammations-2	120	6	2	0.00	1.15	0.80	2.72	9.90	32.45	0.00	12.62	7.19	12.53	93.14	157.59
Hayes-roth	132	5	3	0.00	1.34	0.79	3.53	9.93	45.68	0.00	16.29	6.75	29.46	55.19	356.30
Iris	150	4	3	0.00	1.05	0.78	3.42	9.55	39.78	0.00	15.77	7.67	28.13	56.92	203.80
Teaching-assistant-evaluation	151	5	3	0.00	1.51	0.84	3.91	10.68	47.15	0.00	17.12	6.50	40.81	56.00	441.68
Wine	178	13	3	0.00	3.74	0.96	4.31	12.19	52.91	0.00	34.36	7.25	35.29	71.64	478.00
Breast-cancer-prognostic	194	31	2	0.00	8.88	1.18	5.39	15.59	67.95	0.00	74.90	8.30	44.27	105.58	597.49
Parkinsons	195	23	2	0.00	7.11	1.05	4.68	13.62	57.88	0.00	57.35	7.30	37.63	87.25	380.22
Connectionist-bench-sonar	208	60	2	0.00	22.75	1.72	7.77	21.65	99.13	0.00	173.78	10.31	66.75	127.07	892.06
Image-segmentation	210	19	7	0.00	7.91	1.34	5.96	17.12	74.02	0.00	67.92	8.13	68.55	100.50	796.66
Seeds	210	7	3	0.00	2.62	0.87	3.91	10.90	46.48	0.00	24.94	6.67	31.82	58.06	324.50
Glass	214	9	6	0.00	3.57	1.12	4.88	14.14	60.13	0.00	36.52	6.86	56.22	86.70	632.98
Thyroid-disease-new-thyroid	215	5	3	0.00	1.91	0.80	3.68	9.96	44.64	0.00	20.88	6.79	26.34	56.91	234.94
Congressional-voting-records	232	16	2	0.00	6.01	0.90	3.93	11.54	48.39	0.00	48.21	7.54	27.40	88.18	294.63
Spect-heart	267	22	2	0.00	8.81	1.05	4.58	13.78	58.98	0.00	75.22	7.80	31.33	95.72	451.95
Spect-heart	267	44	2	0.00	19.61	1.51	6.31	19.86	87.09	0.00	155.82	9.83	47.15	110.16	640.49
Cylinder-bands	277	39	2	0.00	15.36	1.41	6.39	18.40	80.88	0.00	144.88	8.62	60.42	107.58	752.22
Heart-disease-Cleveland	282	13	5	0.00	5.87	1.20	5.20	15.39	64.19	0.00	64.40	7.29	66.19	95.96	778.76
Haberman-survival	306	3	2	0.00	1.90	0.73	3.39	9.09	41.21	0.00	24.52	5.62	33.22	67.09	402.00
Ionosphere	351	34	2	0.00	19.05	1.17	4.98	15.16	60.42	0.00	162.68	9.21	43.16	101.98	526.50
Dermatology	358	34	6	0.00	24.21	1.70	6.96	21.68	90.49	0.00	193.46	9.20	53.00	122.02	589.15
Thoracic-surgery	470	16	2	0.00	12.10	0.97	4.42	12.74	56.03	0.00	93.56	8.07	38.39	92.12	450.37
Body	507	5	2	0.00	4.31	0.84	3.86	10.65	45.76	0.00	44.76	5.89	34.27	68.42	412.55
Climate-model-crashes	540	20	2	0.00	16.18	1.10	4.60	14.42	59.34	0.00	128.28	8.18	33.52	102.18	407.13
Monks-problems-3	554	6	2	0.00	5.45	0.83	3.30	10.35	39.52	0.00	55.55	7.16	16.07	83.69	189.03
Monks-problems-1	556	6	2	0.00	5.46	0.82	3.28	10.28	40.84	0.00	58.54	7.08	17.52	80.54	204.06
Breast-cancer-diagnosti	569	30	2	0.00	25.12	1.49	6.10	19.03	78.15	0.00	204.26	8.58	48.27	107.88	708.69
Indian-liver-patient	579	10	2	0.00	8.79	0.94	4.25	12.16	51.38	0.00	91.93	7.52	48.79	82.94	559.09
Monks-problems-2	600	6	2	0.00	5.86	0.87	3.91	11.24	46.87	0.00	62.44	6.53	36.61	76.42	395.99
Balance-scale	625	4	3	0.00	4.20	1.03	4.32	12.95	50.54	0.00	49.39	8.13	53.46	76.30	601.11
Credit-approval	653	15	2	0.00	15.46	1.10	4.76	14.47	58.86	0.00	130.39	7.71	44.36	93.77	541.57
Breast-cancer	683	9	2	0.00	9.69	0.92	4.15	12.00	49.59	0.00	87.19	7.67	32.41	89.10	379.21
Blood-transfusion	748	4	2	0.00	5.22	0.85	3.88	10.65	45.38	0.00	58.32	6.81	41.63	82.70	514.97
Mammographic-mass	830	5	2	0.00	6.20	0.88	3.91	11.24	46.56	0.00	81.66	7.01	40.34	85.36	512.67
Tic-tac-toe-endgame	958	9	2	0.00	13.31	1.04	4.45	14.14	55.23	0.00	115.94	8.09	44.36	94.47	502.23
Connectionist-bench	990	13	11	0.01	24.57	2.21	7.83	28.24	97.48	0.01	213.38	19.91	110.57	245.59	1,313.66
Statlog-project-German-credit	1,000	20	2	0.00	30.00	1.18	5.04	15.90	61.10	0.00	236.96	9.21	67.01	105.36	762.96
Concrete	1,030	8	3	0.00	12.95	1.22	4.82	16.42	59.97	0.00	124.04	9.50	59.39	97.43	696.82
Qsar-biodegradation	1,055	41	2	0.01	73.99	2.12	8.08	27.13	103.84	0.01	508.39	10.80	81.14	134.16	964.18
Banknote-authentication	1,372	4	2	0.00	9.08	1.03	4.23	13.37	50.06	0.00	106.74	7.66	36.38	90.54	385.58
Contraceptive-method-choice	1,473	9	3	0.00	21.34	1.25	4.88	16.51	59.91	0.00	192.06	11.26	67.31	120.09	779.00
Car-evaluation	1,728	6	4	0.00	15.54	1.37	4.41	17.94	56.44	0.00	178.86	13.08	31.40	138.81	360.55
Ozone-level-detection-eight	1,847	72	2	0.02	235.39	3.01	11.94	38.33	150.23	0.03	1,747.03	15.34	95.35	191.84	1,219.34
Ozone-level-detection-one	1,848	72	2	0.02	233.14	2.94	11.38	36.42	141.27	0.02	1,754.11	16.43	67.76	197.19	922.84
Seismic-bumps	2,584	18	2	0.00	72.37	1.37	5.64	17.90	70.56	0.01	540.79	10.38	59.00	130.04	639.22
Chess-king-rook-versus-king-pawn	3,196	36	2	0.00	159.37	1.85	6.31	23.83	84.79	0.00	1,292.29	11.69	37.82	144.30	461.35

Table 24 continued from previous page

Dataset	Sample	Feature	Class	Depth=4					Depth=8						
				CART	LS-OCT	DEOCT	MH-DEOCT	DEOCT (Long)	MH-DEOCT (Long)	CART	LS-OCT	DEOCT	MH-DEOCT	DEOCT (Long)	MH-DEOCT (Long)
Thyroidann	3,772	21	3	0.00	114.58	1.79	4.70	22.24	59.31	0.00	923.30	12.37	26.92	133.75	305.46
Statloglansat	4,435	36	6	0.02	258.21	2.73	11.20	34.45	139.87	0.04	2,087.43	20.71	129.89	261.39	1,579.25
Spambase	4,601	57	2	0.02	415.43	3.00	12.47	38.01	160.54	0.03	3,325.58	14.13	94.37	180.23	1,200.20
Wall-following-robot-2	5,456	2	4	0.00	24.72	1.26	4.36	15.98	55.65	0.00	328.64	12.95	28.15	154.22	370.01
Pageblock	5,473	10	5	0.01	90.58	1.84	6.75	23.16	83.48	0.02	777.79	16.92	71.75	216.61	926.20
Optical-recognition	5,620	62	10	0.02	626.33	4.37	17.77	57.68	224.06	0.05	5,167.74	35.80	210.52	467.53	2,387.90
Statlog-project-landsat-satellite	6,435	36	6	0.03	368.50	2.80	11.67	35.74	147.79	0.05	3,053.10	22.37	142.43	288.80	1,642.84
Thyroid-disease-ann-thyroid	7,200	21	3	0.00	221.40	1.85	5.39	23.76	68.80	0.00	1,737.61	13.94	34.24	151.86	397.96
Pendigits	7,494	16	10	0.02	194.58	3.21	12.22	41.87	154.93	0.03	1,657.67	32.11	144.31	424.74	1,679.99
Avila	10,430	10	12	0.03	183.61	3.68	12.18	47.22	153.63	0.05	1,585.04	45.50	141.46	568.74	1,750.95
Eeg	14,980	14	2	0.03	326.68	1.63	6.81	20.43	83.93	0.06	2,497.69	13.00	91.06	165.83	1,029.16
Htru	17,898	8	2	0.05	230.05	1.51	6.20	18.72	72.53	0.08	1,897.76	13.45	69.22	168.26	788.76
Shuttle	43,500	9	7	0.03	665.52	4.46	13.71	56.99	171.78	0.04	5,655.26	59.69	109.06	777.19	1,323.67
Skinsegmentation	245,057	3	2	0.08	1,471.57	6.57	18.12	84.45	221.48	0.10	15,259.16	87.81	187.88	1,143.90	1,965.37
Htsensor	928,991	11	3	3.63	17,448.31	17.37	60.29	189.84	570.93	6.92	-	115.62	798.46	1,441.01	4,111.95
Average Training Time (s)				0.06	366.77	1.81	6.96	22.99	84.32	0.12	869.29	14.71	68.77	178.33	731.07

Table 25: Depth=4,8 training time standard deviation (s) on 65 datasets with 10 random splits within 1 million samples

Dataset	Sample	Feature	Class	Depth=4					Depth=8						
				CART	LS-OCT	DEOCT	MH-DEOCT	DEOCT (Long)	MH-DEOCT (Long)	CART	LS-OCT	DEOCT	MH-DEOCT	DEOCT (Long)	MH-DEOCT (Long)
Soybean-small	47	35	4	0.00	0.05	0.04	0.42	5.17	8.52	0.00	2.73	0.27	3.34	9.82	25.97
Echocardiogram	61	11	2	0.00	0.02	0.01	0.58	0.20	3.75	0.00	0.31	0.28	3.32	2.72	15.50
Hepatitis	80	19	2	0.00	0.05	0.24	0.56	0.13	0.43	0.00	1.82	0.75	4.27	1.27	38.03
Fertility	100	9	2	0.00	0.14	0.01	0.03	0.63	0.94	0.00	3.17	0.23	5.45	0.65	65.74
Acute-inflammations-1	120	6	2	0.00	0.11	0.02	0.02	0.18	0.49	0.00	2.21	0.09	3.34	4.49	75.42
Acute-inflammations-2	120	6	2	0.00	0.78	0.02	0.27	0.66	1.55	0.00	10.12	0.09	7.18	4.61	95.39
Hayes-roth	132	5	3	0.00	0.06	0.03	0.31	0.59	4.30	0.00	2.10	0.22	6.92	4.13	95.29
Iris	150	4	3	0.00	0.16	0.01	0.12	0.43	1.08	0.00	7.88	1.02	4.58	2.14	42.47
Teaching-assistant-evaluation	151	5	3	0.00	0.11	0.02	0.44	0.60	3.81	0.00	8.19	0.51	3.03	1.03	14.78
Wine	178	13	3	0.00	4.14	0.01	0.48	0.44	9.67	0.00	39.73	0.65	3.41	4.30	33.15
Breast-cancer-prognostic	194	31	2	0.00	0.26	0.02	0.53	0.66	3.46	0.00	6.78	0.14	3.62	3.14	22.28
Parkinsons	195	23	2	0.00	0.16	0.01	0.23	0.27	2.37	0.00	1.55	0.97	4.16	1.59	34.40
Connectionist-bench-sonar	208	60	2	0.00	0.72	0.06	0.17	0.96	2.55	0.00	13.20	0.19	9.47	2.19	72.20
Image-segmentation	210	19	7	0.00	0.26	0.03	0.07	0.34	1.01	0.00	20.52	0.49	5.08	0.69	24.72
Seeds	210	7	3	0.00	0.69	0.02	0.03	0.37	0.79	0.00	12.58	0.58	5.10	6.86	47.95
Glass	214	9	6	0.00	0.25	0.01	0.14	0.62	2.11	0.00	8.23	0.21	4.61	1.29	38.70
Thyroid-disease-new-thyroid	215	5	3	0.00	0.18	0.06	0.14	0.88	3.04	0.00	12.47	0.20	5.93	2.10	52.52
Congressional-voting-records	232	16	2	0.00	0.22	0.04	0.30	0.65	2.72	0.00	14.47	0.16	10.02	2.74	70.95
Spect-heart	267	22	2	0.00	0.03	0.04	0.33	0.51	4.44	0.00	0.46	1.09	4.63	3.21	41.07
Spect-heart	267	44	2	0.00	0.01	0.01	0.49	0.24	2.46	0.00	0.69	1.05	5.21	1.95	45.07
Cylinder-bands	277	39	2	0.00	0.02	0.01	0.15	0.16	0.85	0.00	1.07	0.15	2.93	1.78	46.85
Heart-disease-Cleveland	282	13	5	0.00	0.12	0.01	0.50	0.20	0.74	0.00	0.51	0.97	4.00	1.63	60.04
Haberman-survival	306	3	2	0.00	0.08	0.01	0.06	0.42	0.86	0.00	1.27	0.13	3.19	2.10	57.63
Ionosphere	351	34	2	0.00	0.02	0.01	0.57	0.44	5.96	0.00	0.74	0.30	4.90	3.24	77.37
Dermatology	358	34	6	0.00	0.13	0.02	0.06	0.23	2.54	0.00	4.10	0.82	9.67	3.97	30.70
Thoracic-surgery	470	16	2	0.00	0.08	0.02	0.05	0.32	1.18	0.00	2.05	0.94	5.52	0.99	25.83
Body	507	5	2	0.00	0.38	0.04	1.01	0.81	10.18	0.00	3.08	1.14	8.67	1.34	149.43
Climate-model-crashes	540	20	2	0.00	0.01	0.01	0.49	0.20	5.66	0.00	0.47	3.59	5.10	2.38	23.13
Monks-problems-3	554	6	2	0.00	0.04	0.01	0.03	0.23	0.91	0.00	3.02	0.11	2.58	1.11	22.10
Monks-problems-1	556	6	2	0.00	0.08	0.01	0.36	0.24	4.04	0.00	3.15	1.08	2.10	2.90	26.90
Breast-cancer-diagnosti	569	30	2	0.00	0.20	0.01	0.02	0.30	0.89	0.00	4.95	0.17	5.05	1.79	51.80
Indian-liver-patient	579	10	2	0.00	0.10	0.01	0.19	0.15	2.38	0.00	4.94	0.98	2.33	1.20	27.36
Monks-problems-2	600	6	2	0.00	46.31	0.05	0.23	1.47	4.60	0.00	192.44	0.51	4.57	2.09	33.30
Balance-scale	625	4	3	0.00	10.75	0.03	0.34	0.82	4.62	0.00	19.80	0.07	8.00	2.11	31.82
Credit-approval	653	15	2	0.00	2.57	0.06	0.94	0.84	11.13	0.00	9.08	1.13	12.44	3.47	206.06
Breast-cancer	683	9	2	0.00	0.08	0.03	0.27	0.99	4.13	0.00	2.09	0.37	5.02	2.05	55.92
Blood-transfusion	748	4	2	0.00	0.70	0.09	0.30	1.09	3.42	0.00	8.16	0.13	6.79	1.53	44.02
Mammographic-mass	830	5	2	0.00	0.02	0.01	0.20	0.21	2.38	0.00	0.96	0.24	8.48	1.42	54.00
Tic-tac-toe-endgame	958	9	2	0.00	2.02	0.01	0.08	0.77	1.86	0.00	6.46	0.09	5.53	0.80	38.82
Connectionist-bench	990	13	11	0.00	0.02	0.01	0.25	0.29	2.86	0.00	0.24	1.32	4.42	2.64	51.04
Statlog-project-German-credit	1,000	20	2	0.00	7.78	0.07	0.33	1.69	7.07	0.01	30.66	0.27	9.59	3.08	49.77
Concrete	1,030	8	3	0.00	0.06	0.01	0.25	0.77	2.29	0.00	1.49	0.14	2.82	1.07	93.82
Qsar-biodegradation	1,055	41	2	0.00	0.42	0.05	0.67	0.65	5.15	0.00	3.14	1.29	14.90	1.93	187.00
Banknote-authentication	1,372	4	2	0.00	0.25	0.03	0.08	0.42	1.04	0.00	13.07	1.00	3.19	1.55	58.62
Contraceptive-method-choice	1,473	9	3	0.00	4.94	0.05	0.15	0.91	3.99	0.01	23.02	0.63	4.53	2.78	19.34
Car-evaluation	1,728	6	4	0.00	0.02	0.01	0.02	0.28	1.60	0.00	0.21	0.14	2.90	0.84	44.47
Ozone-level-detection-eight	1,847	72	2	0.00	0.17	0.02	0.15	0.42	1.83	0.00	8.95	1.17	3.87	1.59	30.99
Ozone-level-detection-one	1,848	72	2	0.00	5.62	0.01	0.71	0.59	9.25	0.00	49.69	0.47	5.61	2.55	69.52
Seismic-bumps	2,584	18	2	0.00	0.02	0.01	0.18	0.37	2.09	0.00	0.34	0.97	3.87	0.56	26.00
Chess-king-rook-versus-king-pawn	3,196	36	2	0.00	0.08	0.01	0.03	0.66	1.37	0.00	6.82	0.55	5.34	1.16	20.18
Thyroidann	3,772	21	3	0.00	0.27	0.02	0.63	0.31	8.97	0.00	10.67	0.23	3.70	4.55	84.27
Statloglansat	4,435	36	6	0.00	0.02	0.03	0.25	0.53	3.35	0.00	0.98	0.10	9.38	2.18	44.58
Spambase	4,601	57	2	0.00	0.03	0.01	0.04	0.42	1.97	0.00	1.52	0.45	4.81	0.76	53.88
Wall-following-robot-2	5,456	2	4	0.00	0.02	0.01	0.05	0.23	1.47	0.00	1.18	0.09	4.70	1.14	45.33
Pageblock	5,473	10	5	0.00	0.11	0.01	0.04	0.36	1.29	0.00	2.93	0.10	3.02	1.30	15.88
Optical-recognition	5,620	62	10	0.00	1.85	0.02	0.08	0.69	2.41	0.00	26.89	0.79	2.26	4.57	23.11
Statlog-project-landsat-satellite	6,435	36	6	0.00	4.09	0.03	0.12	0.74	3.87	0.01	86.51	0.72	4.78	2.45	20.96
Thyroid-disease-ann-thyroid	7,200	21	3	0.00	1.14	0.01	0.05	0.54	2.36	0.00	18.64	0.60	4.56	8.88	49.00
Pendigits	7,494	16	10	0.00	6.06	0.01	0.05	0.95	3.02	0.01	49.20	0.50	3.75	15.75	10.33
Avila	10,430	10	12	0.00	4.46	0.03	0.14	0.93	5.38	0.02	47.34	0.35	4.27	24.60	79.57
Eeg	14,980	14	2	0.00	5.17	0.02	0.12	0.45	2.57	0.00	24.40	0.15	5.76	2.13	23.06
Htru	17,898	8	2	0.00	4.83	0.01	0.04	0.58	2.52	0.00	35.74	0.57	2.58	1.14	50.67
Shuttle	43,500	9	7	0.01	6.72	0.02	0.07	0.99	2.81	0.01	51.44	1.26	4.25	15.15	53.92
Skinsegmentation	245,057	3	2	0.03	13.48	0.17									

Table 25 continued from previous page

Dataset	Sample	Feature	Class	Depth=4				Depth=8							
				CART	LS-OCT	DEOCT	MH-DEOCT	DEOCT (Long)	MH-DEOCT (Long)	CART	LS-OCT	DEOCT	MH-DEOCT	DEOCT (Long)	MH-DEOCT (Long)
Htsensor	928,991	11	3	0.10	567.82	0.08	0.22	2.71	8.13	0.14	-	1.85	54.06	3.46	47.88
Average Training Time STD (s)				0.00	10.89	0.03	0.25	0.66	3.39	0.00	22.69	0.60	6.20	3.23	51.67